DOKTORSAVHANDLINGAR
VID
CHALMERS TEKNISKA HÖGSKOLA
Nr. 64

ON THE MOTION OF LOW ENERGY LIGHT IONS IN THIN SINGLE CRYSTAL FILMS

BY

CARL-JOEL ANDREEN

GÖTEBORG 1967

ON THE MOTION OF LOW ENERGY LIGHT IONS IN THIN SINGLE CRYSTAL FILMS

BY

CARL-JOEL ANDREEN

Tekn. lic.

AKADEMISK AVHANDLING

SOM MED TILLSTÅND AV CHALMERS TEKNISKA HÖGSKOLA FRAMLÄGGES TILL OFFENTLIG GRANSKNING FÖR TEKNOLOGIE DOKTORSGRADS VINNANDE MÅNDAGEN DEN 19 JUNI 1967 KL. 10 I PALMSTEDTS-SALEN, ADMINISTRATIONSBYGGNADEN, CHALMERS TEKNISKA HÖGSKOLA, SVEN HULTINS GATA, GÖTEBORG

GÖTEBORG
ELANDERS BOKTRYCKERI AKTIEBOLAG
1967

ERRATA

sid. 1	rad 15	läs:	... N_2^{++} and O_2^{++} are ...
	rad 23	läs:	... of the D^+ beam ...
sid. 8	rad 6	läs:	... mass spectra ... and A gases.
sid. 9	rad 9	läs:	... two peaks [001] and [[011] may ...
sid. 12	Fig. 3b	läs:	... outside the $\{110\}$ plane.
	rad 10	läs:	... along a channel [V] .
sid. 14	Fig. 4	läs:	... Θ and φ in a $\{111\}$ plane.
sid. 15	Fig. 5	läs:	... ion current 10^{-7} A.
sid. 16	Fig. 6	läs:	... I(Θ) ($\mu\mu$A)
sid. 17	rad. 27	läs:	Both functions ...
sid. 18	Fig. 7	läs:	I(Θ) ($\mu\mu$A)
sid. 19	Fig. 8	läs:	I(Θ) ($\mu\mu$ A)
sid. 20	Fig. 9	läs:	I(Θ) ($\mu\mu$A)
sid. 21	rad. 13	läs:	The experimental distributions ...
sid. 22	rad 5	läs:	critical
sid. 24	ekv. (12)	läs:	$U(r) = \int_{-\infty}^{+\infty} \frac{dz}{d} V(\sqrt{z^2 + r^2})$
sid. 25	rad 18	läs:	... of 0,5 Å from the ...
sid. 29	ekv. (25)	läs:	... $\approx$ ...
	ekv. (23)	läs:	... $\sum_{[hkl]} \frac{R(E,t,\Theta)}{R(E,t,\Theta_{h_1k_1l_1})} \cdot F_{\{110\}}(E,t)$ ...
sid. 30	ekv. (34)	läs:	... $r = R_{exp} / R_{theor.}$ and ...
sid. 31	rad 14	läs:	... channeling [[V] .
sid. 36	Fig. 12	läs:	... $r \leq \lvert \bar{u} + a \rvert$
sid. 37	rad. 6	läs:	... 10^{-14} - 10^{-15} A.
sid. 39	rad 4	läs:	... coldfinger connected to a Cu cylinder which..
	rad 18	läs:	... W.M. Gibson, Bell Telephone Laboratories and Rutgers ...
sid. 31	ekv. (38)	läs:	... $\sum_{[hkl]} \cos(k'\Theta) \cdot F_{\{100\}}(E,t)$ ...

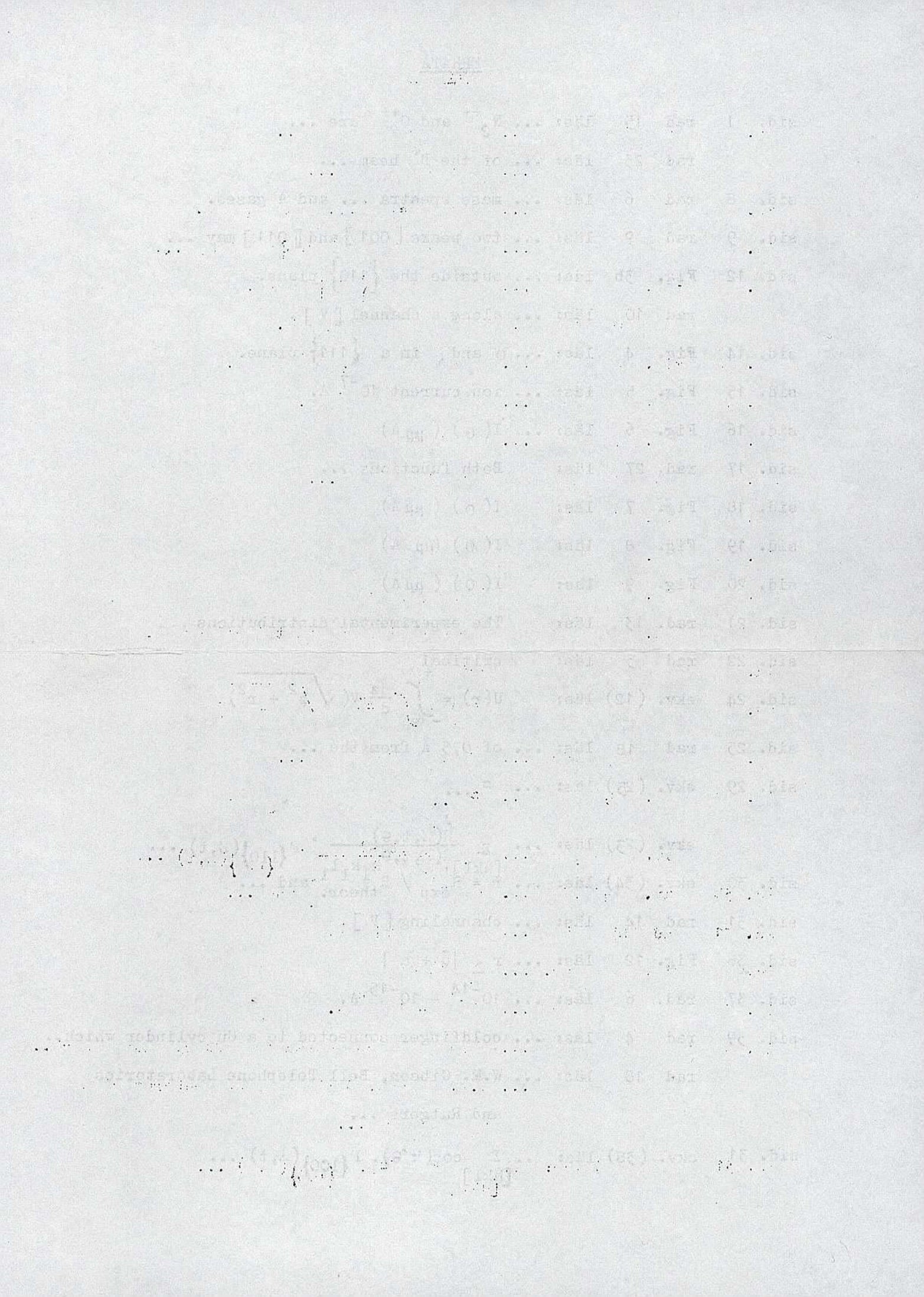

DOKTORSAVHANDLINGAR
VID
CHALMERS TEKNISKA HÖGSKOLA

ON THE MOTION OF LOW ENERGY LIGHT IONS IN THIN SINGLE CRYSTAL FILMS

BY

CARL-JOEL ANDREEN

GÖTEBORG
ELANDERS BOKTRYCKERI AKTIEBOLAG
1967

To my family

This thesis is based on experiments done at Northwestern University, Evanston, Ill., U.S.A., during the period 1964–1966. It contains mainly the following papers

I*a*. C-J. Andreen, R. L. Hines, W. Morris and D. Weber Channeling of 13 keV D^+ ions in gold crystals. Physics Letters *19*, (1966), 116.

b. C-J. Andreen and R. L. Hines, Channeling of D^+ and He^+ ions in gold crystals. Phys. Rev. *151* (1966), 341.

II. C-J. Andreen, E. F. Wassermann and R. L. Hines, Direct observation of channeling in b.c.c. iron films. Phys. Rev. Letters *16* (1966), 782.

III*a*. C-J. Andreen and R. L. Hines, Critical angles for channeling of H^+, D^+ and He^+ ions in single crystal gold films in the energy interval 1–17 keV. Physics Letters 24A (1967), 118.

b. C-J. Andreen and R. L. Hines, Critical angles for channeling of 1 to 25 keV H^+, D^+ and He^+ ions in gold crystals. Phys. Rev. In print.

IV. C-J. Andreen, Experiments on the channeling of ions through thin films of different structures. Arkiv för Fysik. In print.

V. C-J. Andreen, A simple transparency model for the channeling of low energy light ions in crystals. Arkiv för Fysik. In print.

VI. C-J. Andreen, Blocking of D^+ ions in single crystal gold films. Arkiv för Fysik. In print.

Introduction

In the early 1960's investigations on the transmission of heavy and light ions through matter gained an increased interest. A new effect was observed for ions which were incident along low index directions and planes in a single crystal. It was found that the transmission was largely increased. The effect was called channeling or the string effect. The main part of this thesis summerizes some investigations on the channeling of low energy H^+, D^+ and He^+ ions in a few materials of different structures. Some experimental information is added here to demonstrate the effects of damage to the films by bombardment with heavier ions such as C^+, Ne^+ and A^+ ions. The investigations are unique in the sense that the incident ion energy is extremely low (1–30 keV). The transmission of these low energy particles demands sofisticated film preparation techniques. Single crystal films of gold, silver and α-iron have been prepared by evaporation. Details about this part of of the work may be found elsewhere.

The problems with radiation damage and contamination make the interpretation of the transmission profiles sometimes hazardous. A prolonged irradiation changes the film to some extent. A complete study of the channeling characteristics using one single foil is therefore excluded. The production of identical crystals is difficult. The investigations are thus limited to a few values of some important parameters. In order to be able to use not only descrete values but to cover an interval of a parameter one has to lower the vacuum in the target chamber to such a degree that a foil could be bombarded for hours without any influence from a contamination layer. The damage may be minimized by using protons of moderately low energies. Still, an accurate determination of a variable such as the critical angle for channeling ψ_2 as a function of energy E and channel type $[hkl]$[1] is difficult.

The investigations summerized in this thesis deal with thin foils with only one kind of atom. In the near future a study of films with different kinds of lattice atoms, like for instance PbS or PbSe films will be undertaken.

The channeling effect has become a working tool in solid state physics as well as in nuclear physics. In solid state physics one is sometimes interested

[1] The notation $[hkl]$ is used consequently in the following in stead of the notation $\langle hkl \rangle$ to indicate a group of directions of the same kind.

in the lokalization of an impurity atom in the lattice. The position of the impurity may be determined by the channeling effect. The doping technique of semiconductors is developing through the use of forced ion implantation (channeling). In nuclear physics one may use the channeling effect as a tool for the determination of lifetimes of the order of $10^{-17}-10^{-18}$ sec. At present 10^{-12} sec. is the shortest lifetime which can be measured by conventional methods. As pointed out by Gemmell and Holland [1] care should be taken when nuclear cross sections are measured using a crystalline target. The channeling effect in conjunction with the blocking effect discussed below may easily result in a cross section which is one order of magnitude smaller.

It is no overstatement to say that the channeling effect has tied closer together nuclear and solid state physics through all kinds of particle accelerators. This means an extention of the use of isotope separators, van de Graaff generators and other high energy accelerators, a fact which should be encourageing to physicists in both fields.

Apparatus and foil production

The particle accelerator used in the investigations summerized here has been described earlier [2]. The goniometer arrangement for orientation of the crystals and the energy analyzer are shown in Fig. 1. A more detailed description is found in [1*b*]. The detector is a Faraday cage connected to an electrometer with an ultimate sensitivity of 10^{-14} A. The analyzer is mainly meant for separating away the ions which have passed through eventual pinholes in the crystal. It has also been used to measure roughly the most probable energy loss ΔE_{mp} as a function of crystal orientation. Because of the low energy of the ions the width of the peaks due to channeling is relatively large. It was therefore decided that two degrees of freedom would be enough to build into the goniometer. If the crystal surface is parallel to the crystal holder surface this is a correct decision. In mounting the thin films a circular piece of tantalum with a centre hole is used to clamp the crystal down against the holder. A remaining misorientation of the crystal relative to the holder may be checked by looking at the transmitted intensity I as a function of the azimuthal angle φ. This function should be a horisontal line apart from the channeling peaks which may be superimposed on it. For these low energy particles it is found experimentally that two degrees of freedom is sufficient. Still, local parts of the crystal may be misoriented relative to the holder. The influence of such misorientations on the peak width is estimated in [1*b*] and found to be less than a few percent for the best crystals.

It is felt worthwhile to include here some figures showing the mass resolving power of the apparatus. Because of the relatively poor vacuum in the accelerator ($\sim 10^{-5}$ mmHg), molecular ions of the type H_2^+ and D_2^+ may split up at different places in the chamber. Quite a few combinations of mass position and energy may occur and it is obvious that one has to be careful about what kind of particle one uses and their incident energies. Table I shows the different combinations which may be found in the beam at the detector. The beam current as a function of the magnet field B is shown in Fig. 2*a–f* for some of the gases used in the experiments. In Fig. 2*a* the mass spectrum of He is shown. The intense peak in this spectrum corresponding to M = 4 is used as a calibration point for the rest of the spectra. The transmission coefficient in the forward direction for ions with mass number M = 5–7 in Fig. 2*a* is found to be much smaller than for ions with mass number M = 4. A possible explanation for the peak at M = 5–7 is that charged molecules N_2^+ and O_2^+ are present in the ion source. If hydrogen is present as an impurty in the deuterium gas, DH^+ or H_3^+ ions, created in the ion source, would cause the peak at M = 3. The small indication of a peak at M = 0.5 does indicate that hydrogen is present. In Fig. 2*b* showing the hydrogen spectrum the peaks are well separated and no other gases seem to be present as impurities. The peak at M = 3 may be caused by H_3^+ ions with full energy. Fig. 2*c* shows the mass spectrum for deuterium. Fig. 2*d* shows the transmitted intensity of the beam in the forward direction through a 700 Å thick gold single crystal as a function of the magnetic field B. No energy analyzis is done. One observes that all mass components from Fig. 2*c* are present and that the relative intensity between the peaks at mass numbers

Table I. The different components in an ion beam of deuterium is illustrated.

	Direct beam					Transmitted beam				
Point of creation[a]	1–2	1	1	2–3	3–4	1–2	1	1	2–3	3–4
Energy[b]	$E_i/2$	E_i	E_i	$E_i/2$	$E_i/2$	$E_i/2+E_a-\Delta E$	$E_i+E_a-\Delta E$	$E_i/2+E_a/2-\Delta E$	$E_i/2+E_a-\Delta E$	$E_i/2+E_a/2-\Delta E$
Unit on mass scale	1	2	4	4	4	1	2	4	4	4
Particle mass	1	2	4	2	2	1	2	2	2	2

[a] 1. Ion source. 2. Magnet. 3. Acc. gap. 4. Analyzer.

[b] Ion source energy E_i, acc. gap energy E_a, energy loss in the foil ΔE.

6–8 and 4 is greatly reduced. The reduction is approximately 30 times. Due to energy spread in the crystal the peaks are somewhat broader in Fig. 2*d*. It is generally observed that the transmission coefficient is inversely proportional to the mass. It is therefore concluded that the peak at M = 6–8 is caused by particles heavier than helium atoms. Fig. 2*e* and Fig. 2*f* show the mass spectrum for relatively pure Ne and A gas.

The production of thin single crystal foils has been the subject of a vast number of investigations. In connection with anomalous transmission due to channeling it is not enough to know how to produce single crystals. A most important factor for the accuracy and the interpretation of the results is the overall flatness as well as different kinds of wrinkles in the mounted films. The influence of these factors on the peak width is estimated

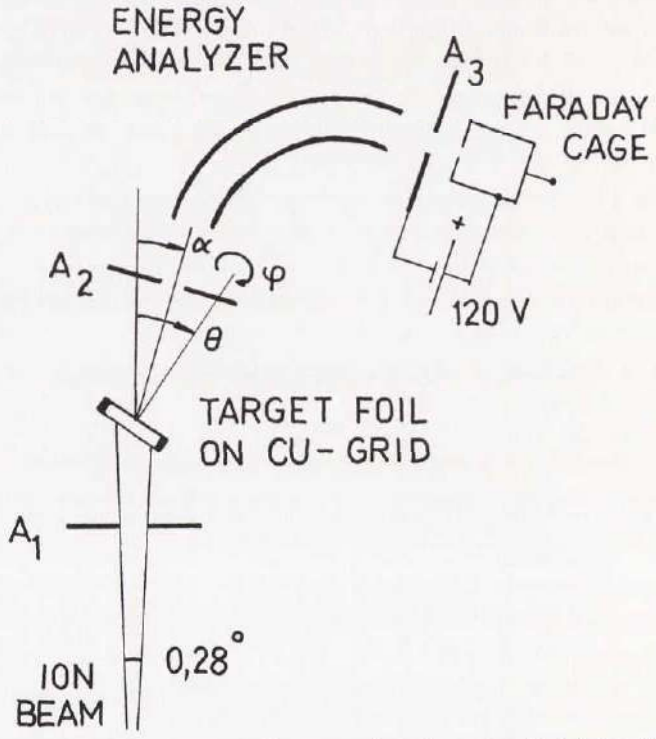

Fig. 1. Experimental arrangement for measuring the transmitted intensities of ions through a crystal as a function of the tilt angle θ and the rotation angle φ. The diameters of the apertures are $A_1 = 0.75$ mm, $A_2 = 0.75$ mm, and $A_3 = 3$ mm. The distance between the foil and aperture A_1 is 50 mm and the distance between the foil and aperture A_2 is 32 mm. The ranges of possible angles are $-60° \leq \theta \leq +60°$, $0° \leq \varphi \leq 360°$, and $-3° \leq \alpha \leq +58°$. The distance between the analyzer plates is about 20 mm. The direction of the ion beam is fixed.

in [I*b*]. The influence of a contamination layer is also discussed. As far as the transmitted intensity is concerned the wrinkles and the contamination is definitely of some importance. The change in intensity due to a contamination build up is studied to some extent in [I*b*]. The effect may be reduced by cutting down the bombarding time or by correcting for the effect by measuring the time dependence of the transmitted ion intensity. The influence of the wrinkles may be checked by using several single crystals with visible wrinkles. A small change in the ratio between the relative intensities in the two peaks may sometimes be observed. As pointed out in [III] only foils which look perfectly flat to the naked eye have been used. The micro wrinkles that still exist in the foils have no detectable influence on this ratio. However, for high energies the influence of even small wrinkles may be fatal. The technique to be used in that case will probably be to prepare thin crystals out of thick crystals through etching methods. The minimum thickness that can be handled without introducing wrinkles in the crystal is of the order of microns. Energies of at least one hundred keV is then believed to be necessary even for the lightest ions.

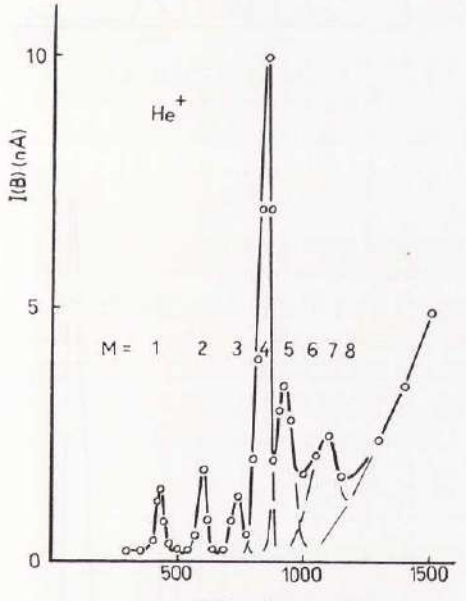

Fig. 2*a*

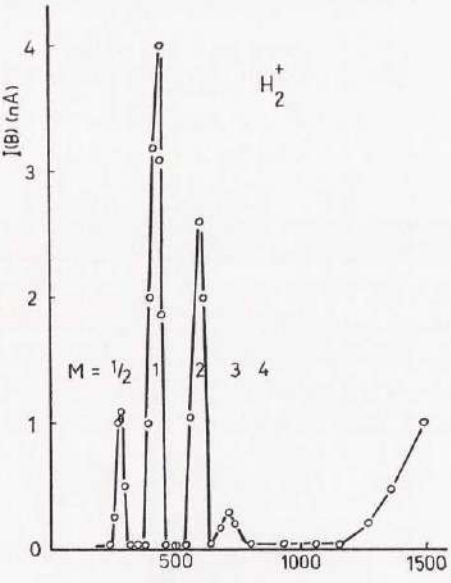

Fig. 2*b*

Fig. 2. The beam intensity of a few different gases is measured as a function of the magnetic field B. The ion current is measured in units of nanoamperes and the energy of the ions is around 10 keV. In Fig. 2*d* the transmitted intensity through a 700Å thick gold film is measured. Compared to Fig. 2*c* the intensity at M=6–8 is greatly reduced.

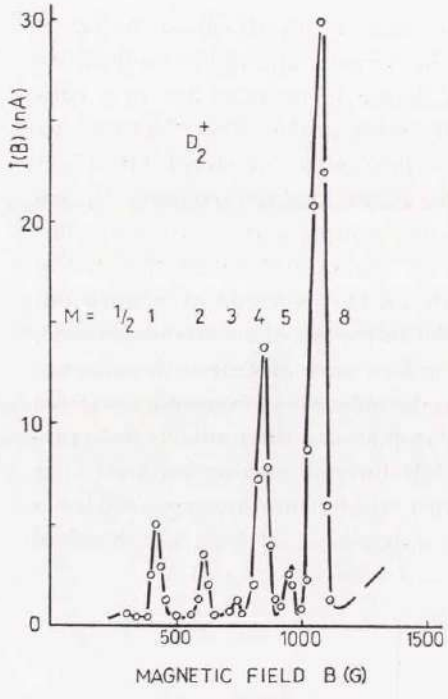

Fig. 2 *c*

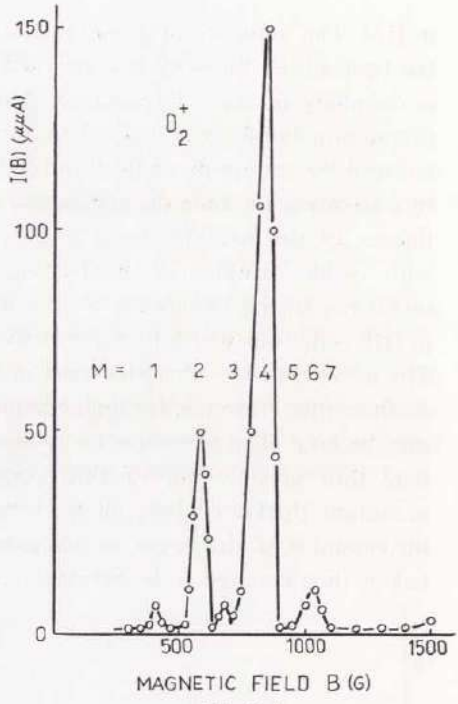

Fig. 2 *d*

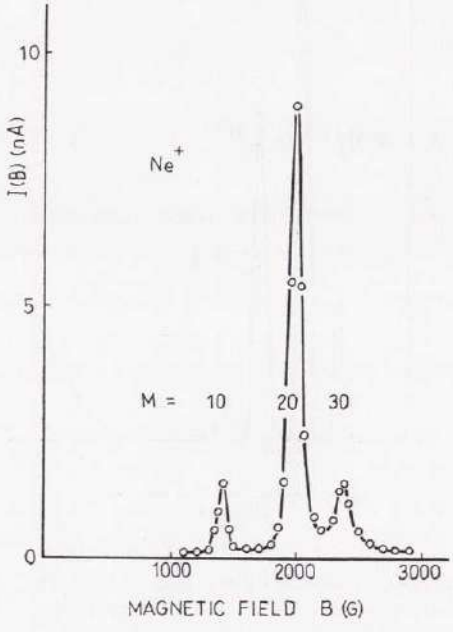

Fig. 2 *e*

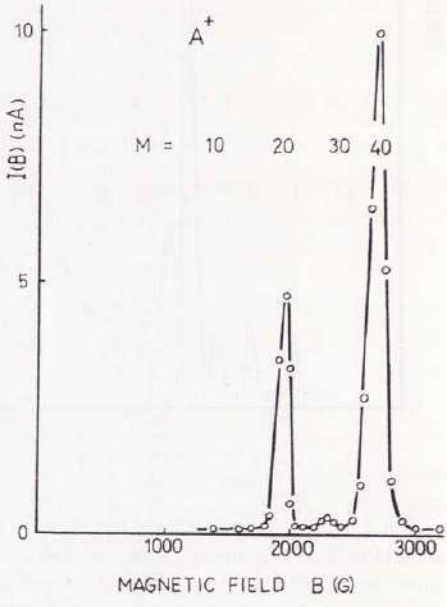

Fig. 2 *f*

Evaporated films are known to have a high defect density. In the investigations this density is kept as low as possible. By optical inspection in an electron microscope those foils are chosen for channeling experiments which on the average show dark areas less than about ten percent. The dark areas are interpreted as being due to defects of different kinds. The inspection is performed with the crystal normal parallel to the electron beam. Some types of defects have a preferred orientation. One example is the slip planes which slip parallel to {111} planes in a f.c.c. lattice. Along this plane the influence of the defects may therefore be reduced. It is observed experimentally that the transmitted intensity is relatively high along these planes. The influence of the defects on the intensity is believed to be small compared to the influence of a large interplanar distance. Measurements of this type are being performed at other laboratories. Good single crystals without pinholes have been prepared by evaporation in the thickness interval 50–2000 Å.

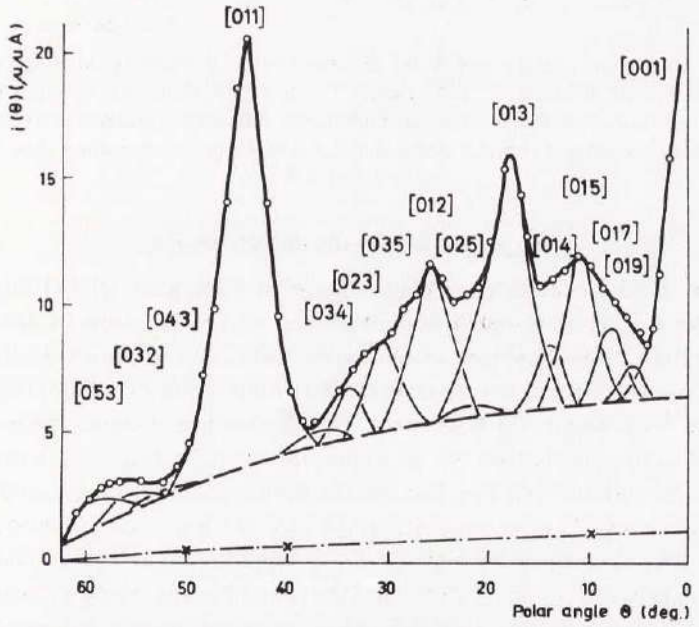

Fig. 3*a*. The intensity $i(\theta)$ of 17 keV D^+ ions transmitted through a gold crystal is shown as a function of θ along a {100} plane. The crystal is about 265 Å thick. The dashed line separates the directional channeling from planar channeling. The dot-dashed line represents the intensity in high index directions outside the {100} plane. Individual directions are resolved and indexed.

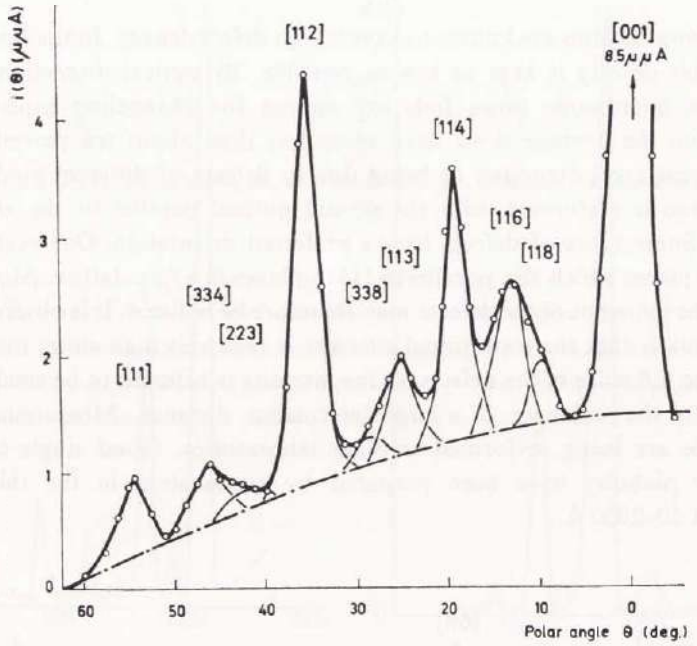

Fig. 3*b*. The intensity $i(\theta)$ of 21 keV D^+ ions transmitted through a gold crystal is shown as a function of θ along a {110} plane. The crystal is about 300 Å thick. The dot-dashed line represents the intensity in high index directions outside the {100} plane. No planar channeling from the {110} plane can be detected. Individual directions are resolved and indexed.

Experimental results and discussion

Some of the experimental results given in the papers [I]–[VI] are given again here. Fig. 3, 4 and 5 show the intensity of D^+ ions of 16–21 keV transmitted through single crystal gold films in the forward direction. Figs. 3*a*–*b* show the intensity transmitted along the {100} and {110} planes in a 265 Å (*a*) and a 300 Å (*b*) thick gold crystal. Fig. 4 shows the transmission along the {111} plane. In all figures the crystal has a [001] channel parallel to the foil normal. Fig. 5 shows the transmission through a gold crystal oriented in a [111] direction. About 12 keV D^+ ions are channeled along a {110} plane. A comparison between Fig. 3*b* and Fig. 5 shows that a correlation exists between channel indices and the peak intensity along a channel. Because of a change in effective foil thickness as a function of θ, a direct comparison between peak intensities and channel areas is impossible. A rough correction method is discussed in [V]. Along the {110} plane in Fig. 3*b* the minima reach the dot-dashed line. This line represents the transmitted intensity along high index planes and reflects the behaviour of a polycrystal

with a random orientation as verified by experiments [IV]. If one divides the peak intensities by the random intensity at the same θ—value and relates this ratio R'_{hkl} to the ratio $R'_{[h_1k_1l_1]}$, one obtains a correlation between this new ratio R'_{exp} and the ratio

$$R'_{theor} = A_{[hkl]}/A_{[h_1k_1l_1]} \tag{1}$$

which can be expressed by the relationship

$$R'_{exp} = R'_{[hkl]}/R'_{[h_1k_1l_1]} = c^{(1)} \cdot A_{[hkl]}/A_{[h_1k_1l_1]} + c^{(2)} \tag{2}$$

$A_{[hkl]}$is the channel area along the direction $[hkl]$, $[h_1k_1l_1]$ is the most open direction in that particular plane under consideration and $c^{(1)}$ and $c^{(2)}$ are constants for a particular foil thickness t and particle energy E. One observes from (2) that the ratio R'_{exp} places the channels in the order expected from simple geometrical calculations. For this reason and because of the fact that the quantitative correlation is acceptable too, this ratio is believed to be a satisfactory way of correcting for changes in effective foil thickness.

If the same technique is applied to the {100} plane in Fig. 3*a* the result is not as good as for the {110} plane. However, if one subtracts a certain part from the peak intensity before dividing by the random intensity, the correlation is made substantially better, in particular the quantitative correlation. The dashed curve in Fig. 3*a* indicates the function $P_{\{hkl\}}(\theta)$ which has to be subtracted along the plane $\{hkl\}$ in order to arrive at an equally good correlation as in the {110} plane. One observes that $P_{\{110\}}(\theta)$ is strikingly similar to $R(\theta)$, the random intensity as a function of θ. In the plane {111}, Fig. 4, the situation is the same as for the {100} plane. The function $P_{\{111\}}(\theta)$, which has to be subtracted, is larger in the {111} plane than in the {100} plane.

The same observations may be made for a b.c.c. lattice as well. Experiments with an α-iron single crystal foil show that for 15 keV D^+ ions transmitted through a 600 Å iron foil, equation (2) is valid along the two planes {110} and {100}. [II], [IV]. Both in the gold and the α-iron lattice the functions $P_{\{hkl\}}(\theta)$, indicated by dashed lines, resemble quite closely the behaviour of $R(\theta)$. In correcting for the change in effective foil thickness with θ, it is therefore not important if the function $P_{\{hkl\}}(\theta)$ or $R(\theta)$ is used. The actual situation may determine which function should be used.

A few experiments have been done with heavier ions in thin single crystal films. It is found that the influence of different damage effects on the transmission profiles is often critical. As pointed out in [I*b*] the change in the transmitted intensity and the most probable energy loss $\Delta E_{mp}(t)$ with time is caused by at least two factors. One is the contamination due to a poor

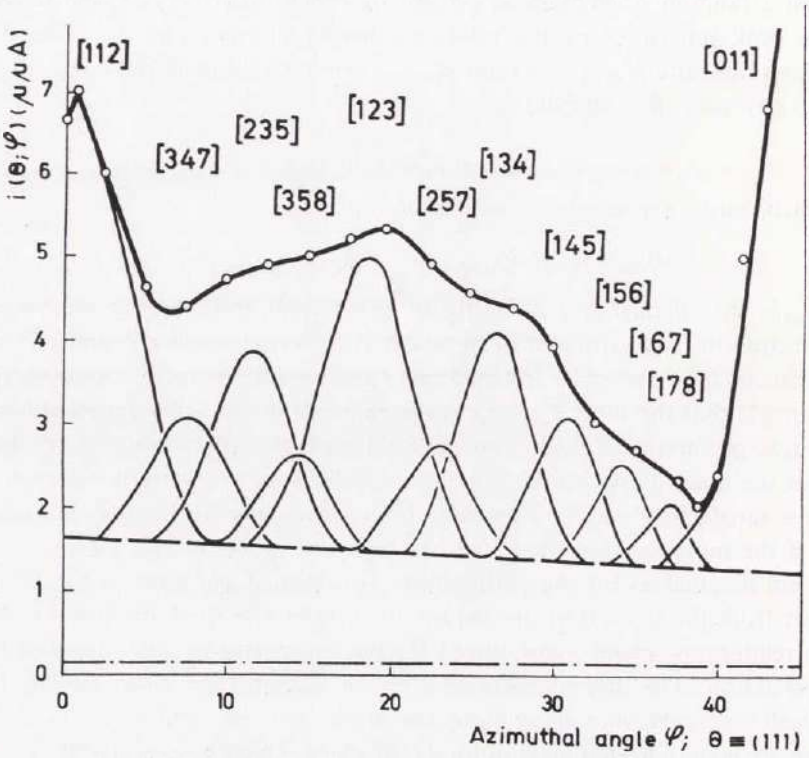

Fig. 4. The intensity $i(\theta, \varphi)$ of 16 keV D^+ ions transmitted through a gold crystal is shown as a function of θ and φ a {111} plane. The crystal is 450 Å thick. The dashed line separates planar channeling from directional channeling. The dot-dashed line represents the transmitted intensity in high index directions just outside the {111} plane. Individual directions are resolved and indexed.

vacuum in the chamber. The contamination layer causes a decrease in the intensity. The influence of such a layer is clearly visible at a preassure of 10^{-5} mmHg when light ions of moderate energies are used. The damage to the crystal lattice which is the second factor is more pronounced at higher energies and for heavier ions. The damage manifests itself through the production of several kinds of defects and a tendency to stuff up open channels through the creation of interstitials. These effects also tend to decrease the transmitted intensity. At the same time sputtering of gold atoms occur which will thin down the foil. Sputtering effects tend to increase the tranmitted intensity because of a decreasing foil thickness. The measureing technique becomes difficult to manage when the damage rate is fast.

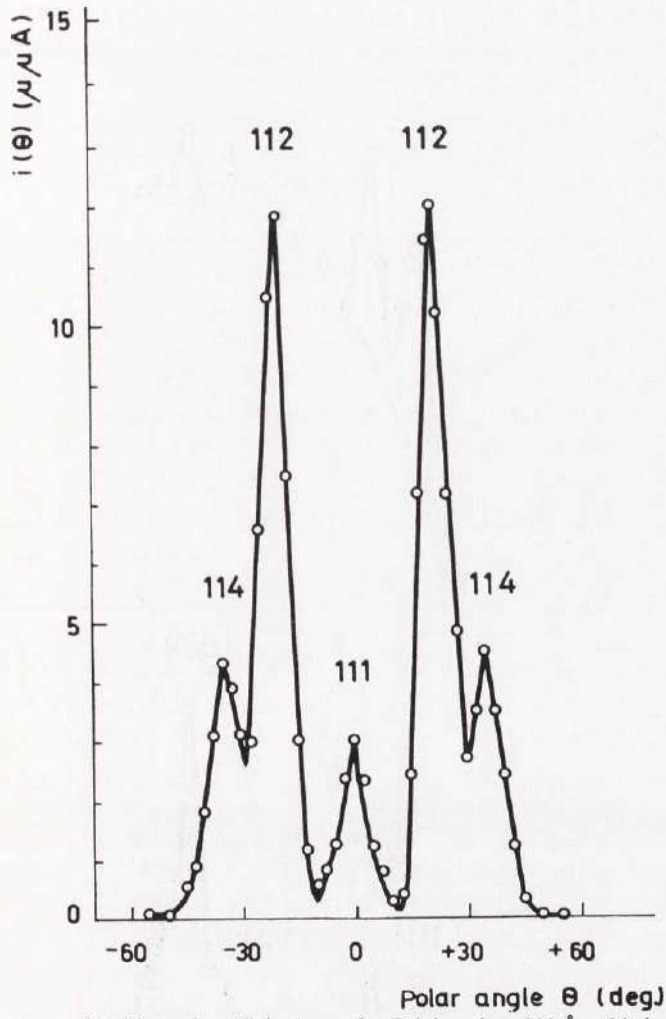

Fig. 5. The transmitted intensity $i(\theta)$ is shown for D^+ ions in a 900 Å gold single crystal film for which the individual crystallites are oriented almost exclusively in the [111] direction (~95%). The incident ion energy is 12 keV and the ion current 10^{-8} A.

The fact that it takes some time to find the most probable energy loss for a certain combination of θ and φ may soon end in a situation where ΔE_{mp} changes appreciably over the time interval necessary to find its value. The situation may be better if individual particle counting is used. This allows the use of much lower beam intensities and perhaps lower incident ion energies as well. Fig. 6 shows the intensity of 25 keV He^+ ions trans-

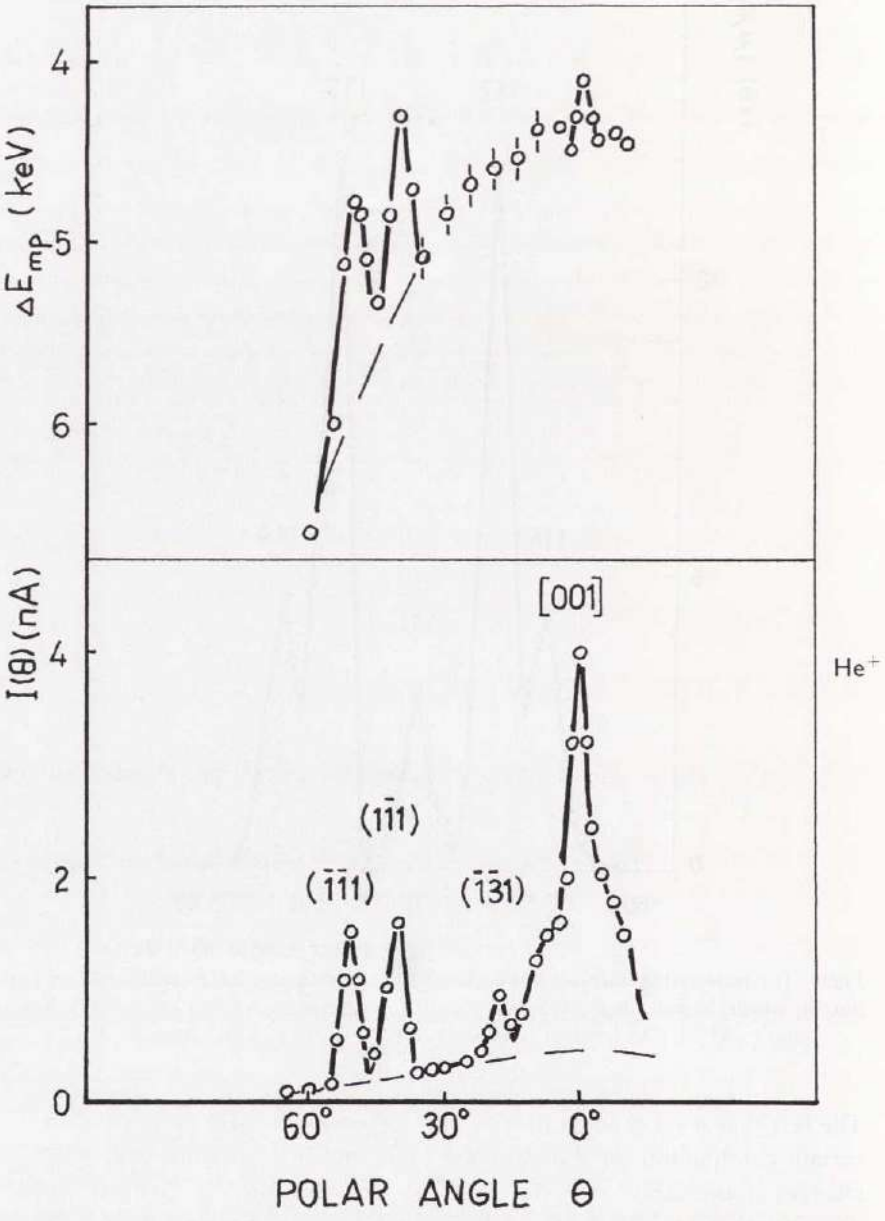

Fig. 6. The intensity of 25 keV He^+ ions transmitted through a 250 Å thick gold foil is shown as a function of θ. The azimuthal angle φ is set at a value corresponding to about 10° off the {100} plane. The most probable energy loss ΔE_{mp} is also given.

mitted through a 250 Å thick gold film as a function of θ. The azimuthal angle φ is set at a value corresponding to about 10° off a {100} plane. The most probable energy loss ΔE_{mp} is shown as a function of θ for the same φ-value. One observes a double peak centered around $\theta = 45°$, due to the $(\bar{1}\bar{1}1)$ and the $(1\bar{1}1)$ planes. At this φ-value the channels [145] contribute appreciably to the intensity in each peak. About two thirds of the peak value is attributed to directional channeling and the rest one third to planar channeling along the {111} planes. The dotdashed lines in Fig. 6 represent the random intensity as a function of θ. At $\theta = 18°$ one finds a small peak due to the $(\bar{1}31)$ plane. No low index channels exist for this combination of θ and φ. The shoulders on each side of the [001] peak are most probably due to the nearness of the {100} plane. Fig. 7 shows the transmitted intensity of 25 keV C^+ ions in the forward direction ($\alpha = 0$) through a 270 Å thick gold crystal as a function of θ. The most probable energy loss ΔE_{mp} is shown as a function of θ in the plane {100}. The total bombarding time is 0.5 hour. One observes that the [001] channel is almost completely gone at the end of the bombarding time. The energy loss ΔE_{mp} decreases fast at the end of the experiment when the foil is thinned down very quickly. At the moment of foil rupture the ΔE_{mp}-value drops instantly to zero. The change is too fast to be followed continously. The transmitted intensity drops to zero at the same time because of the fast change in ΔE_{mp}. Fig. 8 shows the intensity of 32 keV Ne^+ ions transmitted through a 250 Å thick gold film in the forward direction ($\alpha = 0$). The most probable energy loss ΔE_{mp} and the ion intensity I are shown as functions of the polar angle θ. The four channels [011], [001], [112] and [013] may be identified in the intensity curve. The [001] and the [112] channels are also seen in the energy loss curve. No random intensity could be detected at all. Both function are distorted due to damage. Because of a speeded up measuring technique the total interval $-60° \lesssim \theta \lesssim +60°$ could be measured in 10 minutes without breaking the foil. The functions are believed to reflect to a higher degree the damage due to interstitials and vacancies and other defects than due to sputtering. The relatively large peak width shows that the ions are considerably heavier than He^+ ions. This is so despite the fact that the Ne^+ ion energy is higher than the He^+ ion energy. According to Lindhard [3] the width is inversely proportional to the square root of the energy E. The last example of the transmission of heavy ions through thin single crystal films is shown in Fig. 9. The difficulty to detect the transmitted intensity of A^+ ions is overcome by using an extremely thin film and an intense and energetic ion beam. In the case shown in the figure the argon ions have an energy of about 29 keV and the beam intensity is a few times

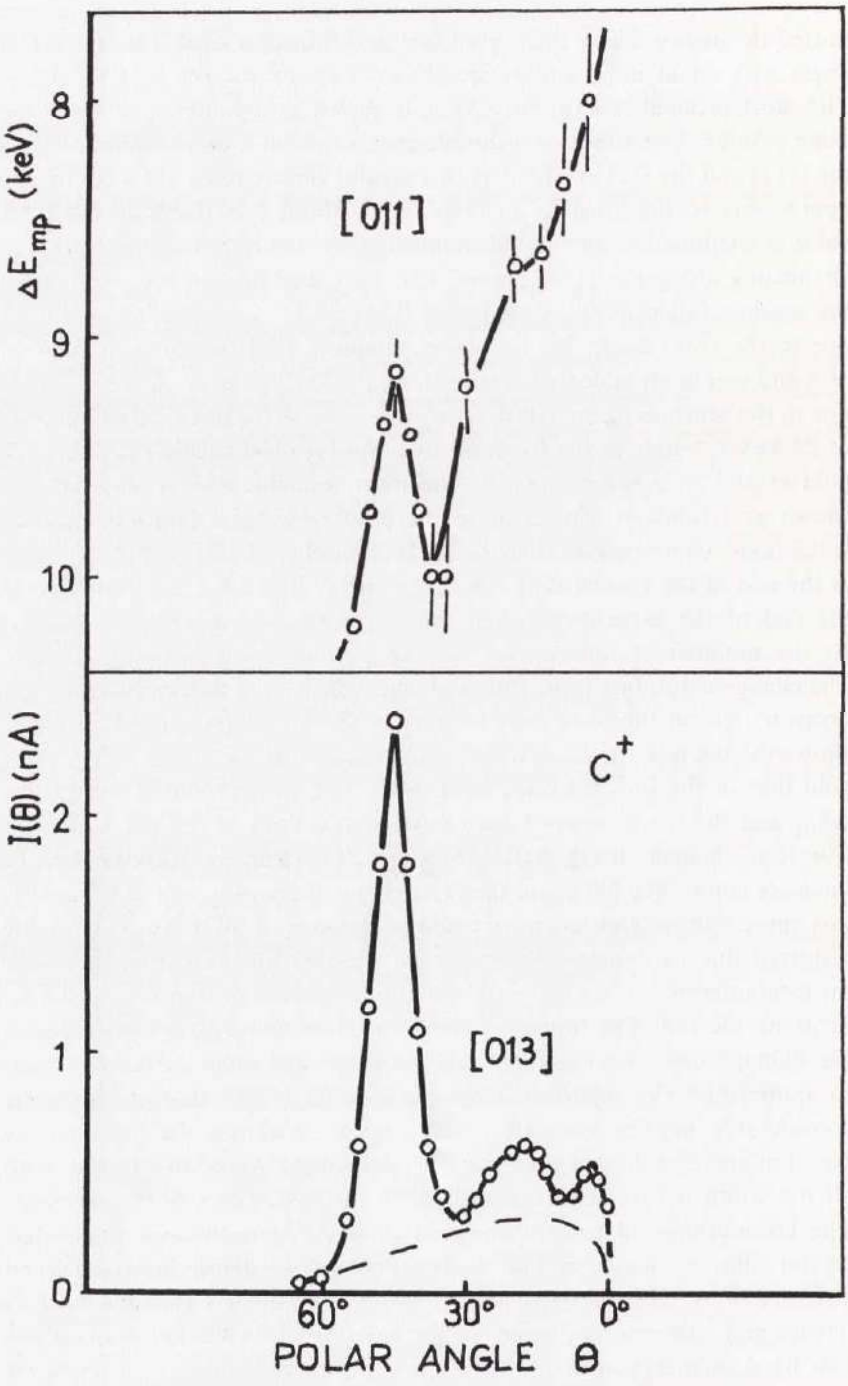

Fig. 7. The transmitted intensity of 25 keV C^+ ions through a 270 Å thick gold film is shown as a function of θ. The total bombarding time is 30 min.

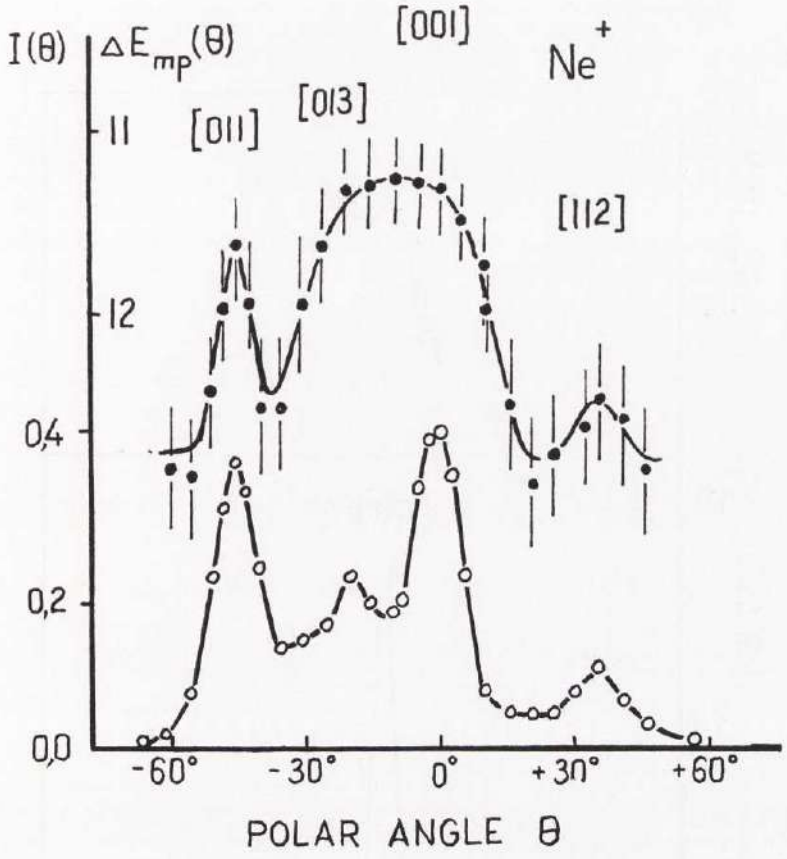

Fig. 8. The intensity of 32 keV Ne^+ ions transmitted through a 250 Å thick gold film is shown as a function of θ. Because of a speeded up measureing technique the total interval of θ could be measured in about 10 min. without breaking the foil.

10^{-8}A. The thickness of the foil is estimated to be about 100 Å. An electron diffraction pattern shows a good single crystal structure. Still, with a speeded up measuring technique the time available for detection of channeled argon ions is less than 10 minutes. The foil broke before the profile of the [001] channel was completed. In this case it is hard to determine wether the structural damage or the sputtering damage of the crystal is dominating. A guess based on the relatively narrow peak width would be that sputtering effects are appreciable.

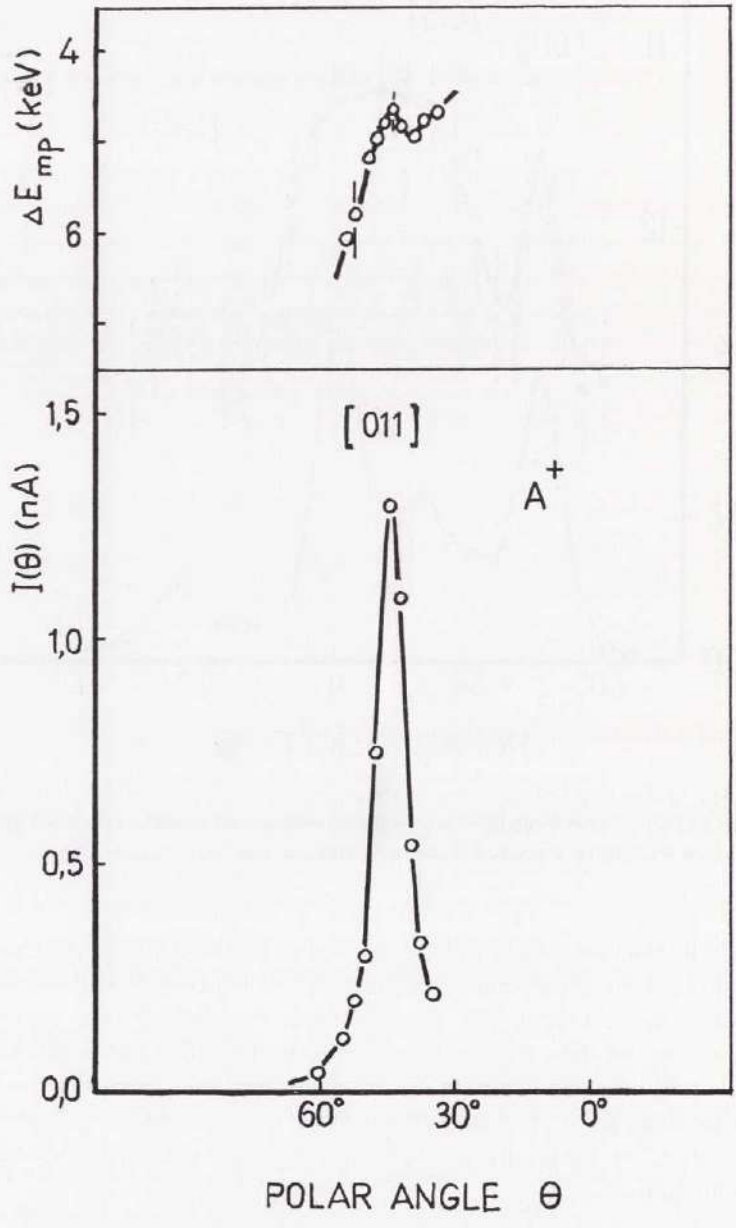

Fig. 9. The intensity of 29 keV A^+ ions transmitted through a very thin gold film, about 100 Å, is shown as a function of θ. The film is broken in less than 10 min.

Analysis of peak widths

If the detector system is rotated relative to the beam direction and the beam is incident parallel to an open channel (θ_0, φ_0) one is able to measure the relative probability $P_{2\alpha}$ for a channeled ion to be detected at an angle α from the channel axis. A similar probability $P_{1\theta}$ may be measured at the entrance side by rotating the foil and the detector system as one unit relative to the incident beam. If the foil is rotated alone relative to a fixed beam and a fixed detector system which is parallel to the beam, the combined relative probability P_θ is measured. It is obvious that $P_{2\alpha}$ also may be measured by rotating the foil and the beam as one unit keeping the detector fixed at $\alpha=0$. This probability may be noted $P_{2\theta}$. Thus we see that

$$P_{2\alpha}=P_{2\theta} \tag{3}$$

If the two probability distributions $P_{1\theta}$ and $P_{2\theta}$ are independent of each other one may write

$$P_\theta=P_{1\theta}\cdot P_{2\theta} \tag{4}$$

The experimental distribution are found to be approximately Gaussian. Fig. 10 shows $P_{2\theta}$ for a D^+ ion beam incident along a [001] channel. One observes that the deviation from a Gaussian curve is very small up to about 2σ. Above 2σ the transmitted intensity is somewhat higher than that predicted by a Gaussian distribution.

A good starting point for the analysis of the peak widths thus seems to be to use the Gaussian curve. We can now write

$$\left.\begin{aligned} P_{1\theta}&=P'\cdot\exp\{-(\theta-\theta_0)^2/2\sigma_{1\theta}^2\} && (5a)\\ P_{2\theta}&=P''\cdot\exp\{-(\theta-\theta_0)^2/2\sigma_{2\theta}^2\} && (5b)\\ P_\theta&=P\cdot\exp\{-(\theta-\theta_0)^2/2\sigma_\theta^2\} && (5c)\end{aligned}\right\}\ \varphi=\varphi_0$$

for $|\theta-\theta_0|$ of the order of a few degrees or less. (θ_0, φ_0) is the direction of the channel under consideration. For $\theta=\theta_0$ we demand by definition that

$$P=P'\cdot P'' \tag{6}$$

In (4)–(5) it is assumed that $\alpha=0$. A situation where $\alpha=\alpha_0$ is discussed to some extent in [1*b*].

For small $|\theta-\theta_0|$ one thus expects to find the following relation fullfilled

$$\sigma_\theta^{-2}=\sigma_{1\theta}^{-2}+\sigma_{2\theta}^{-2} \tag{7}$$

The three characteristic widths σ_θ, $\sigma_{1\theta}$ and $\sigma_{2\theta}$ may be measured separately. Table II gives the result from some measurements of these widths

Table II. The charateristic widths at the entrance and the exit sides of a single crystal foil and the combined widths are measured separately and compared with eq. (7).

E keV	$\sigma_{1\theta}$ deg	$\sigma_{2\theta}$ deg	σ_{θ} deg	$\sigma_{\theta\text{calc.}}$ deg	$\sigma_{1\theta}/\sigma_{2\theta}$
2	4.5	4.3	3.1	3.05	1.04
3	5.3	5.0	3.9	4.05	1.06
11	4.0	3.8	2.8	2.75	1.05
21	2.5	2.9	1.9	1.90	0.86
22	2.4	2.7	1.8	1.79	0.88
25	2.1	2.5	1.6	1.60	0.84

at different energies. From a plot of the ratio $\sigma_{1\theta}/\sigma_{2\theta}$, also shown in the table, as a function of the energy E, one finds that for $0<E<17$ keV

$$\sigma_{1\theta}/\sigma_{2\theta}=1.0\pm0.1 \tag{8}$$

For a Gaussian distribution it is easy to verify that a tangent through the point defining σ meets the abscissa at 2σ. Experimentally it is found that such a tangent meets the abscissa at an angle α_c, the experimental critical angle for channeling, which is found to obey the relationship

$$\alpha_c=(2.1\pm0.2)\sigma_{2\theta} \tag{9}$$

From (7), (8) and (9) one finds that

$$\alpha_c=2.1\sqrt{2}\sigma_{\theta} \tag{10}$$

An experimental determination of σ_θ gives α_c with an accuracy of the order of 10%. The influence of different sources of error on the experimental critical angles or the σ-values is discussed in [1*b*]. From the experimental results one concludes that $\sigma_{1\theta}$ is fairly independant of $\sigma_{2\theta}$ and that the ions thus loose the memory of their incident direction relative to the channel axis when leaving the crystal.

Lindhards theory about the critical angles for channeling

Lindhard has shown that there exists a theoretical criticle angle for channeling ψ_1 and ψ_2 for high and low energies respectively, above which no correlated scattering occurs. The theory is based on a string of atoms in free space with a distance between the atoms equal to d, the string constant. Positive ions with the energy E are allowed to interact with the string at small angles ($\psi<\psi_1$ or ψ_2) of the order of a few degrees. For

distances $R<a$, the screening length, the atomic potential from one single atom may be approximated by a Thomas-Fermi potential

$$V(R)=\frac{Z_1 Z_2 e^2}{R}\,\varphi_0\left(\frac{R}{a}\right) \tag{11}$$

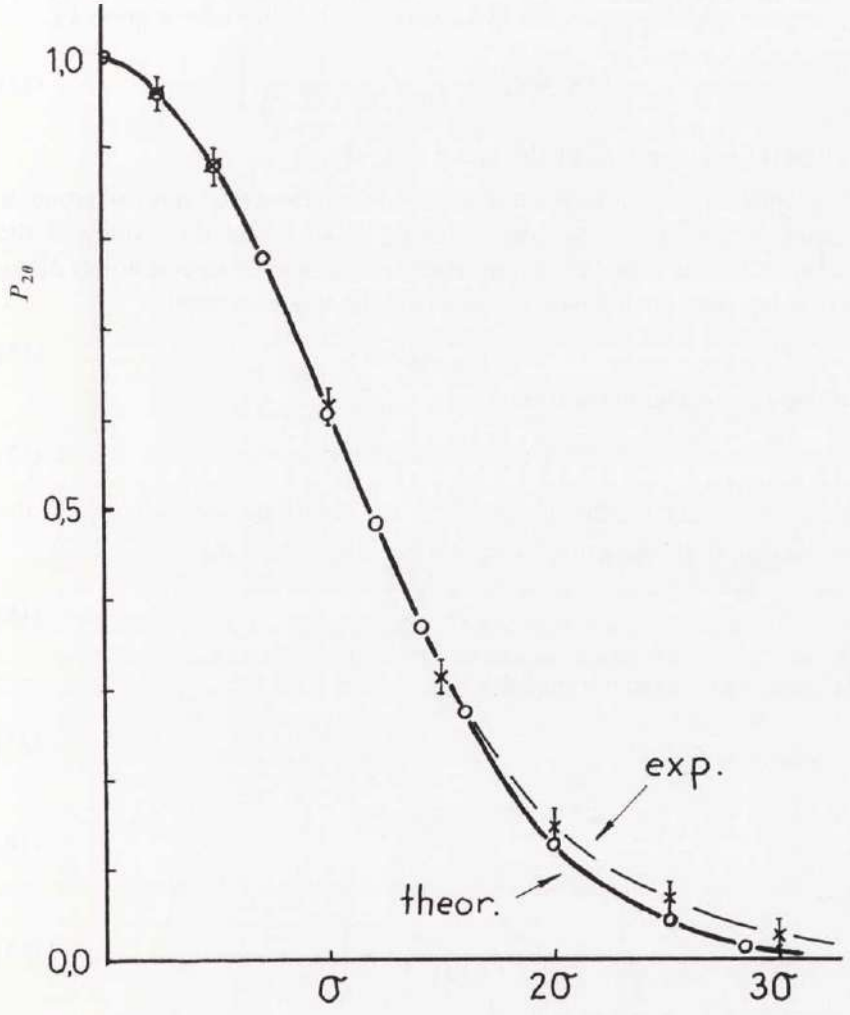

Fig. 10. The probability function $P_{2\theta}$ for a D^+ ion beam, emerging from a [001] channel, is measured as a function of the detector angle α (+). The solid line and the open circles (0) represent a normalized Gaussian distribution. The agreement is good below 2σ.

With this type of atomic potential, a transverse continuum string potential, $U(r)$, may be calculated from

$$U(r)=\int_{-\infty}^{+\infty}\frac{dz}{z}V(\sqrt{z^2+r^2}) \tag{12}$$

which should be a good approximation for incident angles below the critical angles for channeling.

A good approximation for $V(R)$ valid for all values of r is given by

$$V(R)=Z_1Z_2e^2\left(\frac{1}{R}-\frac{1}{(R^2+C^2a^2)^{\frac{1}{2}}}\right) \tag{13}$$

where C is a constant of the order of $1-2$.

A qualitative condition for using a continuum string approximation is found by demanding that the scattering of an ion in the vicinity of the point of closest approach to the string $r_{\min}$ is due to several atoms along the string. For small angles ψ, the condition may be written

$$r_{\min}>\psi\cdot d \tag{14}$$

where $r_{\min}$ is determined from

$$U(r_{\min})=\tfrac{1}{2}M_1v^2\sin^2\psi \tag{15}$$

From (12)–(15) Lindhard arrived at the following expressions for the critical angle at high energies ψ_1 and for low energies ψ_2:

$$\psi_1=\sqrt{\frac{E_1}{E}} \tag{16}$$

subject to the condition that

$$\psi_1\leq\frac{a}{d} \tag{17}$$

where

$$E_1=\frac{2Z_1Z_2e^2}{d} \tag{18}$$

and

$$\psi_2=\left(\frac{Ca}{d\sqrt{2}}\cdot\psi_1\right)^{\frac{1}{2}} \tag{19}$$

subject to the condition that

$$\psi_1>\frac{a}{d} \tag{20}$$

The energy E' separating the high and the low energy regions may be found from

$$E' = E_1 \cdot \left(\frac{d}{a}\right)^2 \tag{21}$$

From (21) it is found that E' is often several hundred times larger than E_1, which is of the order of 500 eV for D^+ ions in gold.

Comparison between experimental and theoretical critical angles

In a laboratory experiment some conditions may be drastically different from those in Lindhards theory, in that one string in a crystal lattice is not isolated from other strings. Further, the energy E is not well defined after the ions have passed through a certain thickness of material. For the most open directions in a f.c.c. lattice a comparison with Lindhards theory may be appropriate. For higher order channels the situation may be different for the following reason. Each channel is bordered by four strings of the same kind, i.e. with the same string constant d. The assymetry caused by the fact that two of the four strings may be shifted along the string direction relative to the other two strings, may result in an effectively smaller string constant d. The effect from nearest neighbour strings is believed to be without any significance. It was found by Nelson and Thompson (1963) [4] that for the [011] channel in gold the string potential has a value of only about 10 eV at a distance of one sixth from the string axis. This means that the channel indices [*hkl*] have to be very large until the nearest neighbour strings are expected to be of any influence. These very high index channels are too narrow to channel any ions at all at the energies discussed here. From the experimental results obtained in [III*a*] and [III*b*], it is concluded that the three or four most open channels in f.c.c. gold satisfy Lindhards conditions. Fig. 11 shows the agreement between theory and experiment for the channels [011], [001] and [112] in gold. The critical angles are shown as functions of the average energy $\bar{E}$ in the foil. For higher order channels the critical angles do not decrease according to Lindhards theory. This is not due to angular resolution limitations in the apparatus. σ-values down to about 1.3° have been obtained for very thin films. The systematic error is, however, increased to an estimated 20% at these low σ-values. For energies around 5 keV, channels of the type [014] should be possible to measure as far as the theoretical critical angle due to Lindhard is concerned.

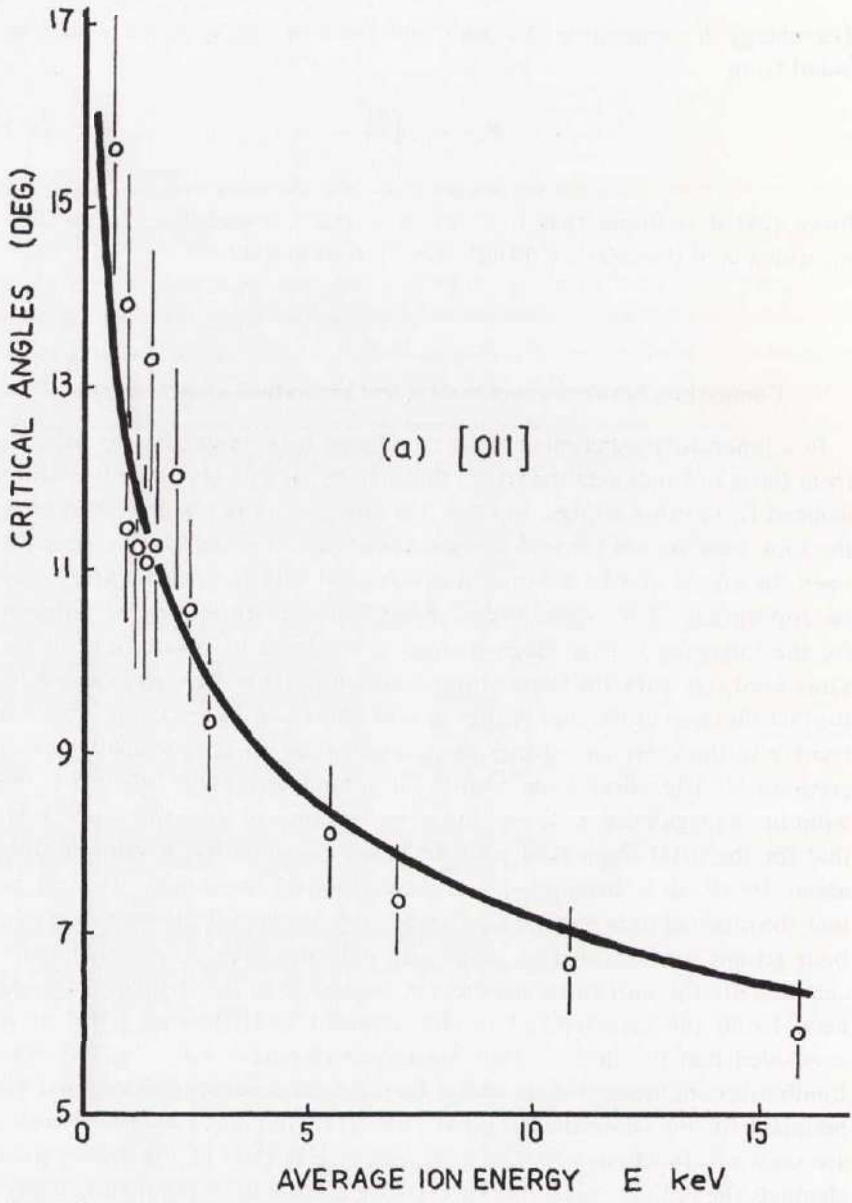

Fig. 11. The critical angle for channeling ψ_2 is shown as a function of the average energy E of the ions in the crystal for the three channels *a*. [011], *b*. [001] and *c*. [112]. The solid lines are the theoretical curves using the theory by Lindhard with a value of $C=2.15$. The filled circles represent the experimental critical angles α_c and the vertical bars show the errors $\Delta\alpha_c$. The errors in average energy vary from 0.3 keV at 1 keV to 0.5 keV at 17 keV. Most of the spread of the experimental points is due to the fact that the information in the figures is based on several films with thickness t in the interval $180 < t < 260$ Å.

The [014] channel is the 11th in Table I in [V] where a few low index channels are listed in order of importance, in the {100} plane. The experimental width becomes constant within the errors from channel [013] and up. This result is believed to be partly due to assymetries in the channel walls discussed above.

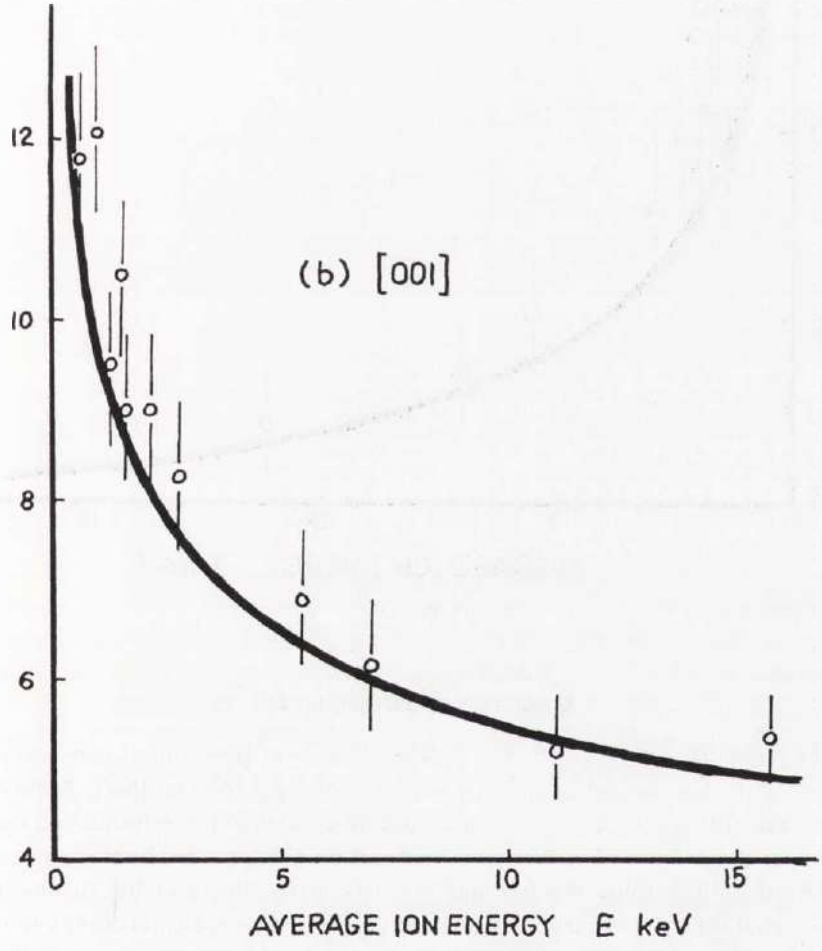

Fig. 11 *b*

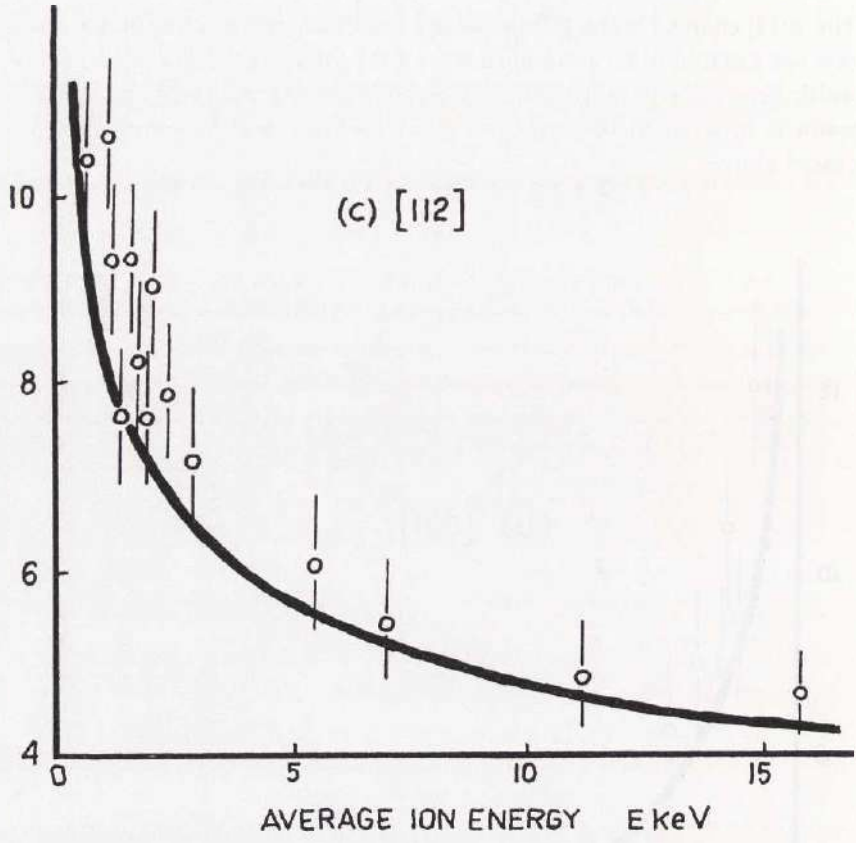

Fig. 11 *c*

A simple transparency model

In paper [I *a*] it is stated that peak intensities of transmitted ions correlated with the channel area $A_{[hkl]}$ per atom along a channel [*hkl*]. A more detailed study of the degree of correlation is given in [V]. It is found that the ratio of the channeled intensity in the direction [*hkl*] divided by the random intensity at the same θ-value and normalized to the ratio for the most open channel in that particular crystallographic plane which is common to the directions, correlates nicely with normalized $A_{[hkl]}$-values. This is found to be the case at least for the {110} plane. The good correlation between theory and experiment indicates that these normalized ratios represent an acceptable way of correcting for changes in effective foil thickness t as the polar angle θ is varied.

The transmitted intensity $I(E, t, \theta)$ along the $\{110\}$ plane may be divided into two parts

$$I_{\{110\}}(E, t, \theta) = D_{\{110\}}(E, t, \theta) + R(E, t, \theta) \tag{22}$$

where

$$D_{\{110\}}(E, t, \theta) \quad \text{and} \quad R(E, t, \theta)$$

represent the directional channeling and the random intensity along the plane $\{110\}$. The directional part may be expressed in the following way:

$$D_{\{110\}}(E, t, \theta) = D_{\{110\}}(E, t, \theta_{[h_1k_1l_1]}) \cdot \frac{R(E, t, \theta)}{R(E, t, \theta_{[h_1k_1l_1]})} \times$$
$$\times F_{\{110\}}(E, t) \sum_{\theta_{[hkl]}} \exp\{-(\theta - \theta_{[hkl]})^2 / 2\sigma^2_{\theta_{[hkl]}}\} \tag{23}$$

In (23) $[h_1k_1l_1]$ is the most open channel to which the other peaks are normalized, in this case the [001] channel. $\sigma_{\theta_{[hkl]}}$ is the characteristic width of the peak at $\theta_{[hkl]}$, where $\theta_{[hkl]}$ is determined from the relation:

$$\operatorname{tg} \theta_{[hkl]} = l^{-1} \cdot (h^2 + k^2)^{\frac{1}{2}} \tag{24}$$

The random intensity which has to be large enough to be experimentally detected may be approximated by

$$R(E, t, \theta) = R(E, t, 0) \cdot \cos(k'\theta) \tag{25}$$

where $k' = 1.385$ is a constant determined by the goniometer. Thus the ratio

$$\frac{R(E, t, \theta)}{R(E, t, 0)} \approx \cos(k'\theta) \tag{26}$$

The function $F_{\{hkl\}}(E, t)$ may be written as a polynomial in x, where

$$x = \frac{A_{[hkl]}}{A_{[h_1k_1l_1]}} \leqq 1 \tag{27}$$

$A_{[hkl]}$ is the geometrical area per atom seen along a direction $[hkl]$ if the lattice atoms are considered as mathematical points.

Thus one may write

$$F_{\{110\}}(E, t) = c^{(1)} + c^{(2)}x + c^{(3)}x^2 + \ldots \tag{28}$$

For D^+ ions with an energy E large enough for several peaks to appear in the plane $\{110\}$, it is found that the third term and higher terms may be disregarded. The parameters $c^{(n)}$ depend on the energy E, foil thickness t and the type of crystallographic plane and should be written

$$c^{(n)} = c^{(n)}_{\{hkl\}}(E, t) \tag{29}$$

For 20 keV D^+ ions channeled through a 300 Å thick gold crystala long the $\{110\}$ plane one finds that

$$F_{\{110\}}(20,300)=1.21x-0.21 \tag{30}$$

When F is a linear function it is easy to show that

$$c^{(2)}_{\{hkl\}}=1-c^{(1)}_{\{hkl\}} \tag{31}$$

and that

$$\begin{aligned} c^{(1)}_{\{hkl\}} &\leq 0 \\ c^{(2)}_{\{hkl\}} &\geq 1 \end{aligned} \tag{32}$$

It is obvious that in (30) the directional channeling is zero when $x_{co}=0.167$. The value of x_{co} is called the cut-off value for directional channeling for a particular energy E and foil thickness t along the plane $\{hkl\}$.

From what is said above it seems desirable to reach the degree of correlation when

$$c^{(n)}_{\{hkl\}}=0, \quad n\neq 2 \quad \text{and} \quad c^{(2)}_{\{hkl\}}=1 \tag{33}$$

For energies around 20 keV it seems unlikely that this could be achieved by choosing a plane with a smaller interplanar distance, like for instance the $\{130\}$ planes. On the contrary it is expected that the larger energy loss of the particles travelling along the $\{130\}$ plane will cause a deviation from the straight line and thus introduce additional terms in (30). For the more widely separated planes $\{100\}$ the lower energy loss may increase the degree of correlation. The degree of correlation may be expressed by the ratio r, where

$$r=R'_{\text{exp}}/R'_{\text{theor}} \quad \text{where} \quad 0\leq r\leq 1 \tag{34}$$

As shown in Fig. 3*a* the intensity transmitted along the $\{100\}$ plane is different from the one along the $\{110\}$ plane (Fig. 3*b*). To achieve a similar degree of correlation as in the latter plane it is found necessary to divide the total intensity along the $\{100\}$ plane into three parts

$$I_{\{100\}}(E, t, \theta)=D_{\{100\}}(E, t, \theta)+P_{\{100\}}(E, t, \theta)+R(E, t, \theta) \tag{35}$$

The directional part D and the random part R may be expressed in the same way as indicated above. The function $P_{\{100\}}(E, t, \theta)$ is found to behave very similar to the random part and may be expressed by

$$P_{\{100\}}(E, t, \theta)\approx P_{\{100\}}(E, t, 0)\cos(k'\theta) \tag{36}$$

One thus finds that

$$\frac{P_{\{100\}}(E, t, \theta)}{P_{\{100\}}(E, t, 0)} \approx \frac{R(E, t, \theta)}{R(E, t, 0)} \tag{37}$$

According to (37) it is possible to use either the random part R or the function P to correct for changes in effective foil thickness. It is found experimentally, however, that $R(E, t, \theta)$ generally represents a shorter range in the material than either of the two other functions whenever they appear in the transmitted intensity. Thus it may sometimes be necessary to use the function P, namely if the incident energy is too low for the random part to be detectable.

The function $P(E, t, \theta)$ depends upon the type of plane in such a way that the value of P at any angle θ is larger for lower indexed planes. Furthermore, P is independant of any low index directions in that particular plane. These facts indicate that the function P may be connected with the planar potential described by Lindhard. P is therefore called planar channeling.

For the $\{100\}$ plane one may now write

$$D_{\{100\}}(E, t, \theta) = D_{\{100\}}(E, t, 0) \cos(k'\theta) \times$$

$$\times \sum_{[hkl]} F_{\{100\}}(E, t) \exp\{-(\theta - \theta_{[hkl]})^2 / 2\sigma^2_{\theta_{[hkl]}}\} \tag{38}$$

$$P_{\{100\}}(E, t, \theta) \approx P_{\{100\}}(E, t, 0) \cos(k'\theta) \tag{39}$$

and

$$R(E, t, \theta) \approx R(E, t, 0) \cos(k'\theta) \tag{40}$$

For 17 keV D^+ ions transmitted through a 265 Å thick gold crystal along the $\{100\}$ plane, the function $F_{\{100\}}(E, t, \theta)$ may be written

$$F_{\{100\}}(17{,}265) = 1.13x - 0.13 \tag{41}$$

The cut-off value $x_{co} = 0.115$ is smaller than for the $\{110\}$ plane. However, in the plane $\{110\}$ the peaks are normalized relative to the channel [001] while in the $\{100\}$ plane the normalization is made relative to the channel [011]. Now

$$\frac{A_{[011]}}{A_{[001]}} = \sqrt{2} \tag{42}$$

and thus one finds for the cut-off areas A_{co} the ratio

$$\frac{A_{co}^{\{100\}}}{A_{co}^{\{110\}}} = \frac{x_{co}^{\{100\}}}{x_{co}^{\{110\}}} \cdot \frac{A_{[011]}}{A_{[001]}} \approx 1 \tag{43}$$

The cut-off areas A_{co} are therefore approximately the same along the two planes and equal to about 0.041 a_0^2, where a_0 is the lattice constant for gold. Taking into consideration the somewhat higher energy for the ions traveling along the {110} plane it is clear that the cut-off area A_{co} in the {100} plane is slightly smaller than along the {110} plane. A comparison between the {110} and the {100} planes at one constant energy thus reveals that the quantitative correlation is only slightly better in the {100} plane.

The intensity transmitted along the {111} plane, $I_{\{111\}}(E, t, \theta)$, has to be divided into three parts as well in order to achieve a good quantitative correlation with relative channel areas x. For a crystal grown in the [001] orientation, the {111} planes do not intersect the point $\theta=0°$ in a stereogram representing the lattice. Instead the {111} planes may be found in the interval $|\theta| \geq 35.2°$. It is found advantageous to trace the {111} planes in the interval $35.2° \leq \theta \leq 45°$ i.e. between the channels [112] and [011]. In this interval the function cos $(k'\theta)$, which takes care of changes in effective foil thickness, may be substituted by the linear function

$$L(\theta)=1{,}64(1.22-\theta) \tag{44}$$

For 16 keV D^+ ions transmitted through a 450 Å thick gold crystal along the {111} plane it is found that

$$F_{\{111\}}(16{,}450)=x \tag{45}$$

where x is related to the [011] channel. (45) indicates that the cut-off value of x is zero along the plane {111}. This is not the case. From experiments it is shown that one has to put a limit to x which is found to be approximately 0.115 for the 16 keV D^+ ions discussed above. If compared with the values for the other two planes it is found that for one constant energy the cut-off value for the {111} plane is slightly smaller than for both the other two planes. The difference between the three planes {111}, {100} and {110} as fas as the cut-off area is concerned is very small, however. To summerize the result of the above discussion one may therefore say that for energies around 18 keV, D^+ ions are not channeled through a single crystal foil in a direction [hkl] for which the channel area is smaller than 0.04 a_0^2.

For the {111} plane one may now write

$$D_{\{111\}}(E, t, \theta, \varphi)=D_{\{111\}}(E, t, \theta_0, \varphi_0)\times \\ \times\sum_{[hkl]}L(\theta)\cdot x\cdot\exp\{-(\theta-\theta_{[hkl]})^2/2(k''\sigma_{\theta_{[hkl]}})^2\} \tag{46}$$

for

$$0.614\leq\theta\leq 0.785 \quad \text{and} \quad x\geq 0.115$$

(θ_0, φ_0) is equivalent to the channel [011], and k'' is a parameter due to the goniometer design.

Because of the fact that when tracing the {111} plane, the azimuthal angle φ is not constant, the width of the peaks in the {111} plane is larger than normal and varies somewhat with θ. This is discussed in some detail in [1*b*]. The parameter k'' in (46) is experimentally found to be about 1.8 for the channel [112]. This value is fairly consistent with the value 1.74 obtained from the relation

$$\sigma_\varphi = \frac{\sigma_\theta}{\sin\theta} \tag{47}$$

given in [1*b*]. The value of the parameter k'' may also be checked for the [011] channel by comparing experimental and theoretical ratios. Thus, from Lindhards formula for the critical angle for channeling one would except a theoretical ratio

$$\sigma_{\theta_{[011]}}/\sigma_{\theta_{[112]}} = 1.5 \tag{48}$$

Experimentally one finds for D^+ ions of about 3 and 10 keV

$$\frac{\sigma_{\varphi_{[011]}}}{\sigma_{\varphi_{[112]}}} = 1.3 \pm 0.1 \tag{49}$$

From (47) and (49) one obtains

$$\frac{\sigma_{\theta_{[011]}}}{\sigma_{\theta_{[112]}}} = \frac{\sigma_{\varphi_{[011]}}}{\sigma_{\varphi_{[112]}}} \cdot \frac{\sin 45^\circ}{\sin 35.2^\circ} = 1.6 \pm 0.1 \tag{50}$$

which agrees satisfactorily with the theoretical value 1.5 above. From here one may use (47), (49) and (50) to arrive at the relationship between σ_φ and σ_θ for the [011] channel

$$\sigma_{\varphi_{[011]}} = 1.3 \cdot 1.7/1.6\sigma_{\theta_{[011]}} = 1.39\sigma_{\theta_{[011]}} \tag{51}$$

It is found that generally

$$k'' = \frac{1}{\sin\theta_{[hkl]}} \tag{52}$$

(52) yields the factor 1.414 relating the characteristic widths in (51).

To complete the description of the transmitted intensity along the {111} plane, it is noted that analogous to the situation along a {100} plane one may write for the function P

$$P_{\{111\}}(E, t, \theta, \varphi) \approx P_{\{111\}}(E, t, \theta_0, \varphi_0) 1.64(1.22 - \theta) \tag{53}$$

in the interval

$$0.614 \leq \theta \leq 0.785$$

A similar relationship exists for the random intensity.

A comparison between $P_{\{hkl\}}$-values at constant energy and effective foil thickness shows that

$$P_{\{111\}} > P_{\{100\}} > P_{\{110\}} \tag{54}$$

Blocking effects

Domeij *et al.* [5] have shown that the α-radiation from active Rn and Po atoms positioned at normal lattice sites in a tungsten lattice shows a marked dip along the direction of a low order channel. The effect is called blocking. It is known that a blocking effect may also show up when ions are transmitted through a lattice and detected at large angles from the incident beam. There are reasons to believe that both directional and planar blocking effects are possible [VI]. Erginsoy [6] has presented some aspects on the phenomenon. As he points out "the observed effects are consistent with the strong scattering that a particle would be expected to undergo whenever it penetrates deeply into an atomic row or a plane and becomes nearly parallell to it". He further suggests that in the presence of thermal vibrations of the lattice atoms this strong scattering is not due to single Rutherford deflections. The phenomenon is more likely to be the result of correlated multiple Coulomb scattering. The situation is similar to the channeling case in that the high anisotropy of the atomic distribution causes the correlated scattering. One difference between the two kinds of phenomena is that the blocked particles loose more energy than normal while the channeled particles loose less energy than normal. The latter kind of particles feel an electron density which is less than normal due to the fact that they do not come closer to an atomic row or a plane than a, the screening length. Instead they sample the low electron density closer to the center of the channel.

The blocked particles sample the atomic density $\overline{N}(r)$ near the center of a plane, $0 < r < a$. According to Erginsoy one may write

$$\overline{N}(r) = \frac{1}{A\sqrt{2\pi\bar{u}}} \exp\{-r^2/2\bar{u}^2\} \tag{55}$$

where r is the distance from the center of the plane, $1/A = \rho_{\{hkl\}}$ [V] is the atomic density in the plane and $\bar{u}$ is the mean amplitude of the thermal

vibrations perpendicular to the string. The average atomic density N_{av} is given by the expression

$$N_{av} = \int_{-s/2}^{+s/2} \bar{N}(r)\, dr = 1/As \tag{56}$$

where s is the interplanar distance $D_{(hkl)}$.

To a good approximation the ratio $\bar{N}(r)/N_{av}$ is equal to the ratio

$$[<\theta^2>_r / <\theta^2>_{av}]_{\Delta x}$$

which is the ratio of the mean square angles for the same small distance Δx traversed by the ions. One may thus write

$$[<\theta^2>_r / <\theta^2>_{av}]_{\Delta x} = \frac{s}{\sqrt{2\pi \bar{u}^2}} \exp\{-r^2/2\bar{u}^2\} \tag{57}$$

Two gold films with approximately the same thickness Δx are used to check (57). One is a single crystal and the other is a polycrystal foil with a random orientation. For the {100} plane it is found experimentally that

$$[<\theta^2>_r / <\theta^2>_{av}]_{\Delta x = 400\,\text{Å}} = 0.175$$

In the experiment it is not possible, however, to follow the exact path of the particle. It is possible and even probable that in the experiment a particle may change from a situation of proper cahnneling into a situation of true blocking or to random scattering during some time of the penetration through the film. The comparison given here between theory and experiment has therefore to be considered as a rough estimate.

For a {100} plane in f.c.c. gold one has approximately at room temperature

$$\begin{cases} s \approx 2\,\text{Å} \\ \bar{u} \approx 0.1\,\text{Å} \end{cases}$$

This gives

$$\bar{N}(r)/N_{av} = 8.1 \exp\{-r^2/0.02\} \tag{58}$$

from which one finds

$$\bar{r} = 0.1\,\text{Å} \quad \text{and} \quad (\bar{r}^2)^{\frac{1}{2}} = 0.13\,\text{Å}$$

The experimental value

$$r_{exp} = 0.28\,\text{Å}$$

is the estimated distance from the center of the plane where the particles experience the blocking in the presence of thermal vibrations. Fig. 12 shows the blocking and the channeling region for a {100} plane. For a static

lattice the distance from the plane where the channeling region starts is $r \gtrsim a$. Thus one would expect a theoretical distance r_{theor} somewhat larger than $\bar{r}$ or $(\overline{r^2})^{\frac{1}{2}}$

$$r_{theor} = f \cdot \bar{u} + a \tag{59}$$

where f is a constant or the order of $1-1.3$.

For D^+ ions in gold $a = 0.12$ Å and

$$r_{theor} \approx 0.22 - 0.25 \text{ Å}$$

which agrees roughly with the experimental value 0.28 Å

One concludes from this estimate that the atomic distribution given by Erginsoy predicts a region close to the crystallographic plane where the blocking effects occur and with outer limits of approximately the right magnitude.

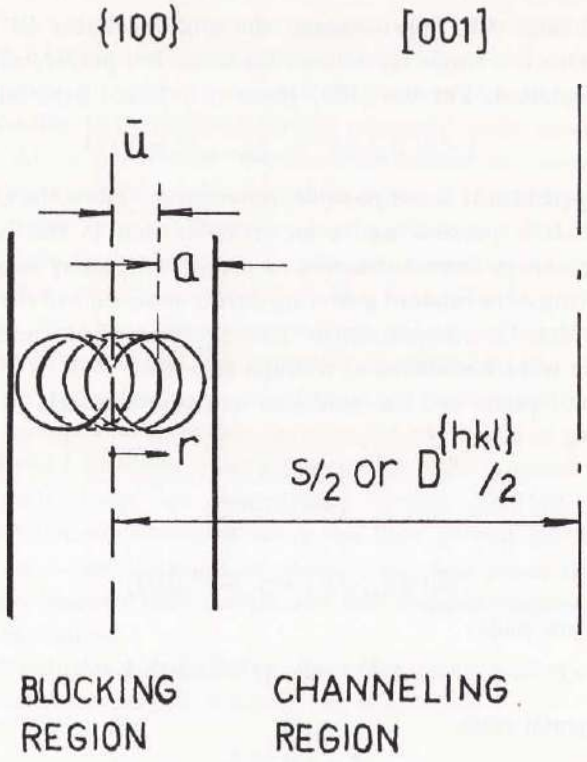

Fig. 12. The blocking region and the channeling region are shown schematically in the figure. The blocking region may be represented by $r \geq |\bar{u} + a|$. A thermally vibrating atom is represented by the circles. The mean amplitude is $\bar{u}$. a is the screening length and s is the interplanar distance.

Determination of structure and energy loss

As shown in [IV] the determination of the structure of a crystalline foil may be performed by the transmission of light ions of quite low energies. By simple means it is possible to use energies down to a few keV still using practical film thicknesses. In this situation the detection of the transmitted current may be performed by a Faraday cage and an electrometer with a sensitivity of $10^{-15}A$. For much lower ion energies and ion currents individual particle counting is necessary. This results in an appreciable reduction in the radiation damage which otherwise is disturbing. For quick checks of the structure of a foil an ion transmission equipment may be as useful as an electron microscope. For ion energies less than 20 keV it is possible to look through a crystal of much greater thickness than is possible with the microscope. Film thicknesses of several thousand angstroms may be checked by protons or deuterons of about 20–30 keV using the channeling effect. Individual particle counting will most probably extend the thickness region up to several microns for ion energies of the order of 100 keV.

The development of the channeling technique is competeing with ordinary electron microscopy in an increasing number of situations. As mentioned above the microscope is already surpassed as far as thick targets are concerned. Fagot and Fert have designed an ion-electron microscope in which the secondary emission of electrons from ion bombardment is used as the source in an ordinary electron microscope. A picture, of for example a single crystal taken by this microscope, reveals the areas misoriented relative to a reference plane in the crystal with excellent contrast. The microscope may also be used for studies similar to the ones summerized here through the detection of secondary electron intensities as functions of the crystal orientation relative to the in cident ion beam. Curves similar to transmission profiles are reported.

Energy loss measurements are performed for the main purpose of separating the direct beam transmitted through small pinholes, which accidentally may be present in the film, from the beam actually penetrating through material. For each combination of θ and φ the transmitted intensity has a maximum corresponding to a most probable energy loss ΔE_{mp}. The function $\Delta E_{mp}(\theta, \varphi)$ is obtained through a variation of the analyzer voltage U. Thus one obtains energy loss values and maximum intensities simultaneously.

The analyzer is not designed for high resolution energy loss experiments. The center line between the two analyzer plates is not on ground potential as is desirable. This fact affects the resolution noticably and for high energy

losses the linearity is spoiled. Still, some information may be gained from the measurements. It is found that along the {100} plane the energy loss is relatively smaller than along the {110} plane which in turn does not deviate from the energy loss of the random beam. Further, the energy loss along the [011] direction is smaller than the loss along the {100} plane at $\theta = 45°$. This is partly due to the {111} planes intersecting at $\theta = 45°$. A comparison between the energy loss at $\theta = 35°$ along the [112] channel (the intersection between a {110} plane and a {111} plane) and at $\theta = 45°$ along the [011] channel (the intersection between a {100} plane and a {111} plane) shows that an energy loss value characteristic of the [011] channel has to be considered. By similar arguments, further discussed in [1*b*] it is found that the expected order of importance amongst the directions and amongst the planes is obtained. No contradictions exist between the results from energy loss studies and from studies of relative transmitted intensities. It is believed that energy loss studies using a high resolution analyzer will add usable important information to the existing knowledge of low energy particle channeling. This will be one of the future experimental tasks.

Summary

The investigations have shown that the characteristic features of a channeled ion beam, the peak widths and the peak intensities, may be explained phenomenologically in rather simple terms and may also be mathematically formulated to make a more stringent analysis possible. It has been shown that planar channeling occurs along some planes. It is not known, however, where this planar intensity originates. There are reasons to believe that a cumulative effect is responsible for the planar intensity. The ion beam directed along a low index channel is believed to loose intensity to the planar beam and to the random beam all the way through the film. This may be caused by the high defect density in evaporated films.

The total picture of the channeling effect as obtained from recent publications, including this work, is fairly complete. The blocking effect is not so completely understood at the present time. The works by Lindhard and by Domeij *et al.* have added valuable information to our knowledge. The blocking effect in transmission studies, as it shows up in this work, is most probably a mixed effect between channeling and extreme blocking, as it is observed by Domeij. This situation can not be subjected to analytical calculations at the present time. As Erginsoy points out, this may possibly be achieved by machine calculations based upon reasonable approximations. Before then, however, the effect has to be more thoroughly investigated

through experiments. A new accelerator for the acceleration of light ions is under construction. The maximum particle energy will be about 50–75 keV. The vacuum in the vicinity of the crystal will hopefully reach the low 10^{-7} mmHg region by help of a coldfinger which completely surrounds the target and which is cooled down to liquid nitrogen temperatures.

Acknowledgement

The experimental information on which this work is based was obtained during my stay at Northwestern University, Evanston, Ill. U.S.A. in the years 1964–1966. The work was financially supported by the Atomic Energy Commission of the United States.

To all my collegues at the Physics Department and in particular to prof. R. L. Hines I would like to express my sincere thanks for un unforgetable visit to the United States and for a fine collaboration under excellent working conditions at the Technological Institute.

Special thanks go to Dr. O. Almén, Chalmers University of Technology, who arranged my visit to Northwestern.

It is also a great pleasure to acknowledge valuable criticism of part of this work from prof. J. Lindhard and many of his collaborators at Aarhus, Denmark. I would also like to thank prof. W. M. Gibson Rutgers University, for all the interest he has shown in my work and for stimulating discussions.

I am grateful to many people at the Physics Department, Chalmers University of Technology for assistance in connection with the publication of this work. My thanks go to the secretaries Mrs. E. Lidö and Miss E. Johansson for typing the manuscripts and to Mr M. Soondra and Mr. G. Tidefors for their help with the figures.

Finally I am indepted to prof. N. Ryde for his encouragement and never failing interest in my work.

References

[1] D. S. Gemmell and R. E. Holland.
Phys. Rev. Letters *14*, (1965) 945.

[2] R. L. Hines and R. Arndt.
Phys. Rev. *119*, (1960) 623.

[3] J. Lindhard.
Fys. Medd. Dan. Vid. Selsk. *34*, No 14 (1965).

[4] R. S. Nelson and M. W. Thompson.
Phil. Mag. *8*, (1963) 1677.

[5] B. Domeij
Arkiv för Fysik *32*, (1966) 179.

[6] C. Erginsoy.
Phys. Rev. Letters *15*, (1965) 360.

[7] B. Fagot and C. Fert.
J. de Microscopie *4*, (1965) 21.
J. de Microscopie *5*, (1966) 389.
J. de Microscopie *5*, (1966) 409.

Additional references may be found in the papers I–VI.

GÖTEBORG
ELANDERS BOKTRYCKERI AKTIEBOLAG
1967

CHANNELING OF 13 keV D^+ IONS IN GOLD CRYSTALS *

C. J. ANDREEN **, R. L. HINES, W. MORRIS and D. WEBER
Northwestern University, Evanston, Illinois

Received 1 September 1965

The effect of symmetry in a crystal lattice on the scattering of ions has recently been reported to be of more importance than was expected. Many authors give experimental proof for the existance of correlated small angle scattering mostly in experiments dealing with sputtering [1-4] and range determinations [7-9]. A transparency model used in the theory of sputtering is moderately successful in accounting for the angular dependence of sputtering. Transmitted distributions through single crystals do also show angular dependence [2, 5, 10]. This is referred to as the channeling effect. It is the purpose of this letter to report some experimental results on channel-

* Research supported by U.S. Atomic Energy Commission.

** On leave of absence from Dept. of Physics, Chalmers University of Technology, Gothenburg, Sweden.

ing at low energies in single crystal gold films using 13 keV D^+ ions and compare the results with the predictions of the transparency model.

The films are grown by vacuum deposition onto a substrate of rocksalt. They are removed by dissolving the rocksalt in water and are then mounted on 75 mesh Cu electron microscope grids 3 mm in diameter. Electron microscope diffraction patterns show that the films are single crystals with a (001) orientation. The electron microscope pictures also show that the films are not exactly uniform in thickness but contain a small fraction of areas which are probably quite thin.

The incident mass separated ion beam has an angular spread of about 0.2°. Transmitted ions travel through a 90 degree electrostatic energy analyzer and are then detected in a Faraday cup. The energy analyzer stops the ions transmitted through holes or thin areas in the foils. The angle subtended by the entrance aperture to the analyzer is about 5°. Channeled H^+ and He^+ ions have been observed but for the present experimental set up D^+ ions give the best results. An aperture is used to confine the bombardment to a central area 1.5 mm in diameter on the grid supporting the film. The grid can be rotated in a goniometer around two perpendicular axis. Thus it is possible to vary the polar angle θ between the film normal and the incident beam axis from -60° to +60°. The azimuthal angle φ of rotation about the film normal can be varied from 0° to 360°. Without the gold film on the Cu grid the detected intensity varies by less than 10% within $-55^\circ \leq \theta \leq +55^\circ$ and decreases rapidly to zero outside this angle interval.

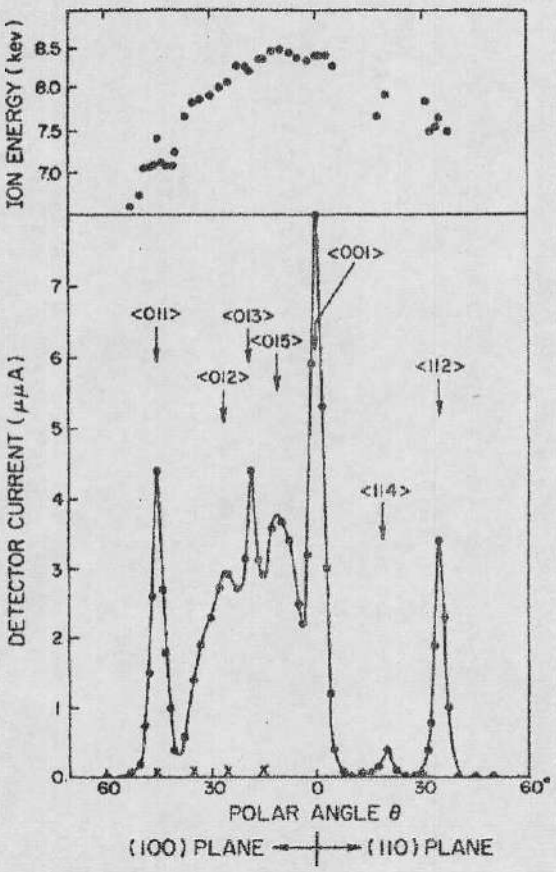

Fig. 1. Transmitted ion currents and energies of D^+ ions incident on a (001) gold crystal in the (100) and (110) planes. Arrows point at the angles for the indicated low index directions. Crosses indicate the transmitted intensities for high index directions. The incident ion energy is 13 keV and incident current intensity is 5×10^{-9} A. The thickness of the foil is about 700 Å.

It seems reasonable to assume that the transparency in terms of the area A_{hkl} per atom can be used to explain the variation in intensity for different channels. This is defined by the relation $A_{hkl} = \text{const} \times \rho_{hkl}^{-1}$, where ρ_{hkl} is the number of atomic rows per unit area used by others [6]. The transmission is expected to be high for crystallographic directions with a high transparency and low for crystallographic directions with a low transparency. It is easily verified that A_{hkl} for a direction for which $h+k+l$ is even, is larger than the neighbouring directions for which $h+k+l$ is odd for the gold lattice.

Fig. 1 shows typical distributions of the transmitted ion intensity in (100) and (110) planes and the energies of the transmitted ions. The voltage across the analyzer plates is always set to give maximum intensity for every combination of θ and φ. The accuracy in determining the transmitted ion energy which gives maximum intensity is about ± 0.13 keV for largest intensity and ± 0.43 keV for the small intensities. The intensity in ⟨001⟩ in fig. 1 dropped 8% in the 200 sec needed to make the measurements. This drop in intensity with time is believed to be the combined effort of radiation damage and hydrocarbon build up. The foil is about 700 Å thick. When φ is set at such values as to give high index directions the transmitted intensity drops below the detection limit of the electrometer with the detector geometry described above. This means that no randomly scattered beam is found with this detector geometry, neither in the angular nor in the energy distribution. It is thus not yet possible to say anything about the channeling energy

loss to distant electronic resonant momentum transfer relative to close electronic collisions for the randomly scattered beam [11].

It can be seen in fig. 1 that relatively pronounced peaks appear for crystallographic directions for which $h+k+l$ is even, except in only two cases where the A_{hkl}-value is large enough even when $h+k+l$ is odd. These two cases are ⟨012⟩ and ⟨001⟩. Directions for which $h+k+l$ is odd generally do not give pronounced peaks. The distributions in fig. 1 show a correlation between peak intensities and directional indexes. No correction is made for the fact that the effective foil thickness is 40% greater for $\theta = 45^{\circ}$ than it is for $\theta = 0^{\circ}$. Measurements made on about 50 foils without the energy-analyzer have so far given well established channeling peaks in the following directions: ⟨011⟩, ⟨001⟩, ⟨112⟩, ⟨111⟩, ⟨013⟩, ⟨015⟩, ⟨012⟩, ⟨114⟩ and ⟨116⟩. The transmitted intensity in (111) planes is found to be relatively high compared to (100) and (110). In (111) planes we have seen peaks in the ⟨123⟩, ⟨134⟩ and ⟨145⟩ directions.

References

1. J.M.Fluit, P.K.Rol and J.Kistemaker, J.Appl. Phys.34 (1963) 690.
2. R.S.Nelson and M.W.Thompson, Physics Letters 2 (1962) 124; Phil.Mag.8 (1963) 1677.
3. A.L.Southern, W.R.Willis and M.T.Robinson, J. Appl.Phys.34 (1963) 153.
4. O.Almén and G.Bruce, Nucl.Instr. and Meth.11 (1961) 257.
5. C.Erginsoy, H.E.Wegner and W.M.Gibson, Phys. Rev.Letters 13 (1964) 530.
6. M.T.Robinson and O.Oen, Phys.Rev.132 (1963) 2385; Appl.Phys.Letters 2 (1963) 30.
7. H.Lutz and R.Sizman, Physics Letters 5 (1963) 113.
8. B.Domeij, F Brown, J.A.Davies, G.R.Piercy and E.V.Kornelson, Phys.Rev.Letters 12 (1964) 363.
9. J.A.Davies and G.A.Sims, Can.J.Chem.39 (1961) 601.
10. E.Bøgh, J.A.Davies and K.O.Nielsen, Physics Letters 12 (1964) 129.
11. A.R.Satchler and G.Dearnaley, Phys.Rev.Letters 15 (1965) 59.

* * * * *

PHYSICAL REVIEW VOLUME 151, NUMBER 1 4 NOVEMBER 1966

Channeling of D^+ and He^+ Ions in Gold Crystals*

C. J. ANDREEN† AND R. L. HINES
Northwestern University, Evanston, Illinois
(Received 3 June 1966)

The transmitted intensity of D^+ and He^+ ions through gold crystals in the forward direction is measured as a function of crystal orientation for energies near 15 keV. The gold crystals have a (100) orientation and are mounted in a goniometer which can tilt the foil normal up to 60° away from the incident beam direction and which can rotate the foil about its normal. The detector can be tilted relative to the beam direction up to a maximum angle of 58°. Pronounced peaks are found in the transmitted intensity at low-index directions. Both directional and planar channeling are present. The peak widths are successfully interpreted in terms of a channel-entrance peak width and a channel-exit peak width. Energy analysis shows that the energy of the transmitted ions also has peaks in the low-index directions. The experimental values for the energy loss of the randomly scattered part of the ion beam agree with the theoretical predictions.

INTRODUCTION

IN two recent papers we show that channeled intensities of low-energy D^+ ions in single-crystal face-centered cubic (fcc) gold[1] and body-centered cubic (bcc) α-ion films[2] are closely related to the crystal structure. For both lattice types we find enhanced transmission in directions corresponding to the five channels calculated by Robinson and Oen[3] to be the most open ones. Planar channels are also confirmed. In both structures they originated from the two widest separated types of planes.

In order to explain long "tails" observed in measured range distributions by Davies *et al.*,[4] Robinson and Oen, in their computer studies, let a computer trace the history of ions traveling in an ordered structure. Different types of interatomic potentials were used. In preliminary studies it was found that 1% of 10-keV Cu atoms, slowing down in Cu according to the Bohr potential, made very long flights, predominantly in the ⟨001⟩ direction. At the present time structural effects due to channeling have been observed in range measurements,[6] ion reflection and transmission measurements,[6] sputtering yields,[7–10] secondary electron yields,[11] conversion-electron measurements,[12] and in nuclear reaction rates.[13–15] Theoretical works on channeling have recently been published by Lindhard,[16] Erginsoy,[17] and Lehmann and Leibfried.[18] The ions are separated in two main groups according to the type of motion they experience during the passage of the film. Ions which are scattered in a random way experience *ungoverned* motion while channeled ions experience *governed* motion.[16] Governed motion is further divided into directional and planar channeling.

The purpose of this investigation is to study channeling of light ions in evaporated gold films at energies lower than previously reported. It will be shown that both directional and planar channels are present. The most striking evidence for channeling is that the transmitted intensity in the forward direction shows pronounced peaks at low-index directions when measured as a function of foil orientation. The angular widths of these peaks are investigated and compared to the geometrical relations between the experimental apparatus and the crystal channels.

A secondary effect of channeling is the anisotropy in the energy loss experienced by the penetrating ions.[19–23] Energy is lost by electron excitation and through displacement of atoms. We call these losses electronic and nuclear energy losses, respectively. The energy loss of the ions experiencing ungoverned motion is compared with calculated values of the stopping power dE/dx according to Nielsen[24] and Lindhard and Scharff.[25] The reduction in the energy loss of the

* Supported by the U. S. Atomic Energy Commission.
† Present address: Chalmers University of Technology, Gothenburg, Sweden.
[1] C. J. Andreen, R. L. Hines, W. Morris, and D. E. Weber, Phys. Letters 19, 116 (1965).
[2] C. J. Andreen, E. F. Wassermann, and R. L. Hines, Phys. Rev. Letters 16, 782 (1966).
[3] M. T. Robinson and O. S. Oen, Phys. Rev. 132, 2385 (1963).
[4] J. A. Davies, J. D. McIntyre, and G. A. Sims, Can. J. Chem. 40, 1605 (1962).
[5] B. Domeij, F. Brown, J. A. Davies, and E. V. Kornelsen, Phys. Rev. Letters 12, 363 (1964).
[6] R. S. Nelson and M. W. Thompson, Phil. Mag. 8, 1677 (1963).
[7] A. L. Southern, W. R. Willis, and M. T. Robinson, J. Appl. Phys. 34, 153 (1962).
[8] O. Almén and G. Bruce, Nucl. Instr. Methods 11, 257 (1961).
[9] A. F. Tulinov, V. S. Kulikauskas, and M. M. Malov, Phys. Letters 18, 304 (1965).
[10] J. M. Fluit, P. K. Rol, and J. Kistemaker, J. Appl. Phys. 34, 690 (1963).
[11] H. Zscheile, Phys. Status Solidi 11, 159 (1965).
[12] G. Astner, I. Bergström, B. Domeij, L. Eriksson, and A. Persson, Phys. Letters 14, 308 (1965).
[13] E. Bøgh, J. A. Davies, and K. O. Nielsen, Phys. Letters 12, 129 (1964).
[14] M. W. Thompson, Phys. Rev. Letters 13, 756 (1964).
[15] B. Domeij and K. Björkqvist, Phys. Letters 14, 127 (1965).
[16] J. Lindhard, Kgl. Danske Videnskab. Selskab., Mat. Fys. Medd. 34, No. 14 (1965).
[17] C. Erginsoy, Phys. Rev. Letters 15, 360 (1965).
[18] C. Lehmann and G. Leibfried, J. Appl. Phys. 34, 2821 (1963).
[19] C. Erginsoy, H. E. Wegner, and W. M. Gibson, Phys. Rev. Letters 13, 530 (1964).
[20] A. R. Sattler and G. Dearnaley, Phys. Rev. Letters 15, 59 (1965).
[21] W. M. Gibson, C. Erginsoy, H. E. Wegner, and B. R. Appleton, Phys. Rev. Letters 15, 357 (1965).
[22] S. Datz, T. S. Noggle, and C. D. Moak, Phys. Rev. Letters 15, 254 (1965).
[23] B. R. Appleton, C. Erginsoy, H. E. Wegner, and W. M. Gibson, Phys. Letters 19, 185 (1965).
[24] *Electromagnetically Enriched Isotopes and Mass Spectroscopy*, edited by M. L. Smith (Academic Press Inc., New York, 1956), p. 68.
[25] J. Lindhard and M. Scharff, Phys. Rev. 124, 128 (1961).

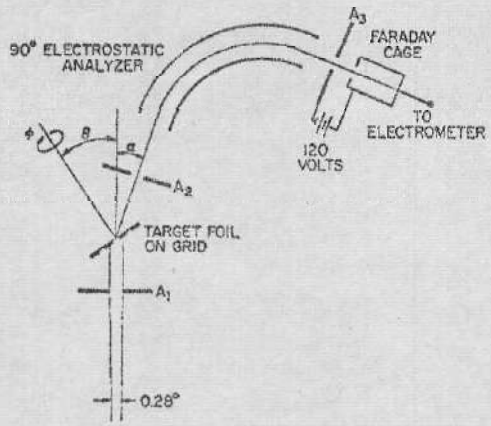

FIG. 1. Experimental arrangement for measuring the transmitted intensities of ions through a crystal as a function of the tilt angle θ and the rotation angle φ. The diameters of the apertures are $A_1=0.75$ mm, $A_2=0.75$ mm, and $A_3=3$ mm. The distance between the foil and aperture A_1 is 50 mm and the distance between the foil and aperture A_2 is 32 mm. The ranges of possible angles are $-60°\leq\theta\leq+60°$, $0°\leq\varphi\leq360°$, and $-3°\leq\alpha\leq+58°$. The distance between the analyzer plates is about 20 mm. The direction of the ion beam is fixed.

channeled ions is interpreted in terms of directional and planar channeling.

EXPERIMENTAL METHOD

Apparatus

The bombardment apparatus has been described earlier.[26] The goniometer, the energy analyzer, and the detector geometries used in this investigation are shown in Fig. 1. Details about the goniometer can be found elsewhere.[1] The angle subtended by the analyzer-detector system is here decreased to 1.4°. In addition the detector alone, or the analyzer-detector system as shown in Fig. 1, can be rotated an angle α about the same axis as the θ rotation. α can be varied from $-3°$ to $+58°$ relative to the beam direction. The beam is confined to a central area on the foil of about 1 mm in diameter. All measurements are done with the foil at room temperature. A copper cylinder in the vicinity of the crystal can be cooled down to liquid-nitrogen temperatures to reduce contamination of the gold target.

Foil Preparation

The gold single crystals are grown in a conventional vacuum system at 10^{-5} Torr by evaporating gold onto hot rocksalt substrates which are cleaved in air just prior to their insertion in the vacuum system. In order to grow continuous films of thicknesses down to 200 Å it is necessary to evaporate an intermediate single-crystal silver film. During the growth of the silver crystal, about 1000 Å thick, the substrate is held at about 150°C. Gold is then evaporated onto the silver at a temperature of about 200°C. The evaporation rates are about 1–5 Å/sec. The gold-silver film is floated on water and the silver is then disolved in 30% HNO_3. The gold crystal is carefully rinsed and picked up on a 75 mesh Cu grid 3 mm in diameter. After the foil has dried on the grid the surface is shiny and without any visible wrinkles. The film is then checked in an electron microscope. No holes are present in the films which have been used for measurements without the energy analyzer and all films had perfect single-crystal diffraction patterns. The epitaxial relations are $\{100\}_{NaCl}\|\{100\}_{Ag}$ and $\{100\}_{Ag}\|\{100\}_{Au}$. The crystals are self supporting down to an estimated thickness of 50Å. Further details about the growth of single-crystal silver and gold films can be found elsewhere.[27] The thickness of the gold crystals has been measured from the optical transmission. The transmission coefficient of a monochromatic light beam is known as a function of the thickness.[28] In addition, the stacking faults, extending diagonally through the foils, have been used to determine the thickness. Results obtained by the two methods do not differ by more than 5–10%.

Measuring Procedure

The azimuthal angle φ in Fig. 1 is an arbitrary angle which has to be related to a known low-index crystallographic direction. The $\langle011\rangle$ channels have been used for this purpose. They are the most open channels in a fcc lattice and are found by rotating φ, keeping θ constant at 45°. The presence of four strong peaks at $\theta=45°$ indicates that the film is a single crystal. When the orientation of the crystal relative to the goniometer is known, the intensity as a function of θ can be measured for different planes. The two planes (100) and (110) have been chosen here. The most important plane {111} can be found for $|\theta|\geq35°$ and the transmitted intensity is then maximized by changing both φ and θ.

When the energy analyzer is put in between the goniometer and the detector, the most probable energy loss ΔE_{mp} is obtained as a function of θ by maximizing the transmitted intensity i for a set of values of θ in a particular plane. This is done by varying the voltage on the analyzer plates. For some of the θ values the intensity is also measured for values of φ corresponding to high-index planes. This intensity does not show any sharp peaks as a function of θ. The energy E of the incident beam is kept constant while ΔE_{mp} and i are obtained as functions of θ and φ. If the analyzer is not used, the detector is attached directly to the goniometer and integrates over all energies in a specific direction.

RESULTS

Transmitted Intensity and Energy Loss

The transmitted intensity i and the most probable energy loss ΔE_{mp} for 25-keV He^+ ions in a 275 Å-thick

[26] R. L. Hines and R. Arndt, Phys. Rev. 119, 623 (1960).

[27] D. W. Pashley, Phil. Mag. 4, 324 (1959).

[28] P. Rouard, D. Malé, and J. Trompette, J. Phys. Radium 14, 587 (1953).

gold film are shown in Fig. 2 as functions of θ in the planes (100) and (110) for $\alpha=0°$. The smooth symmetric curves (solid lines) show the randomly scattered part and the corresponding energy loss in high-index crystallographic planes. These curves reflect the behavior of a randomly oriented polycrystalline gold film as confirmed by measurements. Figure 3 shows the same functions $i(\theta)$ and $\Delta E_{mp}(\theta)$ for 23 keV D^+ ions in a 550-Å-thick gold crystal. In both Figs. 2 and 3 the governed motion in the (100) plane is divided into two parts, indicated by dashed lines. These two parts represent directional and planar channeling. As far as the intensity functions are concerned the separation is made in the way described below.

The minima in the total intensity close to $\theta=-40°$ correspond to a very high index direction. No directional channeling is expected at this point. The intensity therefore originates from planar channeling. The same arguments also hold for the minima at about $\theta=-5°$, although the channel peaks might not be completely resolved at this point. The dashed lines are drawn close to these minima in a way that closely resembles the profile of the random part. Peaks corresponding to the

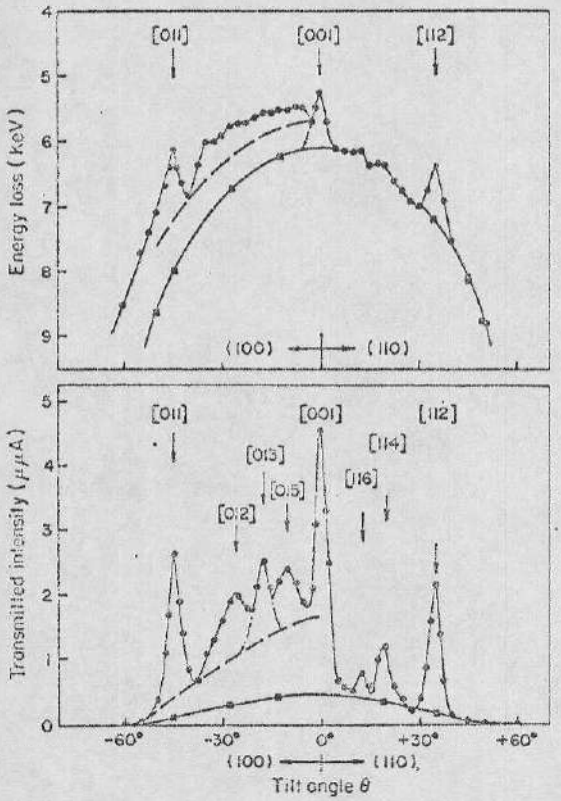

FIG. 2. Energy loss and transmitted intensity distributions for 25-keV He^+ ions transmitted through a 275-Å-thick single-crystal gold film. Arrows point at the angles for the indicated low-index directions in the two planes (100) and (110). Solid lines running through squares represent random quantities. Dashed lines represent dividing lines between directional and planar contributions. The dot dashed line indicates the line shape of channel [013]. Incident ion current is 1.9×10^{-9} A.

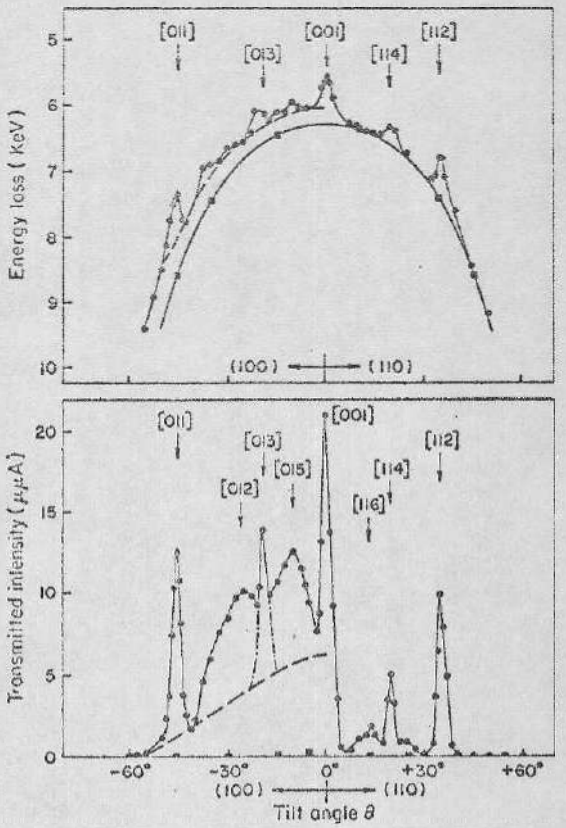

FIG. 3. Energy loss and transmitted intensity distributions for 23-keV D^+ ions transmitted through a 550-Å-thick single-crystal gold film. Arrows point at the angles for the indicated low-index directions in the two planes (100) and (110). Solid lines running through squares represent random quantities. Dashed lines represent dividing lines between directional and planar contributions. The dot-dashed line indicates the line shape of the channel [013]. Incident ion current is 1.1×10^{-9} A.

[012], [013], and [015] directions with a half-width at half-maximum of 2.5° (the same as for the other nicely resolved peaks) can now be superimposed on top of the planar part. The sum coincides nicely with the measured intensity.

The ratios of directional to planar channeling are expected to be much less dependent on the effective foil thickness than are the intensities themselves. If these ratios are compared within the (100) plane, the following expected order of importance amongst the peaks is obtained: ⟨011⟩, ⟨001⟩, ⟨013⟩, ⟨012⟩, and ⟨015⟩. This is found for both D^+ and He^+ ions. No planar channeling is found in the (110) plane. Despite the fact that a "cutoff" in planar channeling exists between {100} and {110} planes, peaks are present in the (110) plane corresponding to the [114] and [116] channels. The presence of the peaks [012], [013], [114], and [116] proves that the peaks can not be accounted for only by adding up planar contributions.

Figure 4 shows the transmitted intensity and the energy loss as functions of φ for $\theta=45°$ for 25-keV He^+ ions in the same foil as in Fig. 2. The curves are obtained

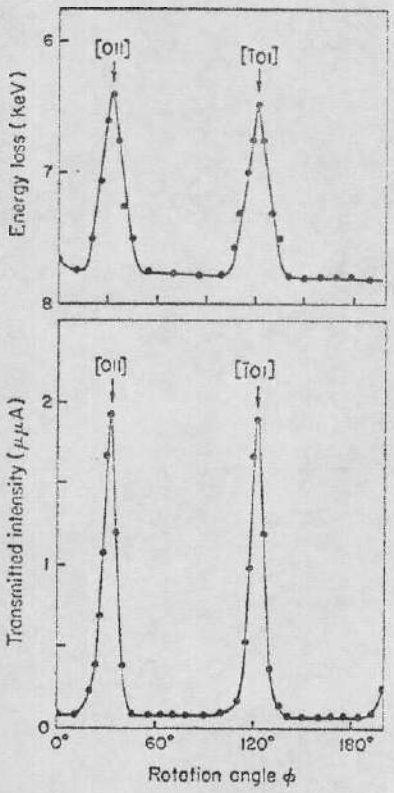

FIG. 4. Energy loss and transmitted intensity distributions for 25-keV He^+ ions transmitted through a 275 Å-thick single-crystal gold film tilted at an angle $\theta=45°$. Arrows point at the φ values for the indicated low-index directions. Incident ion current is 1.9×10^{-9} A. The curves are obtained after about 30 min of bombardment.

after the foil has been bombarded for about half an hour. It is seen that the (110) plane which would appear at $\varphi=76°$ and $\varphi=166°$ is completely absent.

Using 16-keV D^+ ions channeled through a 950-Å-thick gold crystal, it has been found that the relationship between planar contributions from $(\bar{1}\bar{1}1)$, (100), and (110) planes (separated from directional channeling as described above) at $|\theta|=35°$ is about

$$(110):(100):(\bar{1}\bar{1}1)=0:1:2.$$

This relation gives the experimental order of importance amongst the planes. A comparison between Figs. 2 and 3 reveals the following facts:

(a) The peak width is generally smaller for D^+ ions than for He^+ ions.

(b) The transmission of D^+ ions in the forward direction is higher despite the fact that D^+ ions pass through twice the thickness of gold.

(c) The same eight low-index directions are represented by peaks in the intensity functions at the expected angles and with approximately the same relative intensities.

(d) The intensity of ions experiencing ungoverned motion is relatively small for D^+ ions.

The effects of several low-index planes intersecting at a low-index direction are not known in detail at the present time. However, this problem is believed to be intimately related to the hard-sphere radius. For a small hard-sphere radius, the open area seen along a high-index direction in a low-index plane is a large fraction of the total area. In a direction where several low-index planes intersect, the additional open area is small. A calculation based on a radius of 0.04 a_0, where a_0 is the lattice constant for gold, shows that the experimental order amongst the directions present in Figs. 2 and 3 does not change.

TABLE I. The peak widths σ_θ, σ_φ, and $\sigma_\theta/\sigma_\varphi$ are listed for four different channels. Different foils and energies are used. The agreement between $\sin\theta$ and $\sigma_\theta/\phi_\varphi$ is seen to be good.

hkl	θ (deg)	σ_θ (deg)	σ_φ (deg)	$\sigma_\theta/\sigma_\varphi$	$\sin\theta$
015	11.3	2.20	10.45	0.211	0.196
013	18.5	1.65	4.75	0.348	0.316
		2.30	6.50	0.354	
012	26.5	2.20	5.15	0.428	0.448
011	45.0	1.80	2.50	0.720	0.707
		2.00	2.80	0.715	
		2.60	3.80	0.686	
		2.30	3.16	0.724	

The peaks in the intensity curves are approximated by Gaussian curves. In particular, the relative transmitted intensity P_θ as a function of θ near a channel direction is given by the relation

$$P_\theta=\exp[-(\theta-\theta_0)^2/2\sigma_\theta^2] \quad \text{for} \quad \alpha=0,\ \varphi=\varphi_0, \quad (1)$$

where $(\theta_0;\ \varphi_0)$ is the angular position of a low-index direction and σ_θ is the characteristic half-width. P_θ is interpreted as the relative probability that an ion incident at a small angle $(\theta-\theta_0)$ to a channel will be channeled and detected within the small angular interval set by the detector.

The relative transmitted intensity P_φ as a function of φ close to a channel direction $(\theta_0;\ \varphi_0)$ is

$$P_\varphi=\exp[-(\varphi-\varphi_0)^2/2\sigma_\varphi^2] \quad \text{for} \quad \alpha=0,\ \theta=\theta_0, \quad (2)$$

where σ_φ is the characteristic half-width. In addition the relative probability $P_{1\theta}$ for an ion to be accepted into a channel $(\theta_0,\ \varphi_0)$ as a function of θ is denoted by

$$P_{1\theta}=\exp[-(\theta-\theta_0)^2/2\sigma_{1\theta}^2] \quad \text{for} \quad \alpha=\theta-\theta_0,\ \varphi=\varphi_0, \quad (3)$$

where $\sigma_{1\theta}$ is the characteristic half-width. The condition that $\alpha=\theta-\theta_0$ means that the detector is always kept aligned with the channel axis. The relative probability $P_{2\theta}$ for an ion to emerge from a channel at an angle α

TABLE II. The peak shift $\delta\theta$ is listed for three values of the detector position α_0. The ratio $\alpha_0/\delta\theta$ has an average value of 2.57. This value gives the ratio $\sigma_{1\theta}/\sigma_{2\theta}=0.8$ as compared with 0.74 obtained from direct measurements of $\sigma_{1\theta}$ and $\sigma_{2\theta}$.

α_0 (deg)	$\delta\theta$ (deg)	$\alpha_0/\delta\theta$
5.0	1.84±0.13	2.72±0.20
10.0	3.80±0.25	2.63±0.19
15.0	6.40±0.40	2.35±0.15

TABLE III. Calculated and measured values of the total stopping power dE/dx in gold for D^+ and He^+ ions in high-index directions. (N) refers to the theoretical expression for the nuclear energy loss given by Nielsen. (LS) refers to the electronic energy loss given by Lindhard and Scharff.

Ion	E (keV)	b/a	K	ϑ/ϑ_0	$(dE/dx)_n^{(N)}+(dE/dx)_{el}^{(LS)}$ (eV/Å)	expt. (eV/Å)
He^+	25	0.81	300	0.48	10.0	12±1
D^+	13	0.98	160	0.48	4.9	6±1
	23	0.74	260	0.64	7.0	8±1

with respect to the channel axis $(\theta_0; \varphi_0)$ is given by

$$P_{2\vartheta}=\exp[-\alpha^2/2\sigma_{2\vartheta}^2] \quad \text{for} \quad \theta=\theta_0,\ \varphi=\varphi_0, \qquad (4)$$

where $\sigma_{2\vartheta}$ is the characteristic half-width.

Measured values of σ_θ, $\sigma_{2\theta}$, and $\sigma_{2\varphi}$ for ⟨011⟩ channels in a gold foil 660 Å±40 Å thick are $\sigma_\theta=2.7°\pm0.1°$, $\sigma_\theta=3.4°\pm0.1°$, and $\sigma_{2\theta}=4.6°\pm0.1°$. These values are for 9-keV D^+ ions. Measured values of σ_θ and σ_φ for several different channels are given in Table I. If the detector is set at an angle α_0, the peak position is found to be shifted from the channel direction by an amount $\delta\theta$. Table II gives values of α_0, $\delta\theta$ and their ratio for D^+ ions in the 660-Å gold crystal.

Experimental values for dE/dx have been obtained by plotting the total energy loss as a function of effective foil thickness d which varies as $1/\cos\theta$. A straight line is fitted to the experimental points. The results are presented in Table III.

The way of separating directional and planar channeling in the energy loss curves is based on the same arguments which were used above. However, for $\theta>50°$ the separation is somewhat arbitrary. No peaks are observed corresponding to the [012], [013], aud [015] directions. Table IV gives the percentage reduction in the energy loss in the [011], [001], and [112] directions which are the three most open crystallographic directions. No sign of the (110) plane is found in the energy distributions.

TABLE IV. The most probable energy losses for the random part $\Delta E_{mp}{}^r$ and the reduction in energy loss for the channeled parts $\Delta E_{mp}{}^r-\Delta E_{mp}$ for He^+ and D^+ ions in three directions in gold taken from Figs. 2 and 3. The bombarding particle energy is 25 keV for the He^+ ions and 23 keV for the D^+ ions. $(\Delta E_{mp}{}^r-\Delta E_{mp})/\Delta E_{mp}{}^r$ represents the percentage decrease in energy loss due to channeling.

Ion	hkl	θ (deg)	ΔE_{mp} (keV)	$\Delta E_{mp}{}^r$ (keV)	$\Delta E_{mp}{}^r-\Delta E_{mp}$ (keV)	$(\Delta E_{mp}{}^r-\Delta E_{mp})/\Delta E_{mp}{}^r$ (%)
He^+	011	−45	6.1	8.0	1.9	24±2
	001	0	5.2	6.1	0.9	15±2
	112	+35	6.4	7.2	0.8	11±1
D^+	011	−45	7.3	8.6	1.3	15±2
	001	0	5.6	6.3	0.7	11±1
	112	+35	6.8	7.5	0.7	9±1

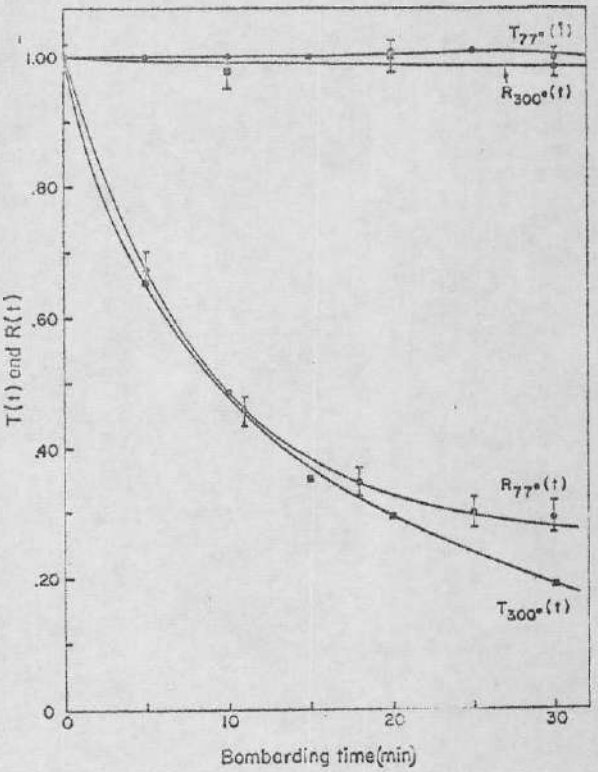

FIG. 5. The transmission coefficient $T(t)$ in the ⟨100⟩ direction normalized to zero time is shown as a function of time. $R(t)$ is the ratio of channeled intensity in the ⟨100⟩ direction to the intensity 7° off the channel axis in the (100) plane normalized to zero time. The figure 300° refers to measurements with the copper cylinder near the gold foil at room temperature and the figure 77° refers to measurements with the copper cylinder at liquid-nitrogen temperatures. Bombarding particles are 8-keV D^+ ions and the current density is on the order of 10^{-7} A/cm².

Time Dependence

The transmitted intensity i and the energy loss ΔE_{mp} are both found to be functions of time. The energy loss increases with time while the intensity normally decreases. The time dependence can easily be measured, however; the rate of change in the energy loss is small enough, so that no correction has to be considered here. The reason for the change in the transmitted intensity is studied to some extent by keeping the copper shield in the vicinity of the gold film at different temperatures. The function $T(t)$ is defined as the ratio of transmitted to incident ion current normalized to zero time. $R(t)$ is defined in the (100) plane as the channeled intensity $(i_{\vartheta=0°}-i_{\vartheta=7°})$ normalized to zero time. This ratio is expected to be sensitive to changes in the gold crystal. In Fig. 5 $T(t)$ and $R(t)$ are shown with the copper shield at room temperature (300°K) and at liquid-nitrogen temperature (77°K). With the copper shield at 77°K the contamination of the gold crystal is reduced and the functions $T(t)$ and $R(t)$ reflect the effects of true radiation damage. With the copper shield at 77°K the normally observed contamination spot was not visible on the gold film at the end of the 30-min bombardment.

Charge Exchange

The interpretation of our results are based on the assumption that for these low energies, charge exchange with the bombarded material is independent of orientation. If we assume that the reflection coefficient is very small, we find that for 30-keV He^+ ions, the fraction of the incident intensity which emerges from a 300-Å gold crystal as He^+ ions is about 0.2. This value is obtained by measuring the transmitted intensity as a function of α and integrating over all forward directions with a correction applied for the finite detector aperture. Neutral He atoms are not detectable with the arrangement used here. It is very likely that in our experiment the charge exchange takes place in the contamination layer which tentatively consists of elemental carbon. The figure 0.2 is then in reasonable agreement with an extrapolation of measurements at higher energies.[29]

Crystal Defects and Thermal Vibrations

Evaporated gold films are known to contain appreciable concentrations of defects. The peak intensities are believed to be affected by these defects and by thermal vibrations. In particular, when the channel area becomes small, the effect might be large enough to knock ions out of the channel direction.

A "cutoff" in the directional channeling has also been observed. The critical area for 23-keV D^+ ions is found to be close to the ⟨019⟩, ⟨1,1,10⟩, or ⟨167⟩ directions. If the root-mean-square (rms) amplitude of the thermal vibrations amounts to about $0.03a_0$ at 300°K and the radius of the D^+ ion is neglected compared to the gold atom, the critical channel area corresponds to a hard-sphere radius of $0.04a_0$.

DISCUSSION

Peak-Width Errors

There are several sources of error which might effect the widths of the peaks. We will give a brief discussion of each of these.

(*a*) *Detector angle.* A numerical estimate of the effect on the peakwidth of different detector openings has been made. It is found that if half of the acceptance angle of the detector, σ_{det}, is equal to $0.5\sigma_{2\theta}$, the measured width is 3% too large. If $\sigma_{det}=\sigma_{2\theta}$ the correction is 8%. In all runs $\sigma_{det}<0.3\sigma_{2\theta}$. A correction of 2% may be applied to $\sigma_{2\theta}$.

(*b*) *Beam spread.* From the diameter of the contamination spot and the beam defining aperture, half of the angular spread σ_{beam} is found to be 0.14°. We thus find that $\sigma_{beam}<0.1\sigma_{1\theta}$. No correction is necessary.

(*c*) *Wrinkles.* All foils have been examined in an optical microscope for wrinkles in the central area of the foil. Only foils with at least 4–9 perfectly flat grid squares in the center have been used. No wrinkles are seen after the bombardment. No correction is necessary. For some of the films, electron microscope photographs show bend extinction contours which indicate the presence of submicroscopic wrinkles. The effect of these is believed to be small.

(*d*) *Grid-Square Misorientation.* Microscope grids looking perfectly flat to the naked eye have been checked in the optical microscope. It is found that individual grid squares can be tilted a small angle relative to their neighbors. A maximum tilt of about 1° is observed. The standard deviation σ_{grid} is equal to about 0.5°. We find that $\sigma_{grid}<0.3\sigma_{2\theta}$. A correction of 2% may be applied to $\sigma_{2\theta}$.

(*e*) *Angular Measurements.* The accuracy in setting the dials for θ and α is about 0.25°. A gear ratio of 2:1 in the dial for φ makes it possible to set φ within 0.15°. The statistical errors in measuring σ_θ, σ_φ, and $\sigma_{2\theta}$ are therefore 0.1°–0.2°. No goniometer play has been observed. We find $\sigma_{gear}\ll\sigma_{2\theta}$. No correction is necessary.

(*f*) *Surface Contamination.* The effect of surface contamination is very obvious from the study of the variation of peak intensities with time (Fig. 5). It is assumed that the contamination layer consists of elemental carbon.[30] From a comparison between the mean-square deflection angles for a 850-Å polycrystalline gold film and a 100-Å carbon film[31] we find that the additional spread in the incident ion beam due to a 100-Å carbon film is about 0.13°. The effective beam spread σ_{beam} is still only $0.15\sigma_{2\theta}$. A correction of 1% may be applied to $\sigma_{2\theta}$ because of the spread in the bombarding ion beam.

Because of (*a*), (*b*), (*d*), and (*f*), the measured values are about 3–5% too high. The statistical errors are about 5–10%.

Errors in Energy Determination

When only a single energy value, corresponding to maximum intensity in a specific direction, is measured the accuracy is ±2% for high intensities and 5–7% for low intensities. When the complete energy profile is determined the accuracy in locating the most probable energy of a particular beam component is about ±1.5%.

The rate of change of ΔE_{max} as a function of time is found to be approximately 20% during the first hour of bombardment. This change in energy loss affects mainly the ungoverned motion. The heights of the peaks above the random energy loss in the energy-loss curves are less dependent on time. No corrections have been applied to any energy values presented in the figures or the tables.

Errors in Intensity Measurements

The experimental error in measuring the transmitted intensity for an individual point is less than 1% for

[29] J. C. Armstrong, J. V. Mullendore, W. R. Harris, and P. Marion, Proc. Phys. Soc. (London) 86, 1283 (1965).

[30] A. E. Ennos, Brit. J. Appl. Phys. 4, 101 (1953).

[31] N. F. Mott and H. S. W. Massey, *The Theory of Atomic Collisions* (Clarendon Press, Oxford, England, 1949), 2nd ed.

high intensities and about 5% for low intensities. The relative error in separating the directional from the planar channeling is about 10%. The error in the transmission coefficient $T(t)$ in Fig. 5 is about 5%.

Analysis of Peak Widths

We now try to find relationships between measured values of σ_θ, σ_φ, $\sigma_{1\theta}$, and $\sigma_{2\theta}$. Assume that the Gaussian distributions on the entrance side $P_{1\theta}$ and exit side $P_{2\theta}$ are independent and symmetric around the channel axis. Assume further that $\sigma_{1\theta}\neq\sigma_{2\theta}$. Then the relationship between $P_{1\theta}$, $P_{2\theta}$, and P_θ should be

$$P_\theta = P_{1\theta}\cdot P_{2\theta}, \tag{5}$$

which gives the relation

$$\sigma_\theta^{-2} = \sigma_{1\theta}^{-2} + \sigma_{2\theta}^{-2}. \tag{6}$$

The measured quantities given earlier do satisfy this relation. It is found that usually $\sigma_{2\theta}$ is larger than $\sigma_{1\theta}$. The critical angle for channeling[16] is expected to increase as the energy decreases. Since the energy decreases as the ion traverses the foil, the larger value of $\sigma_{2\theta}$ may be due to the increased critical angle for the ions emerging from the foil.

When the ions are detected at a fixed angle $\alpha_0\neq 0$, it is found that the peaks in the transmitted intensity measured as a function of θ are shifted. Assuming that $\sigma_{1\theta}=\sigma_{2\theta}$ it is obvious that $P_\theta=\exp\{-[(\theta-\theta_0)^2/2\sigma_{1\theta}^2] -(\theta-\theta_0-\alpha_0)^2/2\sigma_{2\theta}^2\}$ has a maximun for a shift $\delta\theta$ given by

$$\alpha_0/\delta\theta = 2. \tag{7}$$

Table II gives the measured ratios $\alpha_0/\delta\theta$ for three values of α_0 using 9-keV D^+ ions in a 660 Å±40 Å gold film. It shows that in this particular experiment the assumption that $\sigma_{1\theta}=\sigma_{2\theta}$ leading to (7) is not the best assumption. If instead $\sigma_{1\theta}$ is assumed to be $0.8\sigma_{2\theta}$, it can be shown by maximizing P_θ that the calculated ratio $\alpha_0/\delta\theta$ agrees with the average measured value of 2.6 in Table II. The directly measured values of $\sigma_{1\theta}$ and $\sigma_{2\theta}$ given above give a ratio of 0.74.

If φ is changed across a channel peak with $\alpha=0$ and $\theta=\theta_0$, we effectively change the angle β between the channel axis and the beam direction. The relationship between β and a change $\Delta\varphi=\varphi-\varphi_0$ for small values of β and $\Delta\varphi$ around the channel axis can be shown to be

$$\beta/\Delta\varphi = \sin\theta. \tag{8}$$

If the channel peak has rotational symmetry, the characteristic widths σ_θ and σ_φ should be related by the equation

$$\sigma_\theta/\sigma_\varphi = \sin\theta. \tag{9}$$

Figure 6 shows the experimental ratios of $\sigma_\theta/\sigma_\varphi$ for four channel peaks in the (100) plane. The solid curve is the function $\sin\theta$. Six different foils are used. The agreement is very good and proves that the difference between

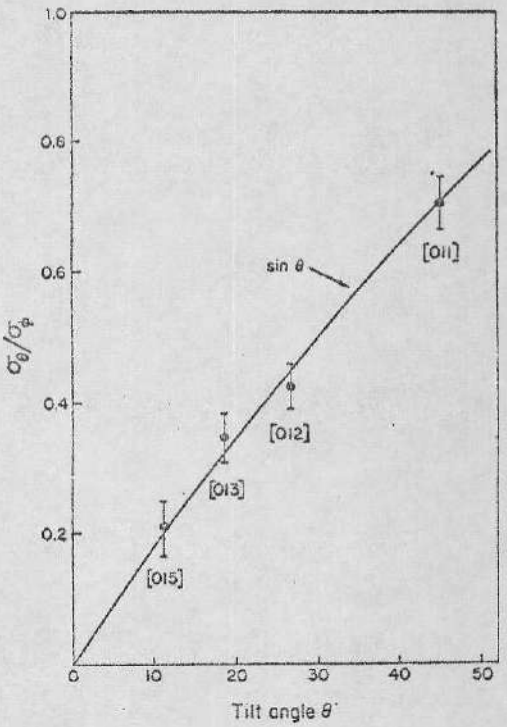

FIG. 6. A comparison between $\sin\theta$ (solid line) and $\sigma_\theta/\sigma_\varphi$ (filled circles) for four channels in the (100) plane; six different gold foils are used. The agreement between $\sigma_\theta/\sigma_\varphi$ and $\sin\theta$ shows that the peaks are symmetric around the channel axis.

σ_θ and σ_φ is not characteristic of the crystal, but originates from geometrical factors in the goniometer. The peaks are thus quite symmetric around the channel axis.

Analysis of Energy Losses

The total energy loss is the sum of nuclear and electronic losses. To compare the measured dE/dx values with theory we have used the expression by Nielsen[24] for the energy loss due to displacement collisions:

$$\frac{dE^{(N)}}{dx} = 3.63\frac{NM_1}{M_1+M_2}\frac{Z_1Z_2e^2}{(Z_1^{2/3}+Z_2^{2/3})^{1/2}}\frac{\hbar^2}{m_e e^2}. \tag{10}$$

For the electronic loss we use the expression by Lindhard and Scharff[25]:

$$\frac{dE^{(LS)}}{dx} = \frac{N8\pi e^2 a_0 Z_1 Z_2}{(Z_1^{2/3}+Z_2^{2/3})^{3/2}}\frac{v}{v_0}\xi_e. \tag{11}$$

In (10) and (11), N stands for the number of nuclei per unit volume. The indices 1 and 2 denote the bombarding and the target particle. a_0 is the Bohr radius and ξ_e is a parameter of the order of unity. v_0 is equal to $e^2/\hbar$. In (10) the ratio b/a between the impact parameter b and the screening radius a is limited to the interval 0.8

$<(b/a)<15$. The ratio $K=b/\lambda$ must be large compared to unity where λ is the de Broglie wavelength of the incident particle.

According to Dienes and Vineyard,[32] the electronic loss (11) to the conduction electrons is important when the energy

$$E>M_1\epsilon_F/16m_e, \tag{12}$$

where ϵ_F is the Fermi energy for gold (5.6 eV). The critical energy for He^+ ions in gold is, according to (12), about 3 keV. Tables III and IV list the calculated and measured quantities for 25-keV He^+ ions traveling through the 275-Å single-crystal gold film in Fig. 2 and for 23-keV and 13-keV D^+ ions transmitted through the 550-Å gold film in Fig. 3. Because of the fairly large energy loss in the foils the average velocity $\bar{v}$ over the region in which dE/dx is measured is used instead of v. In Table IV the last column lists the percentage decrease, $(\Delta E_{mp}{}^r-\Delta E_{mp})/\Delta E_{mp}{}^r$, in the energy loss for He^+ and D^+ ions channeled through three of the most open channels in a fcc lattice. $\Delta E_{mp}{}^r$ denotes the most probable energy loss of the random part of the beam.

In the $\langle\bar{1}12\rangle$ direction $(\Delta E_{mp}{}^r-\Delta E_{mp})/\Delta E_{mp}{}^r$ is found to be about 11% for He^+ ions in gold. Almost the same figure is obtained if the energy loss is measured in the (111) plane at a φ value off the [112] direction and corresponding to a high-index plane of the type $(hk0)$. This fact indicates that the percentage reduction in the (111) plane is also about 11%. At $\theta=0$ only (100) planes contribute to the channeling. The percentage reduction in energy loss due to this type of plane is found to be about 7%. The (110) plane does not show up at all. The order of importance amongst the planes is thus found to be (111), (100), and (110) which is the same order as was found above.

The energy loss has also been measured in the $\langle001\rangle$ direction as a function of foil thickness. In the thickness range 275 Å to 1000 Å, the function is very linear. The slope of the line gives a value 7.4 ± 0.3 eV/Å for the stopping power (dE/dx) in the $\langle001\rangle$ direction.

[32] G. J. Dienes and G. H. Vineyard, *Radiation Effects in Solids* (Interscience Publishers, Inc., New York, 1957).

CONCLUSIONS

(1) The transmitted intensity of D^+ and He^+ ions of 8–25 keV energy through thin single-crystal gold films (275–600 Å) consists of directional and planar contributions as well as of a randomly scattered part. (2) The order amongst the three most open directions is found to be $\langle011\rangle$, $\langle001\rangle$, and $\langle112\rangle$. (3) Intensity as well as energy loss measurements give the order (111), (100), and (110) amongst the three most important planes. (4) A "cutoff" in the planar channeling exists between the planes (100) and (110). (5) The peaks are symmetrical around the channel axes and the over-all peak widths are successfully interpreted in terms of the channel entrance and exit peak widths. (6) Energy-loss measurements in high-index directions agree satisfactorily with theoretical predictions for the stopping power dE/dx. (7) The difference in energy loss between directional and planar channeling is much less pronounced than the difference in the channeled intensity showing that the effect of channeling on the energy loss is a secondary effect. (8) Charge exchange is found to significantly reduce the fraction of the beam which emerges from the foil as ions. (9) From the observed cutoff in the directional channeling at high indices, the effective hard-sphere radius for 23-keV D^+ ions in gold is estimated to be 0.16 Å.

ACKNOWLEDGMENTS

The authors would like to express their sincere gratitude to Dr. E. F. Wassermann for critically reading the manuscript. We would also like to thank W. Morris for many helpful discussions, D. Weber for operating the electron microscope, and W. Krakow for making the gold films.

DIRECT OBSERVATION OF CHANNELING IN bcc IRON FILMS*

C. J. Andreen,† E. F. Wassermann, and R. L. Hines
Northwestern University, Evanston, Illinois
(Received 4 April 1966)

In a recent Letter[1] we reported about transmission of 13-keV D^+ ions in single-crystalline fcc gold films. The results showed that the transmitted intensities in the beam direction are high in low-index directions or along low-index planes. The ions are believed to be channeled between the atom rows and planes in the crystal.[2] We found that the channeled intensities are correlated with calculated transparency values A_{hkl}, the area per atom along the direction $\langle hkl \rangle$, given by $A_{hkl} = \text{const}\,\rho_{hkl}^{-1}$ where ρ_{hkl} is the number of atom rows per unit area.[3] A good agreement exists between the strongest five peaks and low-index directions calculated by Robinson and Oen[3] to be the most open channels in fcc crystals.

In this Letter we report the direct observation of channeling in a bcc structure. We compare the results with those obtained on gold films in our previous investigations and show that planar channeling plays an important role. Penetration distributions of ^{125}Xe ions in bcc tungsten have been obtained earlier.[4] The anomalous long-range "tails" in the curves are interpreted as being due to channeling. However, these authors do not discuss the distinction between directional and planar channeling.

Single-crystal α-iron films are used in our investigations. The films are grown by ultra-high-vacuum (10^{-8} Torr) deposition of iron onto hot rocksalt substrates. Growing techniques similar to those described by Matthews[5] and Shinozaki and Sato[6] are used. The film thickness is measured with a quartz crystal microbalance. The epitaxial relation between the films and the substrates as seen in an electron microscope is that the (001) plane of iron is parallel to the (001) plane of the rocksalt. The

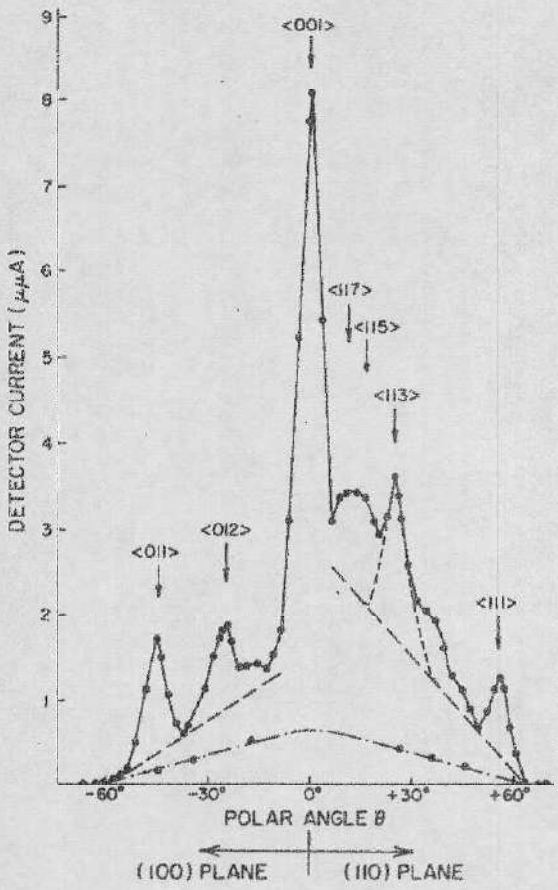

FIG. 1. Transmitted currents of D^+ ions in the beam direction through a 1000-Å-thick α-iron film are shown as a function of film orientation. The film normal is ⟨001⟩. Arrows point to the angles for low-index directions in the (100) and (110) planes. Dashed lines indicate the separation of directional and planar contributions. The dot-dashed line represents transmitted intensities in high-index planes. Incident ion current is 10^{-9} A. Incident ion energy is 15 keV.

films are picked up on 3-mm-diameter Cu grids and mounted in a goniometer. With the goniometer, the foil normal can be inclined to a polar angle θ with respect to the beam direction, and the foil can be rotated about its normal through an azimuthal angle φ. A mass-separated D^+ ion beam is used for the bombardment. Details about the apparatus and the goniometer geometry have been described earlier.[1,7]

Figure 1 shows the channeled intensities in the beam direction in a (100) and a (110) plane for a 1000-Å-thick iron film. The D^+ ions have an energy of 15 keV. The incident ion current is 10^{-9} A. Because of the film orientation the ⟨001⟩ direction appears at $\theta = 0$, the intersection

Table I. Most-open channel directions $\langle hkl \rangle$ as found experimentally are shown for fcc[a] and bcc structures. A plus sign refers to resolved peaks and a minus sign to directions where no resolved peaks are seen. The parentheses indicate that the ⟨012⟩ direction has a relatively low intensity.

$\langle hkl \rangle$	bcc	fcc
001	+	+
011	+	+
111	+	−
012	+	(+)
112	−	+
013	−	+
113	+	−
114	−	+
015	−	+
133	+	−
115	+	−
117	+	−

[a]See Ref. 1.

between the two planes. In the (100) plane, peaks are found in directions corresponding to the channels ⟨011⟩ and ⟨012⟩. In the (110) plane we find channels in the ⟨111⟩, ⟨113⟩, ⟨115⟩, and ⟨117⟩ directions. The smooth background shown by the dot-dashed line in Fig. 1 is obtained from measuring the intensity in high-index planes. In these planes the foil acts like a polycrystalline film with random orientation. Similar curves are obtained from measurements on randomly oriented iron films.

In Table I we list 12 low-index directions in increasing order of the sum $h+k+l$. Directions for which resolved peaks are found are marked with a plus sign. No peaks have been seen in directions marked with a minus sign. Table I shows clearly that most of the peaks present in one structure are absent or unresolved in the other. This fact proves that the channeled intensities are closely related to the lattice structure and therefore gives strong support to the transparency model discussed by Robinson and Oen.[3] Their transparency values (expressed by the row densities ρ_{hkl}) suggest a certain order among the channel directions. The order is different for fcc and bcc structures. For both structures we do obtain the first five most open channels. The peak intensities, however, do not give the expected order because of an unknown dependence on effective foil thickness. The most striking difference between the fcc and bcc structures occurs for the two directions ⟨112⟩ and ⟨013⟩. In gold[1] both directions are

very pronounced while they are hardly visible at all in iron.

Figure 2 shows the transmitted intensities as a function of azimuthal angle φ for a constant value of $\theta = 45°$. Peaks at $\varphi = 10°$ and $\varphi = 100°$ correspond to $\langle 011 \rangle$-type channels. The shoulders on each side of these maxima belong to the channels of the type $\langle 133 \rangle$. At $\varphi = 55°$ and $\varphi = 145°$ no low-index directions are expected from theory. The high peaks at these angles must, therefore, be due to channeling in (110) planes. The total intensities in Fig. 1 thus also have to contain planar contributions. For $\theta = +49°$ and $-37°$ only very high-index directions exist, and we expect only planar channeling at these points. Using these minima and observing the fact that the width at half-maximum is roughly constant for all peaks, we can find the planar part on top of which the directional contributions appear. The separations are done in Fig. 1 (dashed lines). It can now be seen that the (110) plane is more transparent than the (100) plane, which is expected from calculated values of interplanar spacings.

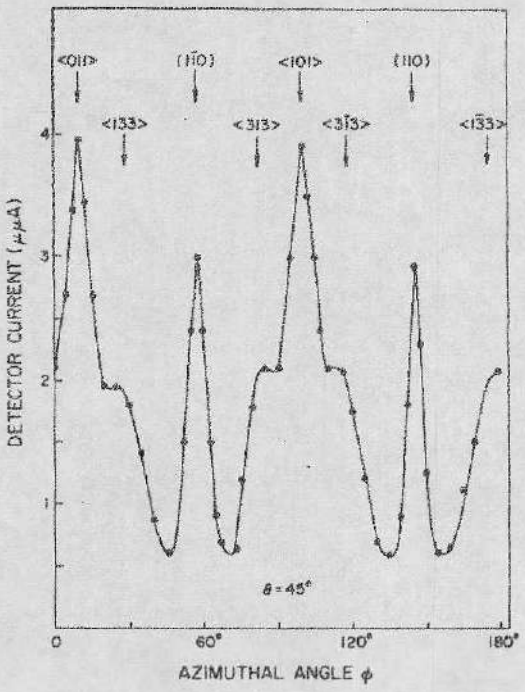

FIG. 2. Transmitted current of 15-keV D^+ ions in the beam direction in a 1000-Å α-iron film is shown as a function of azimuthal angle φ. The polar angle is $\theta = 45°$. Arrows point to the angles for the indicated low-index directions and planes. Incident ion current is 10^{-8} A.

No sign of the next important plane (112) is found. This means that in our experiment only the two most important planes (110) and (100) show planar channeling. In directions where these planes intersect ($\langle 111 \rangle$, $\langle 011 \rangle$, and $\langle 001 \rangle$), the net effect of several planes has to be considered. So far we do not know exactly how this could be done; but a calculation based on an estimated hard sphere radius of $0.06a$, where a is the lattice constant for gold, gives a maximum correction of about +20% for the planar contribution indicated in Fig. 1 in the $\langle 011 \rangle$ direction. In the $\langle 001 \rangle$ and $\langle 111 \rangle$ directions the upward shift is much smaller.

The energy loss of the ions in the iron films can be determined by a 90-deg energy analyzer. For the $\langle 001 \rangle$ channel this energy loss is found to be about 50%. Energy losses for other directions are higher.

Provided that the D^+ ion energy is kept constant, a comparison between peak widths for iron and gold films of the same thickness can be made. We find that the channel peaks are broader in iron than in gold. H^+, D^+, He^+, C^+, O^+, and Ne^+ ions have been used for channeling experiments in gold foils. It is found that the peak width increases when the mass ratio between the target and the bombarding particle decreases. The data on iron agree with this relation.

Radiation damage reduces the peak intensities because the channels are blocked by displaced atoms. By looking at the films in an electron microscope after bombardment, the damage can also be observed as a high density of defect clusters.

*Research supported by U. S. Atomic Energy Commission.

†Present address: Department of Physics, Chalmers University of Technology, Gothenburg, Sweden.

[1]C. J. Andreen, R. L. Hines, W. Morris, and D. Weber, Phys. Letters 19, 116 (1965).

[2]R. S. Nelson and M. W. Thompson, Phil. Mag. 8, 1677 (1963).

[3]M. R. Robinson and O. S. Oen, Phys. Rev. 132, 2385 (1963).

[4]B. Domeij, F. Brown, J. A. Davies, G. R. Piercy, and E. V. Kornelsen, Phys. Rev. Letters 12, 360 (1964).

[5]J. W. Matthews, Appl. Phys. Letters 7, 225 (1965).

[6]S. Shinozaki and H. Sato, J. Appl. Phys. 36, 2320 (1965).

[7]R. L. Hines and R. Arndt, Phys. Rev. 119, 623 (1960).

CRITICAL ANGLES FOR CHANNELING OF H^+, D^+ AND He^+ IONS IN SINGLE CRYSTAL GOLD FILMS IN THE ENERGY INTERVAL 1 - 17 keV*

C. J. ANDREEN** and R. L. HINES
Northwestern University, Evanston, Illinois

Received 12 December 1966

The critical angles for channeling are obtained from measurements of transmitted ion intensity in the forward direction through gold crystal foils as a function of foil orientation. The results agree with theoretical predictions for the low energy region.

Recent theoretical calculations by Lindhard [1] have provided an approximate expression for the critical angle ψ_2 for channeling in the low energy region. The experiment results given here for H^+, D^+ and He^+ ions channeled through thin single crystal gold films in the ⟨011⟩, ⟨001⟩, and ⟨112⟩ directions are in good agreement with the theoretical predictions.

* Work supported by the Atomic Energy Commission.
** Present address: Department of Physics, Chalmers University of Technology, Gothenburg, Sweden.

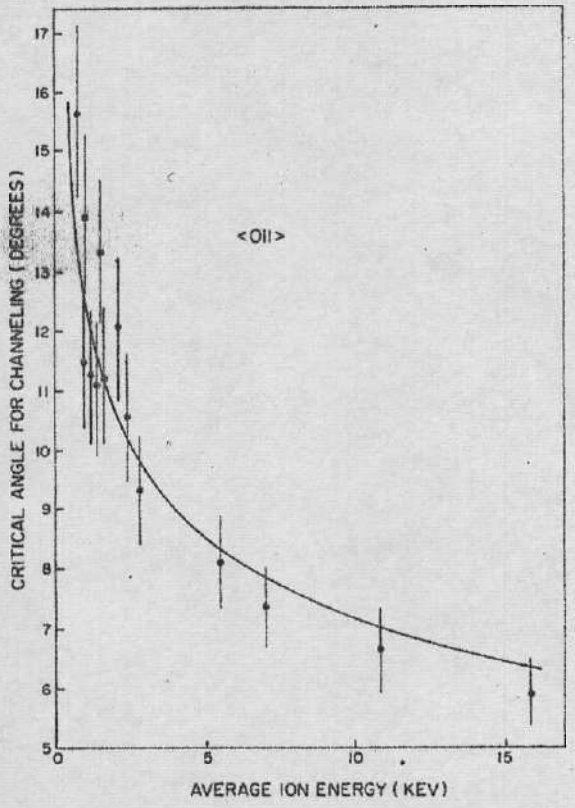

Fig. 1. Critical angles for channeling for D^+ ions in 180-260 Å thick single crystal gold films as a function of the average ion energy $\bar{E}$. The solid curve shows the theoretical value for the ⟨011⟩ channel with C = = 2.15. The vertical bars give the errors in critical angles. The errors in energy vary from 0.3 keV at 1 keV to 0.5 keV at 17 keV.

The apparatus has been described elsewhere [2,3]. The gold films are prepared using standard techniques [4]. The most probable energy loss ΔE_{mp} is measured as a function of E with a 90° electrostatic energy analyzer. The average ion energy $\bar{E}$ is gound by subtracting $\frac{1}{2}\Delta E_{mp}$ from the incident ion energy.

The half width of a channel peak obtained by tilting the foil an angle θ relative to the beam, keeping the detector fixed on the beam, has earlier been characterized by σ_θ [3]. This parameter is related to $\sigma_{1\theta}$ and $\sigma_{2\theta}$ through the equation

$$\sigma_\theta^{-2} = \sigma_{1\theta}^{-2} + \sigma_{2\theta}^{-2} \quad (1)$$

where $\sigma_{1\theta}$ and $\sigma_{2\theta}$ are characteristic half widths for the angular probability function of acceptance into a channel and emergence from a channel, respectively. In the energy interval 1 - 17 keV we find that

$$\sigma_{1\theta} = (1.0 \pm 0.1)\,\sigma_{2\theta} \quad (2)$$

which together with (1) gives

$$\sigma_{1\theta} = \sqrt{2}\sigma_\theta\,. \quad (3)$$

To find experimentally the critical angle for channeling α_c, we draw a tangent to the channel peak distribution through the point defining $\sigma_{1\theta}$. The point where this tangent meets the intensity of the ungoverned motion is the experimental value of α_c. This gives the experimental result

$$\alpha_c = (2.14 \pm 0.18)\sigma_{1\theta} \quad (4)$$

and thus from (3)

$$\alpha_c = 2.14 \cdot \sqrt{2}\sigma_\theta\,. \quad (5)$$

For a perfect Gaussian distribution of the peak intensities one would expect a factor $2\sqrt{2}$. By measuring σ_θ as a function of $\bar{E}$ for different channel directions the critical angle α_c can be compared with ψ_2. Local misorientations of the film surface due to microwrinkles are measured from the Laue zones of the electron diffraction pattern. The standard deviation for the angle of misorientation is found to be $0.5^\circ \pm 0.2^\circ$. According to an earlier estimate [3] of the foil condition on the peak width, the error introduced by the microwrinkles is less than 1%.

Fig. 1 shows the experimental points for D^+ ions of different average energies $\bar{E}$ in the interval $0.7 \leq \bar{E} \leq 16$ keV in ⟨011⟩ channels. Several different films in the thickness range from 180 Å to 260 Å have been used in order to reduce the effects of contamination build up and radiation damage as much as possible. The solid curve shows the behavior of ψ_2 for the ⟨011⟩ channel. It is found that ψ_2 fits the experimental points within the errors for the three directions ⟨011⟩, ⟨001⟩, and ⟨112⟩ in the total energy interval if the constant C in the expression for ψ_2 is given the value 2.15.

In order to look for a mass dependence H^+ ions are used as bombarding particles on several gold films both before and after a bombardment with D^+ ions. No difference in the critical channeling angle between D^+ and H^+ ions is found. He^+ ions are also used as bombarding particles. It is found that with the other parameters constant the critical angle for channeling α_c for 17 keV He^+ ions incident on gold is 1.13 ± 0.04 times larger than for D^+ ions. The theoretical value is 1.17. From the experimental results we observe that ψ_2 accounts for the dependence of the critical angle on the average energy $\bar{E}$, the string

constant d_{hkl} and the nuclear charge Z_1. Furthermore the results confirm that ψ_2 is mass independent.

1. J. Lindhard, Mat. Fys. Medd. Dan. Vid. Selsk. 34, no. 14 (1965).
2. R.L. Hines and R. Arndt, Phys. Rev 124 (1961) 128.
3. C.J. Andreen and R.L. Hines, Phys. Rev. 151 (1966) 341.
4. D.W. Pashley, Phil. Mag. 4 (1959) 324.

* * * * *

DOKTORSAVHANDLINGAR
VID
CHALMERS TEKNISKA HÖGSKOLA
Ny serie Nr 64 (B.T.36)

Critical Angles for Channeling of 1 to 25 keV H^+, D^+, and He^+ Ions in Gold Crystals.*

C. J. Andreen† and R. L. Hines

Northwestern University

Evanston, Illinois

(Received)

The critical angle for channeling in the low energy region is measured for H^+, D^+, and He^+ ions transmitted through single crystal gold foils. It is found that the theoretical calculation by Lindhard fits the experimental points within the experimental errors if the constant C is given the value 2.15. No difference is found between H^+ and D^+ ions. The critical angle for He^+ ions is found to be 1.13 ± 0.04 times larger than for D^+ or H^+ ions of the same energy.

*Supported by the U. S. Atomic Energy Commission.

†Present address: Chalmers University of Technology, Gothenburg, Sweden.

Critical Angles for Channeling of 1 to 25 keV H^+, D^+, and He^+ Ions in Gold Crystals*

C. J. Andreen† and R. L. Hines

Northwestern University

Evanston, Illinois

(Received)

The critical angle for channeling in the low energy region is measured for H^+, D^+, and He^+ ions transmitted through single crystal gold foils. It is found that the theoretical calculation by Lindhard fits the experimental points within the experimental errors if the constant C is given the value 2.15. No difference is found between H^+ and D^+ ions. The critical angle for He^+ ions is found to be 1.13 ± 0.04 times larger than for D^+ or H^+ ions of the same energy.

*Supported by the U. S. Atomic Energy Commission.

†Present address: Chalmers University of Technology, Gothenburg, Sweden.

Critical Angles for Channeling of 1 to 25 keV H^+, D^+, and He^+ Ions in Gold Crystals*

C. J. Andreen† and R. L. Hines

Northwestern University

Evanston, Illinois

(Received)

The critical angle for channeling in the low energy region is measured for H^+, D^+, and He^+ ions transmitted through single crystal gold foils. It is found that the theoretical calculation by Lindhard fits the experimental points within the experimental errors if the constant C is given the value 2.15. No difference is found between H^+ and D^+ ions. The critical angle for He^+ ions is found to be 1.13 ± 0.04 times larger than for D^+ or H^+ ions of the same energy.

*Supported by the U. S. Atomic Energy Commission.

†Present address: Chalmers University of Technology, Gothenburg, Sweden.

Nelson and Thompson have shown that it is possible to detect surprisingly high intensities of H^+ ions transmitted through thick (3000-4000Å) single crystal gold films in the ⟨110⟩ direction at an ion energy of 75 kev.[1] The presence of the channeled ions showed up as peaks in the ion intensity measured as a function of crystal orientation with respect to the incident beam direction. Peaks due to the channeled ions were seen for both transmitted and reflected ions. However, no energy analysis was made of the ions and no detailed comments were made concerning the angular widths of the peaks. Recently we have reported preliminary results on the angular widths of the peaks at low energies.[2] At higher energies (15-25 keV) a detailed investigation has shown the geometrical relationships between the angular widths of the peaks measured under different conditions.[3]

A recent analysis of the influence of a crystal lattice on the motion of energetic charged particles by Lindhard[4] shows that one can expect to find certain specific characteristics in the transmission curve. One such characteristic is a critical angle for channeling. This critical angle can be related to the half width of the experimentally observed peak. The critical angle is derived for both a high energy and a low energy region. The analysis is primarily concerned with high energies but an approximate expression is given for the low energy region.

This paper gives experimental results for the angular widths of the channeled peaks for 1 to 25 kev H^+, D^+, and He^+ ions in gold crystals and compares these results with the theoretical predictions of Lindhard in the low energy region.

THEORY

The approximate expression derived by Lindhard[4] for the critical angle ψ for channeling is based on the continuum string approximation. It is demanded that the scattering at the point of closest approach to a nucleus along the path is due to several atoms. At reasonable distances from the nucleus the average potential of many atoms lined up in a row (as for example along a low index crystallographic direction in a single crystal) is described by the so-called string potential. This transverse potential U(r), where r is the distance from the string, is an average of potentials V(R) of the Thomas-Fermi type,

$$V(R) = Z_1 Z_2 e^2 R^{-1} \varphi_o (R/a). \tag{1}$$

R is the ion-atom distance, Z_1 is the atomic number of the incident particle, Z_2 is the atomic number of the stopping medium, $a = .885\, a_o (Z_1^{2/3} + Z_2^{2/3})^{-1/2}$ and $\varphi_o(R/a)$ is the Fermi function belonging to one isolated atom. U(r) is then given by

$$U(r) = Z_1 Z_2 e^2 d^{-1} \xi(r/a) \tag{2}$$

where d is the distance between atoms along the string. An approximate expression for $\xi(r/a)$ which is applicable for all values of r is given by

$$\xi(r/a) = \log\left[(Ca/r)^2 + 1\right]. \tag{3}$$

The adjustable constant C may be given the value $C = \sqrt{3}$ to give a good overall fit but it will be slightly higher for large values of r/a.

The condition that the scattering in the vicinity of the minimum distance of approach, r_{min}, is due to many atoms leads to the relation

$$r_{min} > d\psi \tag{4}$$

where ψ is the critical angle for channeling. The minimum distance of approach is determined by

$$U(r_{min}) = \frac{1}{2} M_1 v^2 \sin^2\psi \tag{5}$$

where M_1 is the mass of the incident particle and v its velocity. From (2), (3), (4), and (5) it can be shown that the critical angle, ψ_1, for channeling in the high energy region is given by

$$\psi_1 = (2 Z_1 Z_2 e^2/d E)^{1/2} \tag{6}$$

where E is the energy of the incident ion. (6) is valid as long as $Ca/\psi_1 d$ is larger than unity which is approximately equivalent to the condition

$$E > E' = 2 Z_1 Z_2 e^2 d/a^2. \tag{7}$$

At low energies where $E < E'$, the quantity $Ca/\psi_1 d$ is small compared to unity which gives

$$\psi_2 = (C^2 a^2 Z_1 Z_2 e^2/E d^3_{hkl})^{1/4} \tag{8}$$

where ψ_2 is the critical angle for channeling in the low energy region and d is given the subscript hkl to denote a particular direction. This equation for ψ_2 is a rough estimate and can hardly be expected to hold at very low energies.

A classical treatment for the motion of the particles is appropriate here. The stopping is almost exclusively due to electronic stopping. The nuclear stopping is only 1% of the electronic stopping in this energy region for a random system.[5] The nuclear stopping is further reduced when the particles are moving along an open direction in the crystal. At low velocities, $v < v_o$, the electronic energy loss can be approximately calculated from the equation

$$(dE/dx)_e = 8\pi N e^2 a_o Z_1 Z_2 \xi_\epsilon (Z_1^{2/3} + Z_2^{2/3})^{-3/2} v/v_o \tag{9}$$

given by Lindhard and Scharff[5] where v is the incident particle velocity, $v_o = e^2/\hbar$, and $\xi_\epsilon \simeq Z_1^{1/6}$.

EXPERIMENTAL APPARATUS AND PROCEDURE

The bombarding equipment and the goniometer and detector geometry have been described elsewhere.[3,6] The important parameter which is varied in this experiment is the energy of the incident particle. The lowest incident ion energy is set by the thickness of the gold foil and the sensitivity of the detection system. The upper energy limit is set by voltage isolation conditions in the equipment. Because of radiation damage and contamination build up, the time available for bombardment without introducing large errors is shorter at the higher energies. A practical energy interval for the present equipment is found to be about 1 to 25 kev. The measuring procedure has been described in detail earlier.[3] The only difference in this experiment is that the bombarding times and thus the total amounts of radiation damage are kept small by concentrating the measurements on the peaks and their immediate surroundings. Measurements for all orientations of the foil are taken for only a few of the foils.

The gold films are made by vacuum evaporation of gold onto silver which in turn has been vacuum evaporated onto rocksalt. After the gold films have been stripped from the rocksalt and silver they are mounted on 75 mesh grids. The details of the growing technique can be found elsewhere.[7] The mounted foils are examined for wrinkles using an optical microscope and foils with any visible wrinkles are discarded. The foils are also examined with an electron microscope. The thicknesses of the foils are checked by measuring the projections of the stacking faults on the plane of observation. The foils usually show bend extinction contours which indicate the presence of submicroscopic wrinkles. The amount of the variation in

foil orientation is checked by observing the selected area diffraction patterns from small areas. The diffraction pattern for a perfectly flat thin single crystal foil shows Laue zones where the diffraction spots are strong.[8] If the foil is normal to the electron beam, the circular Laue zones are centered on the incident beam spot. If, however, the film is not normal to the electron beam due to the submicroscopic wrinkles, then the center of the zeroth Laue zone is displaced from the incident beam spot and the displacement gives the relative local orientation of the foil. With reasonable care it is possible to set the selected area mask to a small enough opening so that the variations in orientation within the selected area do not obscure the Laue zone structure. It is then easy to check the orientation at different points by moving the sample. A typical good foil has a standard deviation in orientation angle of $0.5° \pm 0.25°$. According to an earlier estimate of the influence of the foil misorientation on the angular resolution of a channel peak, the effect of the submicroscope wrinkles is found to be less than 1%.

RESULTS AND DISCUSSION

Fig. 1a shows the energy spectrum for 12 kev D^+ ions channeled along the $\langle 011 \rangle$ direction in a 350-400 Å thick gold foil. The final particle energy E_f in kev is determined from the voltage U in kilovolts applied to the plates of the electrostatic analyzer. In this case $E_f = 8.13$ U. This relationship is found from energy analysis of the incident beam with the foil removed and agrees with the value calculated from the geometry of the analyzer. Fig. 1b shows the energy spectrum for an azimuthal angle of rotation φ around the foil normal such that the ions travel along a high

index direction in the crystal. One observes that the intense peak decreases by a factor of about 40 when φ is changed from a low index direction (Fig. 1a) to a high index direction (Fig. 1b). The small peaks in both figures indicate the energy of the direct beam. In this particular run the intensity of the direct peak relative to the channel peak is extraordinarily high and is probably due to a small tear in the foil. Normally nothing is seen at all of the direct beam. The most probably energy loss $\Delta E_{mp}^{(r)}$, as determined from Fig. 1b for hkl large, is given the superscript (r) to indicate that the direction has a high index. The difference $\Delta E_{mp}^{\langle 011\rangle} - \Delta E_{mp}^{(r)}$ is due to the effect of channeling on the energy loss. The results of the energy loss measurements are summarized in Table I. The transmission T which is the ratio of the transmitted intensity in the forward direction to the incident intensity is also given in Table I. It is a function of the foil perfection and flatness and is included here to give an idea of its magnitude.

Figure 2 shows the transmitted intensity as a function of tilt angle for D^+ ions of 1.8 kev incident on a 225 Å thick gold single crystal. Fig. 3a shows the angular distribution in the transmitted intensity when the detector angle α with respect to the incident beam direction is varied with the foil fixed in the $\langle 001 \rangle$ direction. Fig. 3b shows the distribution for a variation of both θ, the tilt angle, and α such that $\theta = \alpha$ which means that the detector is kept fixed along the $\langle 001 \rangle$ direction. In this particular case we obtain for the channel entrance characteristic half-width a value $\sigma_{1\theta} = 4.5^\circ \pm 0.2^\circ$. For the channel exit characteristic half-width we obtain the value $\sigma_{2\theta} = 4.3^\circ \pm 0.2^\circ$. From Fig. 2 we obtain a value $\sigma_\theta = 3.1^\circ \pm 0.2^\circ$ by changing θ. This value agrees very well with the value 3.1° calculated from simple geometrical considerations.[3] From several other measurements of this kind we obtain the relationship

$$\sigma_{1\theta} = (1.0 \pm 0.1)\, \sigma_{2\theta} \quad . \tag{10}$$

A previous estimate[3] of the ratio $\sigma_{1\theta}/\sigma_{2\theta}$ gave the value 0.7 for 25 kev D^+ ions in gold. The suggestion was made that due to the energy loss the value of $\sigma_{2\theta}$ should be slightly higher than $\sigma_{1\theta}$. The ratio is checked here at 1.8, 3.3 and 11.3 kev and is found to be 1.0 ± 0.1. It is true that the energy loss due to electronic excitations and ionizations becomes less important as the energy $\bar{E}$ decreases. Consequently, the focusing effect due to correlated nuclear collisions, which is the origin of the channeling

effect, may play a larger role at very low energies and thus make the ratio $\sigma_{1\theta}/\sigma_{2\theta}$ less dependent on energy. Fig. 4 shows the pronounced change in angular resolution when the incident D^+ ion energy is increased to 8.5 kev. The same foil is used to obtain the data shown in Figures 2, 3, and 4.

In order to obtain the critical angle for channeling α_c, the following construction is performed. At the point defining σ, a tangent is drawn towards the background intensity. The angle where the tangent meets this intensity is defined as the experimental critical angle α_c. We find that

$$\alpha_c = (2.14 \pm .18)\sigma_{1\theta} \quad . \tag{11}$$

From (10) and elsewhere[3] we thus find that $\sigma_{1\theta} = \sqrt{2}\,\sigma_\theta$ so that the final relation is

$$\alpha_c = 2.14\sqrt{2}\,\sigma_\theta \quad . \tag{12}$$

Thus by measuring σ_θ, the characteristic half-width of a channel peak, α_c can be determined. As a comparison it is worthwhile mentioning that if the peak profiles are perfect Gaussian distributions, one would obtain a factor $2\sqrt{2}$ relating α_c and σ_θ.

Figures 5a, 5b, and 5c show the critical angle for channeling α_c as a function of the average ion energy $\bar{E}$ in the foil for the three low index crystallographic directions $\langle 011\rangle$, $\langle 001\rangle$, and $\langle 112\rangle$. The average ion energy is obtained from the incident ion energy E by the relation $\bar{E} = E - \frac{1}{2}\Delta E_{mp}$. The solid curves represent the theoretical expression $\psi_2(E)$ and the filled circles represent the experimental values. Several different foils have been used in order to avoid errors from contamination

build up and radiation damage. The foil thickness cannot be exactly reproduced in the evaporation equipment. Consequently the foil thicknesses are found to range between 180 and 260 $\mathring{A}$. This spread in thickness explains most of the spread in α_c. It is seen in Fig. 5 that the approximate expression given by Lindhard fits the experimental points for all three of the channels if the constant C is given the value 2.15. The low energy value ψ_2 is the appropriate one to use since it can be seen that E' = 810 keV for an H^+ ion in the low index directions.

The critical angle for channeling ψ_2 is symmetrically dependent on Z_1 and Z_2. The choice of practical values for Z_2 is limited but it is possible to get suitable silver foils for use as targets. Silver foils were used in a few of the experiments but the fact that ψ_2 varies as $\left[Z_1 Z_2/(Z_1^{2/3} + Z_2^{2/3})\right]^{1/4}$ causes only a small change in ψ_2 for a change of Z_2 from 79 to 49. The expected change of 5% is less than the experimental error.

The change in ciritcal angle as a function of Z_1, is investigated by comparing the results for H^+, D^+ and He^+ ions. When H^+ ions are used instead of D^+ ions, the mass is decreased by a factor of 2 while Z_1 is constant. A comparison between D^+ ions and H^+ ions is made by using the same foil and the same incident energy E. A similar comparison is made between D^+ ions and He^+ ions. The use of these ions gives a change in both Z_1 and the mass M, of a factor of 2. The results of these measurements are best presented in Table II. An approximate correction is made for the different energy losses experienced by the three different particles so that the critical angles are compared at about the same energy $\bar{E}$. Table II shows that there is no difference between $\sigma_\theta(H^+)$ and $\sigma_\theta(D^+)$. It is also seen that $\sigma_\theta(He^+)$ is larger than $\sigma_\theta(D^+)$ by a factor of 1.13 ± .04 which is significantly larger than 1. The theoretical factor expected from (8)

is 1.17 so the experimental result agrees with the theoretical prediction.

CONCLUSION

The critical angles for channeling of light ions at low energies are in good agreement with the approximate expression for ψ_2 calculated by Lindhard if the arbitrary constant, C, in Lindhard's expression is assigned the value of 2.15.

ACKNOWLEDGEMENTS

The authors would like to express their sincere gratitude to J. Lindhard, H. Shiött and J. U. Andersen for helpful discussions and valuable comments.

REFERENCES

1. R. S. Nelson and N. W. Thompson, Phil. Mag. 8, 1677 (1963).
2. C. J. Andreen and R. L. Hines, Phys. Letters, 24A, 118 (1967).
3. C. J. Andreen and R. L. Hines, Phys. Rev. 151, 341 (1966).
4. J. Lindhard, Kgl. Danske Videnskab. Selskab., Mat. Fys. Medd. 34, No. 14 (1965).
5. J. Lindhard and M. Scharff, Phys. Rev. 124, 128 (1961).
6. R. L. Hines and R. Arndt, Phys. Rev. 119, 623 (1960).
7. D. W. Pashley, Phil. Mag. 4, 324 (1959).
8. Electron Microscopy of Thin Crystals, P. B. Hirsch, A. Howie, R. B. Nicholson, D. W. Pashley, and M. J. Whelan, (Butterworth, Inc., Washington, 1965), p. 112.

CAPTIONS

Fig. 1. The transmitted D^+ intensity in the forward direction through a gold foil is shown as a function of the emerging ion energy as determined with an electrostatic analyzer.

(a) The foil is oriented in the ⟨011⟩ direction. The arrow indicates the energy of the direct beam.

(b) The foil used in (a) is now oriented in a high index direction with the same tilt angle θ as in (a). The arrow again indicates the energy of the direct beam.

Fig. 2. The transmitted intensity is shown for D^+ ions in the (100) plane as a function of the tilt angle θ. The incident ion energy is 1.8 keV, the incident current is 100 $\mu\mu$A and the foil thickness is about 225Å. The characteristic half-width is found to be $\sigma_\theta = 3.1^\circ \pm 0.2^\circ$ for the ⟨001⟩ peak.

Fig. 3. (a) The transmitted intensity is shown as a function of the detector angle α with respect to the forward direction for the foil oriented on the ⟨001⟩ channel. The chacteristic half-width $\sigma_{2\theta} = \sigma_\alpha$ is found to be $\sigma_{2\theta} = 4.3^\circ \pm 0.3^\circ$. The same foil is used as in Fig. 2.

(b) The transmitted intensity is shown as a function of α with the foil tilted so that $\theta = \alpha$ about the ⟨001⟩ channel. The characteristic half-width is found to be $4.5^\circ \pm 0.3^\circ$. The same foil is used as in Fig. 2.

Fig. 4. The transmitted intensity is shown as a function of θ in the two planes (100) and (110) for 8.5 kev D^+ ions. The incident current is 1000 $\mu\mu$A. The dot-dashed line indicates the randomly scattered ions. The difference between the dashed line and the dot-dashed line represents the planar channeling in the (100) plane. No planar channeling is seen in the (110) plane. The widths of the stronger peaks are quite a bit smaller than in Fig. 2. The same foil is used as in Fig. 2.

Fig. 5. The critical angle for channeling ψ_2 is shown as a function of the average energy $\bar{E}$ of the ions in the crystal for the three channels (a) ⟨011⟩, (b) ⟨001⟩, and (c) ⟨112⟩. The solid lines are the theoretical curves using the theory by Lindhard with a value of $C = 2.15$. The filled circles represent the experimental critical angles α_c and the vertical bars show the errors. The errors in energy vary from 0.3 keV at 1 kev to 0.5 keV at 17 keV. Most of the spread of the experimental points is due to the fact that the information is obtained using several films with different thicknesses between 180 and 260 Å.

Table I. The most probable relative energy loss $\Delta E_{mp}^{(hkl)}/E$ in the directions ⟨011⟩ and ⟨001⟩ and the transmission coefficient T in the forward direction along the ⟨001⟩ channel are given for H^+, D^+, and He^+ ions at a few different values of the incident energy E. The relative energy loss is larger in the ⟨011⟩ direction due to the fact that the effective foil thickness is $\sqrt{2}$ times larger than in the ⟨001⟩ direction.

Table II. The characteristic half-widths σ_θ for transmitted H^+, D^+, and He^+ ions respectively are given for the three crystallographic directions ⟨011⟩, ⟨001⟩, and ⟨112⟩ for five different single crystal gold foils. The probable errors of the numbers are between 5 and 10%.

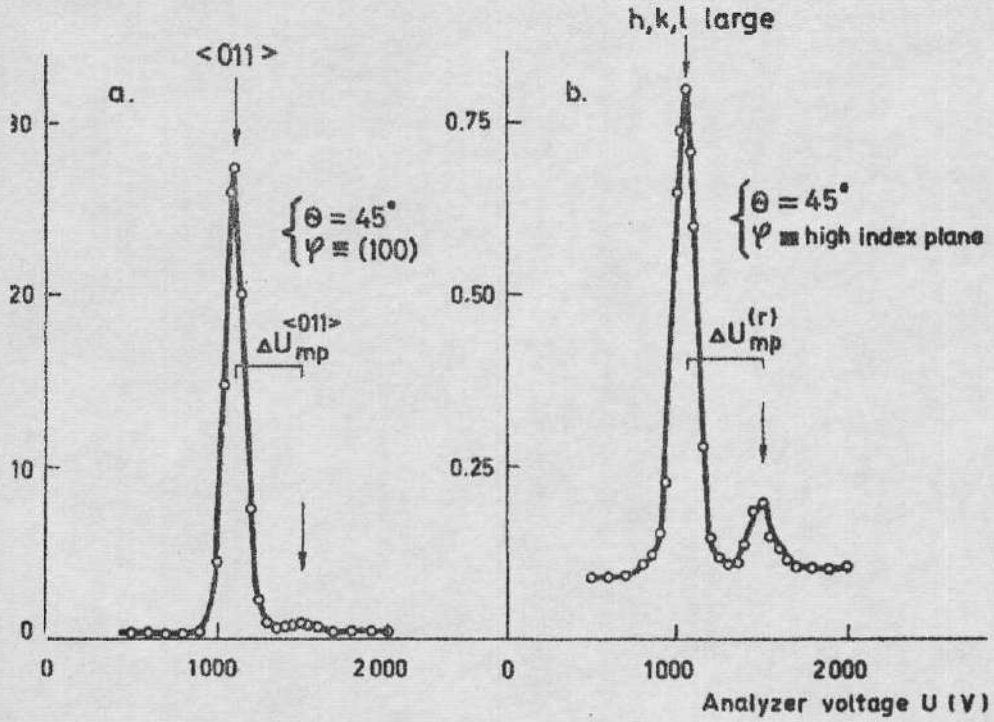
a.
<011>
Θ = 45°
φ ≡ (100)
ΔU_mp^<011>
b.
h,k,l large
Θ = 45°
φ ≡ high index plane
ΔU_mp^(r)
30
20
10
0
0.75
0.50
0.25
0
1000
2000
Analyzer voltage U (V)

Fig.1.

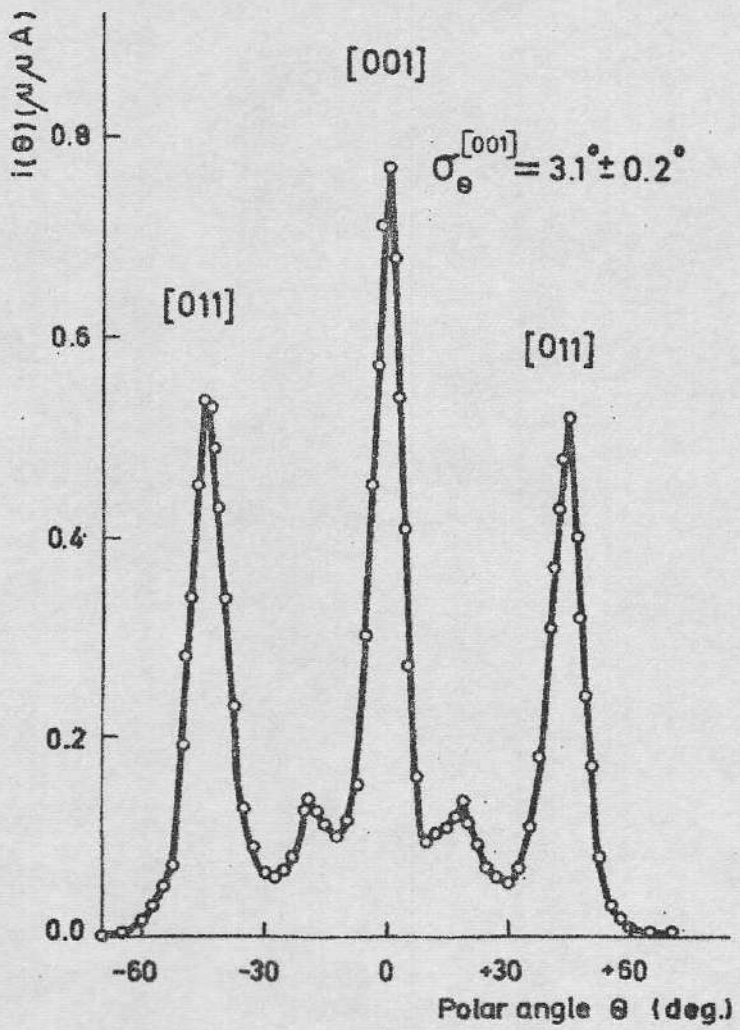
i(Θ)(μμA)
[001]
σ_Θ^[001] = 3.1° ± 0.2°
[011]
[011]
0.8
0.6
0.4
0.2
0.0
-60
-30
0
+30
+60
Polar angle Θ (deg.)

Fig.2.

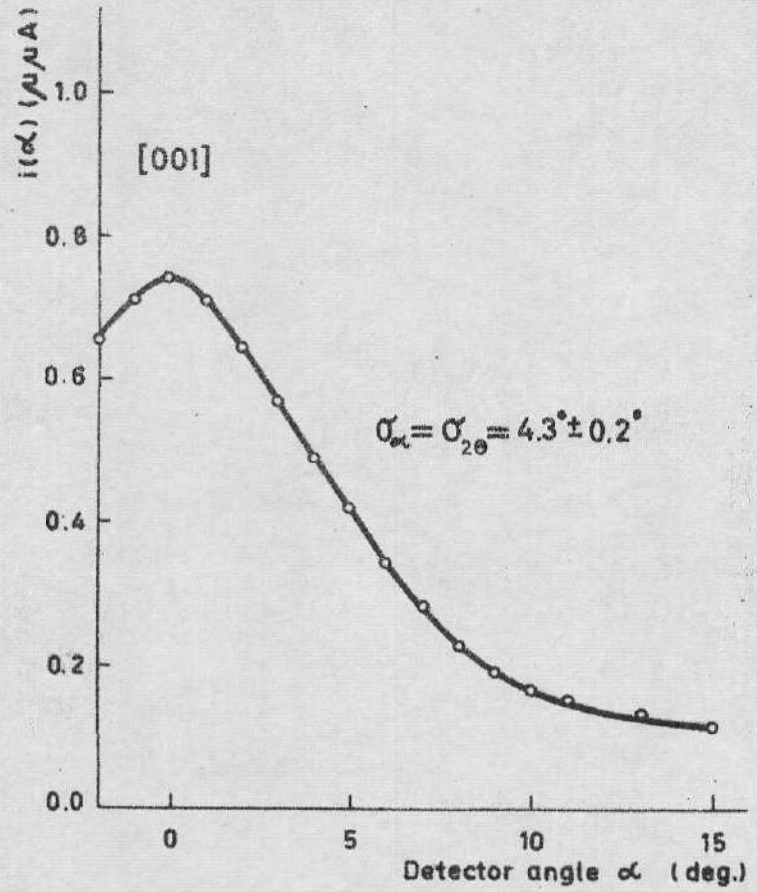
i(α) (μμA)
1.0
0.8
0.6
0.4
0.2
0.0
[001]
$\sigma_\alpha = \sigma_{2\theta} = 4.3^\circ \pm 0.2^\circ$
0
5
10
15
Detector angle α (deg.)

Fig.3a.

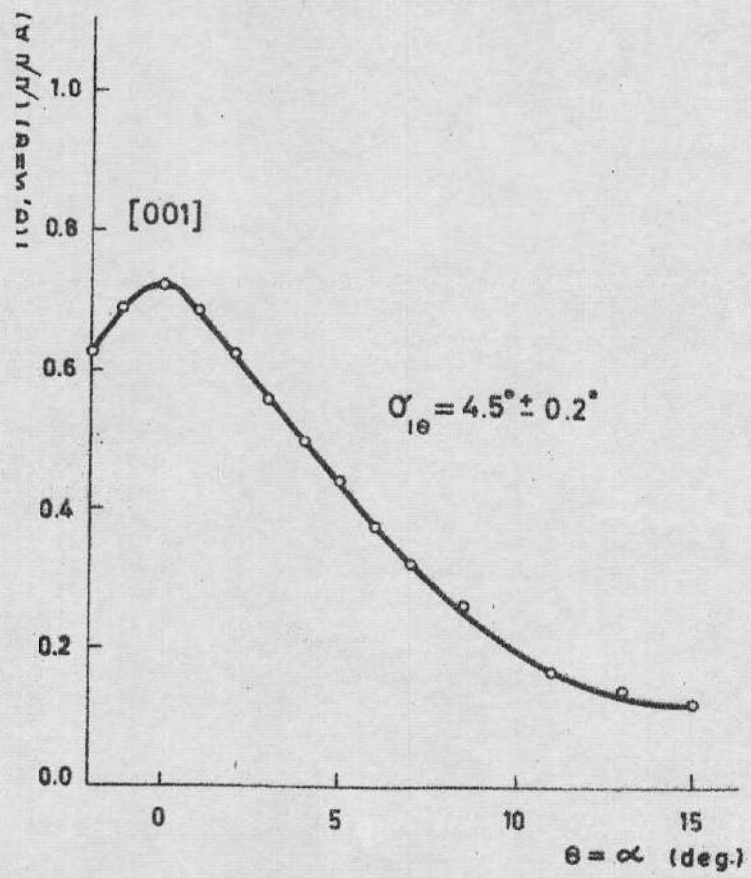
i(θ, α=2θ) (μμA)
1.0
0.8
0.6
0.4
0.2
0.0
[001]
$\sigma_{1\theta} = 4.5^\circ \pm 0.2^\circ$
0
5
10
15
θ = α (deg.)

Fig.3b.

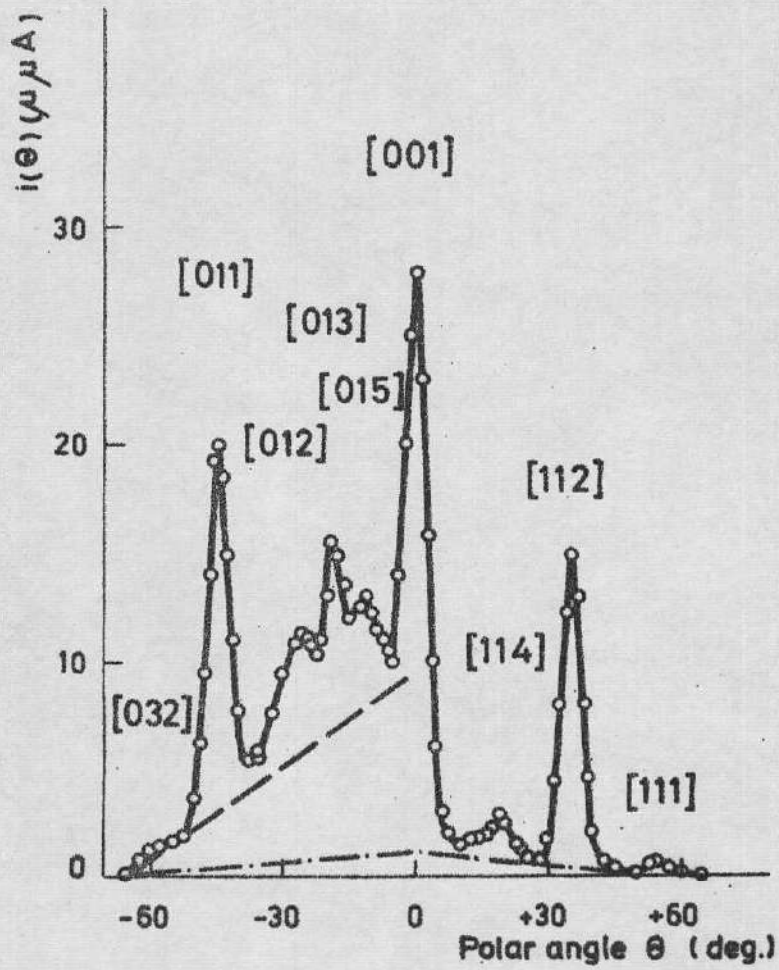
i(Θ)(μμA)
30
20
10
0
[001]
[011]
[013]
[015]
[012]
[112]
[114]
[032]
[111]
-60
-30
0
+30
+60
Polar angle θ (deg.)

Fig.4.

Fig.5.

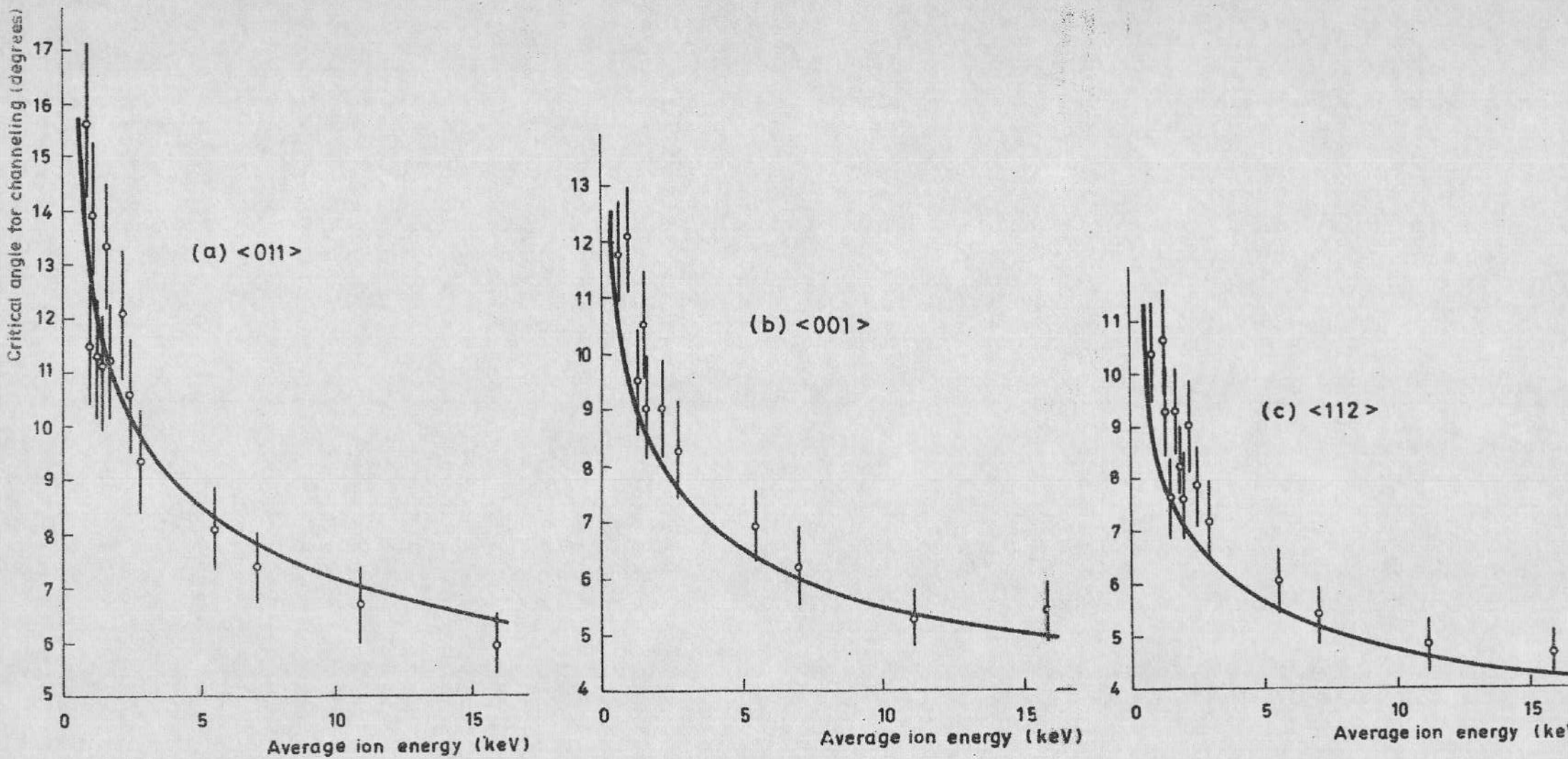
Critical angle for channeling (degrees)
(a) <011>
(b) <001>
(c) <112>
Average ion energy (keV)
Average ion energy (keV)
Average ion energy (ke

Foil. No.	Ion	E keV	$\Delta E^{<011>}_{mp}/E$ %	$\Delta E^{<001>}_{mp}/E$ %	$T_{<001>}$ %
852 NK	H^+	14.3	29.3	21.7	2
~265 Å	D^+	14.3	21.7	16.6	4
	He^+	14.9		21.0	0.1
	He^+	28.8		15.4	2
853 NK	H^+	14.2	27.0	20.7	3
	H^+	28.3	18.9	14.5	13
~250 Å	D^+	14.3	19.2	14.3	6
	D^+	28.5	13.7	10.0	15
	He^+	14.8		17.0	0.2
854 NK	H^+	14.2	29.8	23.7	2
	H^+	28.4	21.2	16.8	10
	D^+	14.1	24.4	18.3	5
~260 Å	D^+	28.4	17.4	13.6	13
	He^+	14.9	30.3	22.0	0.03

Table I

Foil. No.	E keV	$\sigma_\Theta(H^+)$ deg			$\sigma_\Theta(D^+)$ deg			$\sigma_\Theta(He^+)$ deg		
		<011>	<001>	<112>	<011>	<001>	<112>	<011>	<001>	<112>
823 MN	23	2.2	2.1	1.9	2.3	2.1	2.0			
837 NH	3	4.0	3.5	3.0	4.0	3.5	3.0			
883 NR	18				2.1	1.9	1.6	2.5	2.4	1.9
885 NS	17				2.6	2.5	2.1	2.8	2.7	2.1
892 NT	18				2.2	2.1	1.6	2.4	2.3	1.9

Table II

DOKTORSAVHANDLINGAR
VID
CHALMERS TEKNISKA HÖGSKOLA
Ny serie Nr 64

Experiments on the Transmission of low Energy Light Ions Through Thin Films of Different Structures

by

C.J. Andreen

Chalmers University of Technology

Gothenburg, Sweden

Abstract

Transmitted intensities of D^+ ions through polycrystalline, textured and single crystal films of Au are shown as functions of the polar angle θ and the azimuthal angle φ. Ag, α-Fe and mica have also been used. In one case the most probable energy loss $\Delta E_{mp}(\theta)$ is shown. It is found that governed motion exists in films which are not single crystals. It is shown that a gold lattice may grow on top of a silver lattice in such a way that the gold atoms occupy normal silver lattice sites. A semiconductor doping technique is suggested based upon a precanalisation of the ions.

INTRODUCTION

Since quite recently [1-4] it is known that correlated small angle scattering of ions is possible along low index crystallographic directions and planes in a lattice. Most of the work on this so called channeling effect has been done at energies in the MeV region. Very few investigations [5,6] dealt with ion transmission of energies below 50 keV. The main reason for this fact is the increasing difficulties to obtain targets thin enough to transmit low energy ions. It has been shown[7], that it is relatively easy even with quite rough detecting systems to use thin gold films which allow the use of energies down to about 1 keV.

Conventional electron microscopy limits the thickness of a gold film to about 1000 Å. A comparison between the transmission characteristics for electrons and ions transmitted through matter can therefore be made by using film thicknesses below this value.

The purpose of this paper is to show that the interpretation of the ion transmission curves for light ions transmitted through thin foils is consistent with the interpretation of electron microscope pictures taken on the same foils. Only one illustrative diffraction pattern is included here. The advantage of using the channeling effect to get information about the structure of a target much thicker than 1000 Å is obvious. The observation that channeling of ions does occur from the low keV region[8] up till about 100 MeV[9], makes it possible to use conventional machines such as the isotope separator and the van de Graaff generator to study among other things the structure of a target. In the high energy region the conventional apparatus in nuclear physics is directly applicable to channeling work.

In this investigation all characteristics of the transmitted distribution other than the position of the peaks and their relative intensities, are left without notice. Experiments on the critical angle for channeling ψ and the most probable energy loss ΔE_{mp} are reported elsewhere[7,8]. Normal intensity distributions (the intensity as a function of the polar angle θ and the azimuthal angle φ) can be found below for single crystal gold films and single crystal α -iron films. A drastic difference as far as these distributions are concerned, between crystals grown in the same orientation will be interpreted as a difference in the structure of the films. In one case a <111> oriented f.c.c. crystal is shown. The transmitted distribution of this film is naturally different from a <001> oriented film.

EXPERIMENTAL

The experimental apparatus is described in ref. 10. The possibility to vary the detector angle α is not used here. The bombarding particles are D^+ ions of about 15 keV energy. A description of the foil preparation techniques may be found elsewhere [11, 12]. The foils are grown on glass, rocksalt and rocksalt-silver. They are mounted on 3 mm Cu microscope grids. An electron microscope is used to check the results from the ion transmission measurements. An optical microscope is also used to select those gold films which have no visible wrinkles. The influence of microwrinkles is less disturbing.

RESULTS AND DISCUSSION

Polycrystalline films of Au and Ag

Au. 99,99% gold wire is evaporated on to a glass substrate at about 40 - 60°C. Fig. 1 shows the transmitted distribution i (Θ) of D^+ ions as a function of the polar angle Θ . The most probable energy loss ΔE_{mp} of the transmitted ions is also given as a function of Θ. No variation in the intensity is observed when the azimuthal angle φ is varied for constant θ ($\Theta \neq 0$). The variation in the intensity i(Θ) as well as in the energy loss ΔE_{mp}(Θ) in Fig. 1 is due to changes in the effective foils thickness t traversed by the ions in different directions. t varies as $1/\cos \Theta$. A variation of φ with Θ = const. means that the effective foil thickness is constant. The diffraction pattern taken for this foil shows that it is a polycrystal with a random orientation. It is known that it is impossible to produce amorphous gold films by simple means such as evaporation. If not so there is no way of telling the structure in the actual foil from an amorphous one by using the ion transmission.

If rocksalt is used as a substrate in stead of glass the structure of the film becomes more and more ordered as the substrate temperature increases. Fig. 2 shows the transmitted intensity i(Θ) through an 850 Å thick film evaporated onto rocksalt at 40 - 60°C. The diffraction pattern for this film shows that the rings are less homogenous and that occational strong spots appear. The energy spectrum indicates a small deviation from the smooth cosine like curve in Fig. 1. The ion transmission curves give more direct information than electron transmission in this particular case. The anomalous energy loss is more pronounced in Fig. 3. The rocksalt tempe-

rature is here 70 - 100°C. A variation of φ still does not result in any change of the intensity. The dot-dashed lines indicate the intensity due to randomly oriented crystallites. In Fig. 2 the orientation of the crystallites giving rise to the peaks is almost exclusively in the <111> direction. Apart from this preferred <111> axis, the orientation of the crystallites is random. In Fig. 3 there is a growing component oriented in the <001> direction. The diffraction pattern shows more frequent spots of higher intensities. Again ion transmission gives more direct information than electron diffraction. The curves in Fig. 2 and Fig. 3 are interpreted as being due to two types of recrystallisation textures. Each type of texture has one preferred axis of orientation. If the foil is tilted inside the electron microscope it is found that the two textures are present simultanously. Under specific conditions one texture is able to grow faster than the other.

When the substrate temperature is increased till just below the epitaxial temperature the mobility of the gold atoms on the rocksalt is high enough for the crystallites to start to grow with two axes in common. This is shown in Fig. 4a and 4b. In Fig. 4a the angle φ corresponds to the plane {110}. In Fig. 4b the angle Θ is set at 35.5 degrees, the angle for one of the peaks in Fig. 4a. It is immediately seen in Fig. 4b that instead of a constant intensity there is now a peak for every 30° in φ. This observation can be explained by the presence of twinned crystallites oriented in the <111> direction, which is also the twin axis. The twins are rotated 180° relative to each other. If the value of φ in Fig. 4a is changed slightly it becomes clear that the foil also contains a second component. Fig. 5a shows the transmitted intensity i(Θ) as a function of Θ for a φ-

value about 15° off the {110} plane. Peaks now also appear at $\theta = 45°$. Fig. 5b shows the transmitted intensity $i(\varphi)$ as a function of φ for $\theta = 45°$. It is observed that every third peak is more intense than the others. These peaks are partly due to a component with an <001> direction parallell to the foil normal, while the weaker peaks are planar contributions from the {111} planes due to the twins in the <111> orientation. This interpretation is consistent with the result obtained from two overlapping stereograms drawn in the <001> and the <111> orientations, respectively. The diffraction pattern shows 12 spots located on the normal positions of the rings for a polycrystalline material. Some of the spots are in common with both types of orientations. The angular relationship between the <111> and the <001> orientations is shown in Fig. 6.

In a few cases it was possible to obtain thick gold films with almost exclusively the <111> twin orientation (~95 %). Fig. 7 shows the transmitted intensity $i(\theta)$ for a 900 Å thick gold crystal in one of the {110} planes. In order to explain further the intensity distribution in Fig. 4a we show again in Fig. 8 the {110} plane in an <001> oriented single crystal gold film. It is quite obvious that if the profiles in Fig. 7 and Fig. 8 are added together properly, one obtains Fig. 4a. This fact gives extra support to the statement that the foil shown in Fig. 4a consists of two different orientations one of which is twinned. The half width of the peaks in Fig. 7 is relatively large due to the large energy loss of the ions during the passage through the gold film.

Ag. Polycrystalline silver films are grown only at one low temperature, about 30°C, on rocksalt. The ion transmission curves and the diffrac-

tion pattern give the same result as the gold film in Fig. 1.

Single crystal films of Au and Ag

Au. Above the epitaxial temperatures for gold on rocksalt or gold on silver-rocksalt, the foil is found to be a good single crystal. The epitaxial relations are $\langle 001 \rangle_{NaCl} // \langle 001 \rangle_{Au}$ and $\langle 001 \rangle_{NaCl} // \langle 001 \rangle_{Ag} // \langle 001 \rangle_{Au}$. Fig. 9a shows the transmitted intensity $i(\Theta)$ for φ-values corresponding to the {100} and the {110} planes. Fig. 9b shows the intensity $i(\varphi)$ for $\Theta = 45^{\circ}$. These two distributions constitute the normal behaviour for a good f.c.c. crystal at energies around 15 keV. The diffraction pattern is a normal single crystal pattern for a cubic lattice without any extra spots.

Ag. Fig. 10 shows the transmitted intensity $i(\Theta)$ and the most probable energy loss ΔE_{mp} as functions of Θ in the two planes {100} and {110}. The foil thickness is about 800 - 1000 Å. A variation of φ for $\Theta = 45^{\circ}$ gives the intensity curve exemplified in Fig. 9b. The diffraction pattern is typical for a cubic lattice with a lattice constant very close to the one for gold. No fundamental difference is observed between silver and gold as far as the channeling characteristics are concerned. The preparation of very thin homogenous silver films is difficult, however. All silver films have a thickness around 800 Å or thicker.

Polycrystalline films of Fe

Iron films are prepared by evaporation of iron wire and by iron wire explosions onto hot rocksalt surfaces. At low substrate temperatures

the films are polycrystalline and have a diffraction pattern similar to the one described above in connection with Fig. 1. The film thickness is determined by the change in frequency for a crystal oscillator.

Single crystal films of Fe

Above about 400°C the iron films are good single crystals. The diffraction pattern is characteristic of a cubic lattice. The lattice constant is found to be in good agreement with earlier measurements for α-iron. Details about the preparation of iron films can be found elsewhere [12, 13]. Fig. 11a shows the transmitted intensity i(Θ) for 15 keV D^+ ions channeled through a 600 Å thick single crystal α-iron film. Peaks due to the crystallographic directions, calculated to be the most important ones in a b.c.c. lattice, are shown both in the {110} and the {100} planes. The dot-dashed curve represents the intensity transmitted along high index directions. Dashed lines divides the channeled intensity into directional and planar channeling [14]. Fig. 11 b and Fig. 11c show the transmitted intensities as functions of φ for $\Theta = 45^\circ$ and $\Theta = 25^\circ$, respectively. Both directional and planar channeling are present as indicated in the figures. Fig. 11a, b and c are typical transmission curves for light ions of low energies in b.c.c. lattices.

Mica

A thin sheet of mica with an estimated thickness of a few hundred Ångström is examined by ion transmission. No structural effects whatsoever could be observed neither in a Θ-function nor in a φ-function. The diffrac-

tion pattern shows a good crystal structure of the hexagonal type. The distance between the spots in the diffraction pattern shows, however, that the lattice constants for mica is several times larger than for gold or silver. Electron microscope pictures show that the sheet of mica is free from pinholes and is quite homogenous. This is confirmed by the very small transmission coefficient of ions in the forward direction. The absence of structural effects in the ion transmission curves may be explained by a few possible facts. First, the number of channels is larger in the hexagonal structure than in the f.c.c. or the b.c.c. structure. The overlapping of many broad peaks may result in a fairly smooth distribution. The complete absence of any sign of a structure makes this explanation less probable. Second, the fact that the lattice constants are quite large in mica may result in an uncorrelated or random scattering. It may be that there is an upper limit for the lattice constant, above which no correlated scattering can occur, other parameters being constant. A third possible explanation is that the electron microscope is less sensitive to the interior of a crystal than the channeling mechanism is found to be. If the mica sheet is composed of several layers dislocated relative to each other, the directional channels may be effectively blocked.

Application of channeling to growth characteristics

Without separating the silver and the gold from each other for a silver-gold sandwich, the two layers are investigated simultaneously by channeling of 25 keV D^+ ions. The silver is then dissolved and the same gold is used again. The transmitted intensity i(0) for the double film shows

a normal distribution like the one in Fig. 9a. The total thickness of the sandwich is about 2000 Å. The ratio normally found between the intensities in the <001> and the <011> peaks is confirmed and the <013> channel is clearly visible. The width of the peaks is consistent with the large energy loss of the ions in the film. The intensity $i(\varphi)$ for $\theta = 45^{\circ}$ shows the four normal <011> peaks. If the gold foil alone is used, the φ-function for $\theta = 45^{\circ}$ again shows four normal peaks. The diffraction pattern for the gold films shows a normal cubic lattice. The double film is too thick, however, for the electrons to give a diffraction pattern. It is clear that in this particular case ion transmission is superior to conventional electron microscopy. The result of this experiment is that the gold lattice grows with its three main axes parallell to the three main axes for the silver lattice. A relative rotation $\Delta\varphi$ between the silver and gold lattice would result in a double pattern [14]. A translatory shift along one of the main axis may be possible. Such a shift would not block a channel completely but merely influence the transmitted intensity to some degree. In order to block the channels <001> and <011> simultaneously the gold atoms have to occupy the positions$(2n+1/4,\ 2n+1/4,\ 2n+1/4)$ relative to a reference lattice point. This position is less probable than the lattice site itself. No indications of blocking either the <001> or the <011> channels is observed. Despite the long irradiation time used on the silver-gold sandwich on the silver side, the gold exhibited a surprisingly low damage rate. Almost no damage could be observed. This supports the conclusion that the gold atoms actually occupies normal silver lattice sites. The small misfit of 0,3 % should be of no influence.

The observations made here with a silver-gold sandwich may be valuable for the application of channeling to the doping of semiconductors without introducing heavy damage. The technique of annealing during the ion inplantation is found to reduce the remaining damage drastically. An other way of attacking the problem may be to grow a single crystal film onto the surface of the crystal to be doped. If the lattice constant and the orientation of the crystal film could be chosen to match the semi-conductor surface exactly (or with only a very small misfit) the damage would preferably occur in the film. The film should then be dissolved from the semiconductor. Oen[15] has shown that along an open channel the damage is reduced by a large factor. By using a precanalisation in combination with annealing the damage may be reduced, to an absolute minimum.

S U M M A R Y

The investigation exemplifies governed motion as well as ungoverned motion[16]. It is shown that governed motion is exibited in films which are not necessarily single crystals. The lowest order of governed motion is found in textured films. It seems possible to distinguish between at least three different types of governed motion namely in growing textures, recrystallisation textures and single crystals, the last two types being exemplified here. The result of the comparison between electron and ion transmission shows that the use of ion transmission to study the structure of a material is in many respects similar to electron diffraction studies. With quite simple and inexpensive means it is possible to look at a material of much greater thickness using ions of energies below 25 keV than is possible with electrons of

100 keV energy. If individual particle counting is used instead of an intergrating electrometer to detect the ions it will most probably be found easy to use ions of energies near 100 keV and target thicknesses of the order of microns. In a few cases ion transmission gives more direct information about the foil structure than does the electron diffraction. The damage to the foil after long irradiations with light ions is unfortunate. The contamination of the foil is also disturbing but can be avoided by effective cooling and shielding. For thicker targets the channeling of light ions is superior to conventional electron diffraction. The experiment with the silver-gold sandwich shows that the two lattices most probably are lined up exactly relative to each other. This suggests a doping technique of semiconductors based on a precanalisation of the ions in a lattice which can easily be removed after the irradiation. The investigation further demonstrates the importance to avoid any structural effects in a foil in connection with cross section measurements in nuclear physics. It is shown in ref. 17 that in some directions the detector indicates a smaller than normal transmission probability due to the so called blocking effect. If the beam is incident along a low index direction and the detector is in a blocked direction, it is thus possible to find a cross section which is one order of magnitude too low.

Acknowledgement

The author would like to take this opportunity to thank Prof. R.L. Hines for his hospitality during my stay at Northwestern University. The cooperation with Dr. E. Wassermann, Fred Morris, Donald Weber and Willian Krakow is also deeply acknowledged.

The work is supported by the Atomic Energy Commission of the United States of America.

References

1. M.T. Robinson and O.S. Oen
Phys. Rev. 132, 2334 (1963)

2. R.W. Nelson and M.W. Thompson
Phil. Mag. 8 1677 (1963).

3. G. Dearnaley,
IEEE Trans. Nucl. Sci. 11, 249 (1964).

4. C. Erginsoy, H.E. Wegner, and W.M. Gibson
Phys. Rev. Letters 13, 530 (1964).

5. C.J. Andreen, R.L. Hines, W. Morris, and D. Weber
Phys. Letters 19, 116 (1965).

6. C.J. Andreen, E.F. Wassermann, and R. L. Hines
Phys. Rev. Letters 16, 782, (1966).

7. C.J. Andreen and R.L. Hines
Phys. Rev. 151, 341, (1966).

8. C.J. Andreen and R.L. Hines
Phys. Letters 24A, 118 (1967).

9. S. Datz, T.S. Noggle, and C.D. Moake
Phys. Rev. Letters 15, 254 (1965).

10. R.L. Hines and R. Arndt
Phys. Rev. 119, 623 (1960)

11. D.W. Pashley
Phil. Mag. 4, 324 (1959).

12. J.W. Mathews
Appl. Phys. Letters 7, 225 (1965)

13. S. Shinozaki and H. Sato
J. Appl. Phys. 36, 2320 (1965)

14. C.J. Andreen
Arkiv för Fysik. In print

15. O. Oen
Phys. Rev. Letters (1966).

16. J. Lindhard
Mat.Fys. Medd. Dan. Vid. Selsk. 34, 14 (1965)

17. C.J. Andreen
Arkiv för Fysik. In print

Figure captions

Fig. 1 The transmitted intensity i(Θ) and the most probable energy loss ΔE_{mp} for D^+ ions are shown as functions of the polar angle Θ for a polycrystalline gold film grown on glass at about 50°C. The film thickness is about 600 Å. The incident ion energy is 13 keV and the ion current $1.5 \cdot 10^{-8}$ A.

Fig. 2 The transmitted intensity i(Θ) and the most probable energy loss ΔE_{mp} for D^+ ions are shown as functions of Θ for a 850 Å thick gold film grown on rocksalt at about 50°C. A recrystallisation texture with the <111> orientation is becoming visible in both the intensity and the energy loss curves. The dot-dashed lines indicate the random distributions. The curves have rotational symmetry around a vertical axis through $\Theta = 0^\circ$.

Fig. 3 The transmitted intensity i(Θ) of D^+ ions and their most probable energy loss ΔE_{mp} are shown as functions of Θ . The incident ion energy is 13 keV and the incident ion current $2 \cdot 10^{-8}$ A. The film thickness is about 800 Å. The dot-dashed lines indicate the random distributions. The texture is more evident than in Fig. 2. A small component of a recrystallisation texture in the <001> orientation is becoming visible.

Fig. 4a. The two types of growing textures seen in Figs. 2 and 3 are present in higher percentages. The two sets of indices represent in order the <001> oriented texture and a twinned texture in the <111> orientation. The dot-dashed lines indicate the completely random distributions. The incident ion energy is 11 keV and the current 10^{-8} A. The gold film is about 700 Å thick.

Fig. 4b. The transmitted intensity $i(\varphi)$ of D^+ ions is shown as a function of the azimuthal angle φ for the gold film in Fig. 4a. The value of Θ is 35.5°. For every 30° degrees in φ there is a peak mainly due to <112> channels in the <111> oriented twin-crystals. Other channels contribute too but to a smaller degree.

Fig. 5a. If the φ-value corresponding to one of the minima in Fig. 4b is chosen ($\varphi = 0^\circ, 30^\circ, 60^\circ, 90^\circ, \ldots$) one obtains this quite different function $i(\Theta)$. Each of the intense peaks in Fig. 4a, except the <001> peaks, seems now to be split up into two peaks. The peaks at $\Theta = 45^\circ$ reveal the <001> oriented component. They represent contributions from the {111} planes belonging to the <001> orientation.

Fig. 5b. The transmitted intensity i(θ) is shown for $\theta = 45^{\circ}$ corresponding to the two peaks in Fig. 5a. It is now definitely clear that a <001> oriented texture component is present. For this component the periodicity is 90° while for the twinned <111> texture the periodicity is 30°. The fact that each of the smaller peaks is split up into two is due to contributions from {111} planes symmetrically positioned around the φ-values 30°, 60°, 90°, 120° etc.

Fig. 6. The relative orientation between the <111> oriented twins and the <011> oriented crystals is shown. It is found that the angle between a {100} plane in a <001> oriented crystal and a {110} plane in a <111> oriented crystal is 15°. It is clear from this fig. that every third peak should be more intense than the other due to the presence of the <001> oriented component.

Fig. 7. The transmitted intensity i(θ) is shown for D^{+} ions in a 900 Å gold single crystal film oriented almost exclusively in the <111> direction (~ 95 %). The intensity along a {110} plane is shown for comparison with Fig. 4a and Fig. 8. The incident ion energy is 12 keV and the ion current 10^{-8} A.

Fig. 8. The same {110} plane as in Fig. 7 is shown for a <001> oriented film. The <111> directions are too far out to be visible at the actual foil thickness and ion energy. The dot-dashed line indicates the completely random distribution. About 20 keV He^+ ions are used.

Fig. 9a. The transmitted intensity i(θ) is shown for D^+ ions in a very good single crystal of gold along the {100} and the {110} planes. This distribution is a normal one for an f.c.c. lattice. The incident ion energy is 17 keV and the ion current $1.7 \cdot 10^{-9}$ A. The film thickness is about 300 Å. The dot-dashed line represents the random distribution. The dashed line indicates the dividing line between directional and planar channeling.

Fig. 9b. The transmitted intensity i(φ) for $\theta = 45^\circ$ is shown for a similar film as in Fig. 9a. This is a normal profile as a function of φ for $\theta = 45^\circ$. The film thickness is about 200 Å. The incident D^+ ion energy is about 20 keV and the ion current 10^{-9} A.

Fig. 10. The transmitted intensity i (θ) and the most probable energy loss ΔE_{mp} are shown for D^+ ions of 21 keV energy along the {100} and the {110} planes in a 800 Å thick single crystal silver film. No significant difference can be found compared

to a single crystal gold film. Dot-dashed lines represent random distributions. Dashed lines indicate the dividing lines between directional and planar channeling.

Fig. 11a. The transmitted intensity $i(\theta)$ is shown as a function of θ along the planes {100} and {110} for D^+ ions of 13 keV in a b.c.c.α-iron film of about 600 Å. The dot-dashed line represents the random distribution. The dashed lines indicate dividing lines between directional and planar contributions to the total channeled intensity.

Fig. 11b and c. The transmitted intensity $i(\varphi)$ is shown for b. $\theta = 45^\circ$ and c. $\theta = 25^\circ$. In b. we identify the $\langle 011 \rangle$ type channels and $\{110\}$ type planes. In c. the largest contributions come from the two directions $\langle 113 \rangle$ and $\langle 012 \rangle$.

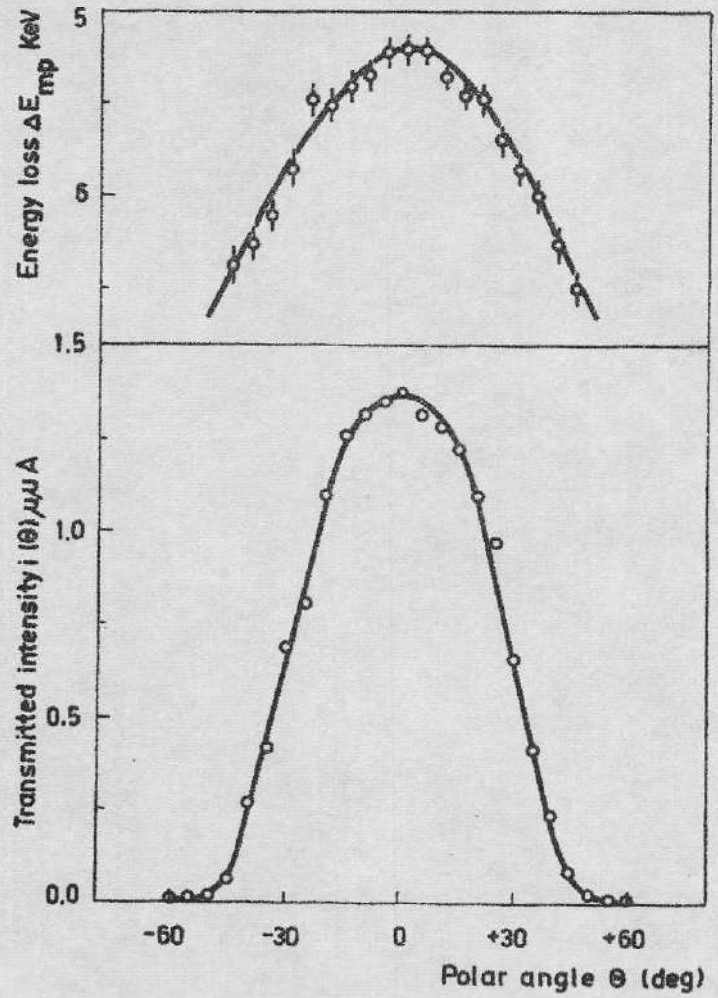
Energy loss ΔE_mp KeV
5
6
1.5
Transmitted intensity i (θ) μμ A
1.0
0.5
0.0
-60
-30
0
+30
+60
Polar angle θ (deg)

Fig.1.

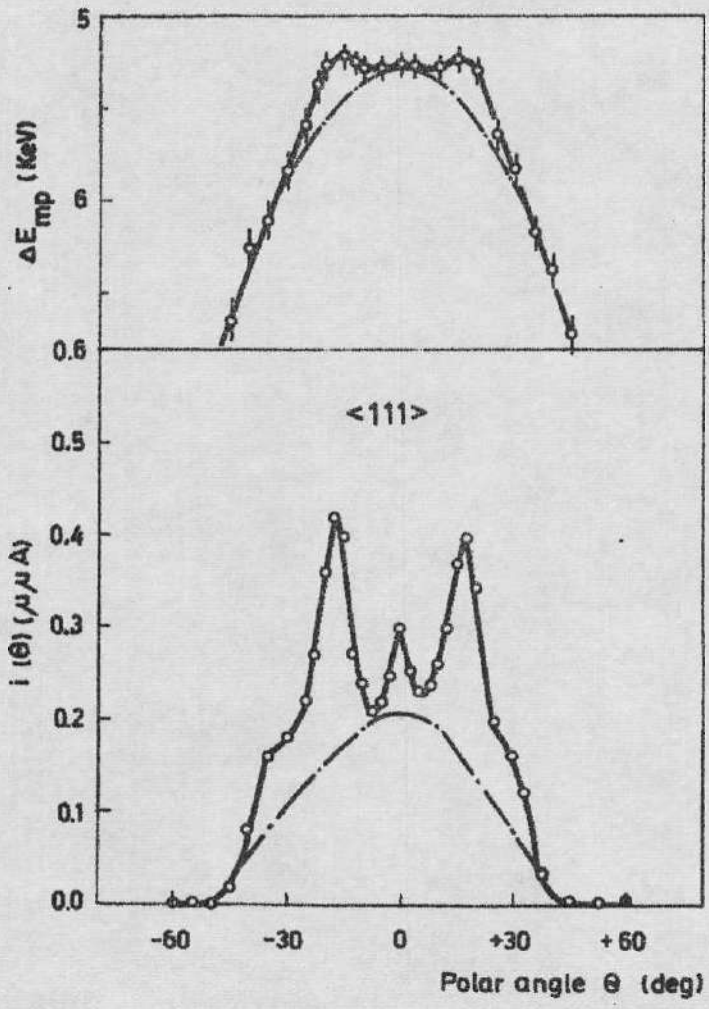
ΔE_mp (KeV)
5
6
0.6
<111>
0.5
0.4
i (θ) (μμ A)
0.3
0.2
0.1
0.0
-60
-30
0
+30
+60
Polar angle θ (deg)

Fig.2.

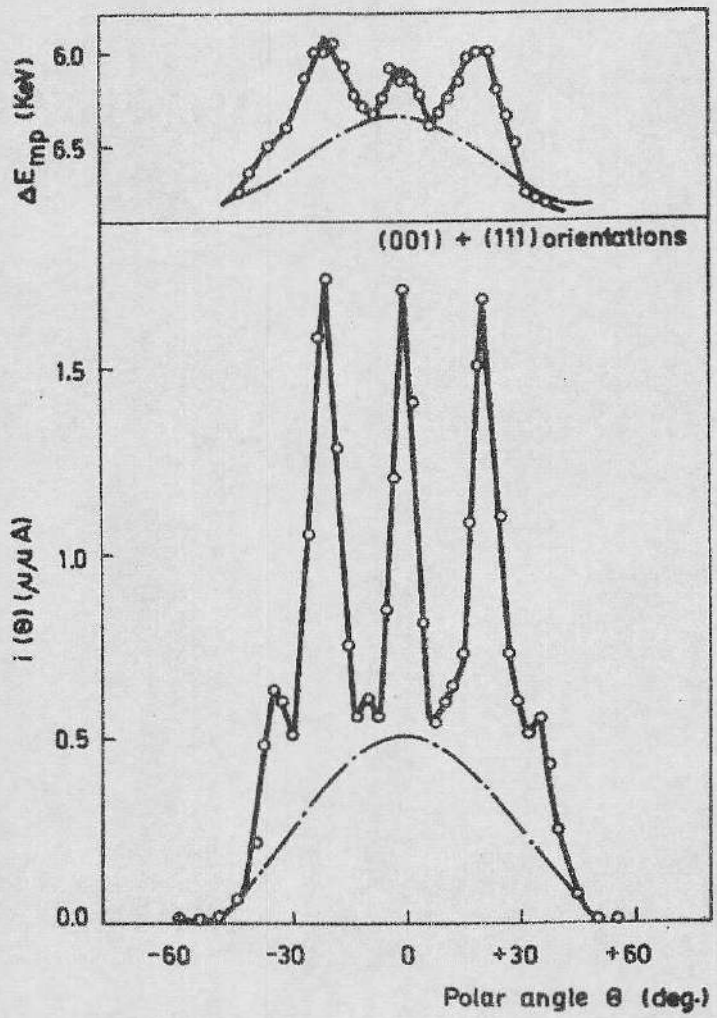
ΔE_mp (KeV)
6.0
6.5
(001) + (111) orientations
i (θ) (μμA)
1.5
1.0
0.5
0.0
-60
-30
0
+30
+60
Polar angle θ (deg.)

Fig.3.

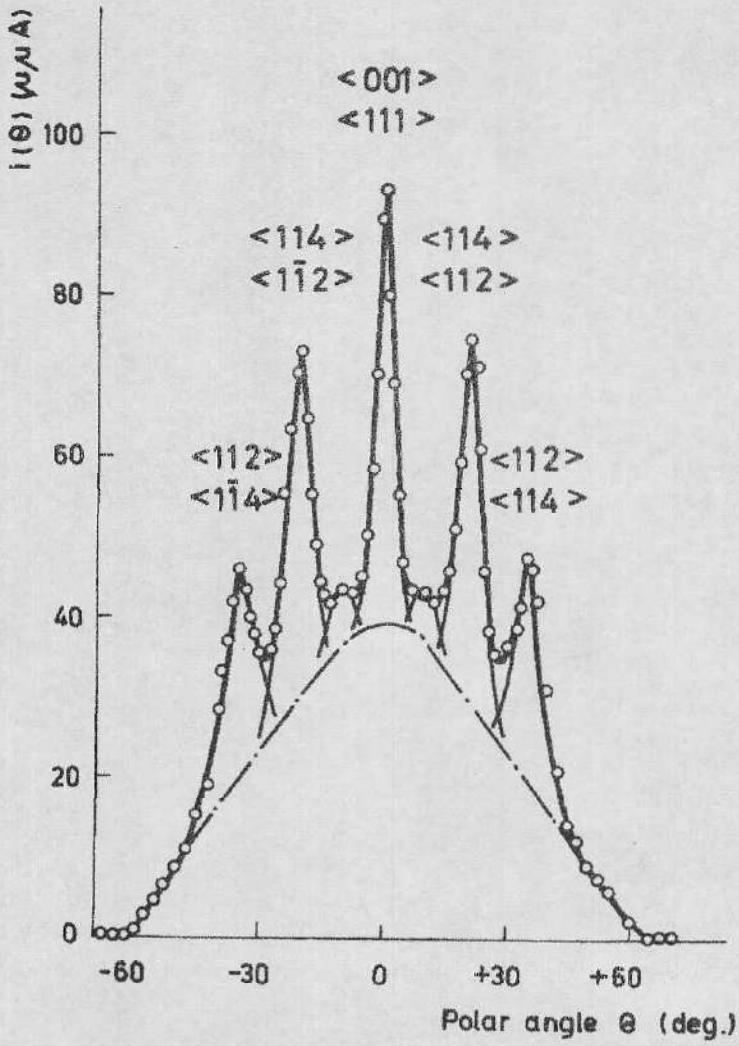
i(θ) (μA)
100
80
60
40
20
0
<001>
<111>
<114>
<1$\bar{1}$2>
<114>
<112>
<112>
<1$\bar{1}$4>
<112>
<114>
-60
-30
0
+30
+60
Polar angle θ (deg.)

Fig.4a.

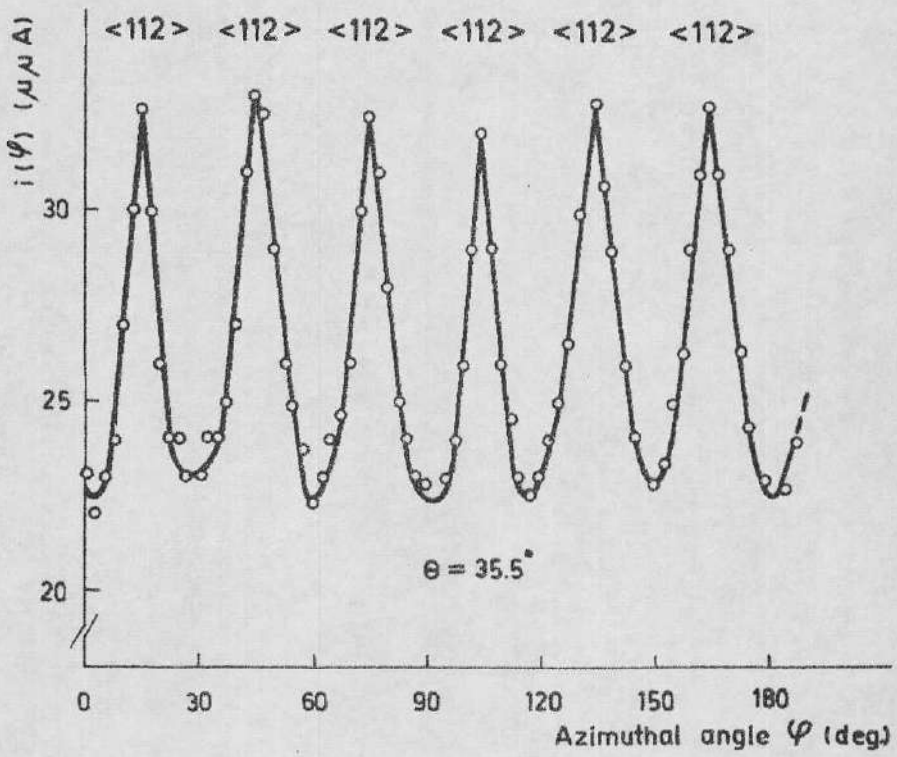
i(φ) (μA)
<112>
<112>
<112>
<112>
<112>
<112>
30
25
20
θ = 35.5°
0
30
60
90
120
150
180
Azimuthal angle φ (deg.)

Fig.4b.

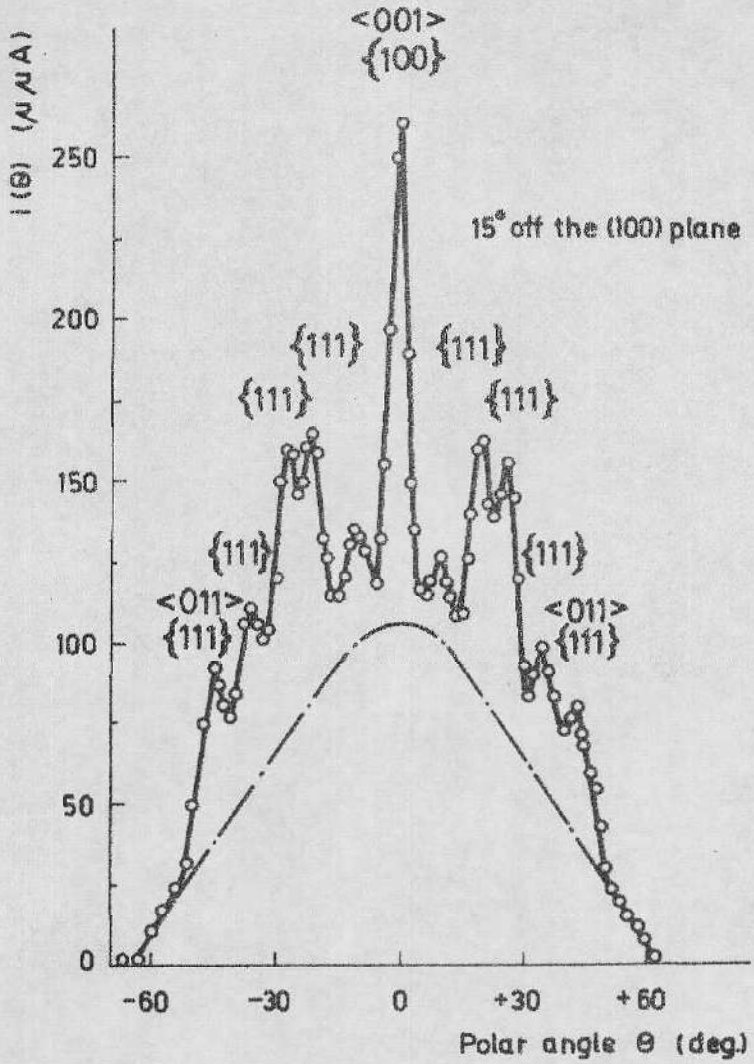
<001>
{100}
15° off the (100) plane
{111}
{111}
{111}
{111}
{111}
{111}
<011>
{111}
<011>
{111}
i (Θ) (μA)
250
200
150
100
50
0
-60
-30
0
+30
+60
Polar angle Θ (deg.)

Fig.5a.

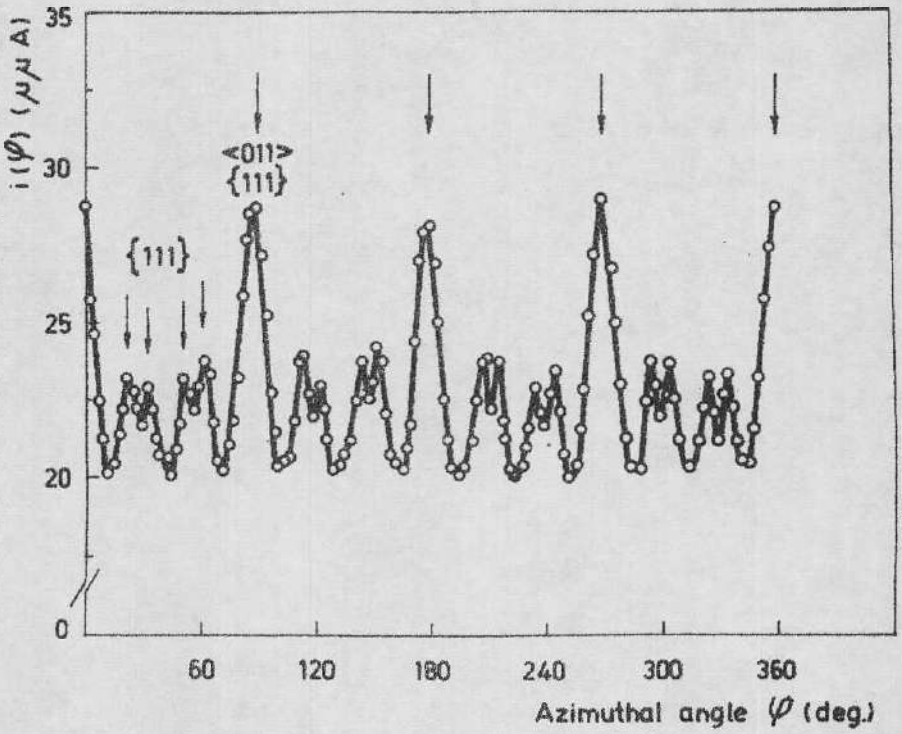
i (φ) (μA)
35
30
25
20
0
<011>
{111}
{111}
60
120
180
240
300
360
Azimuthal angle φ (deg.)

Fig.5b.

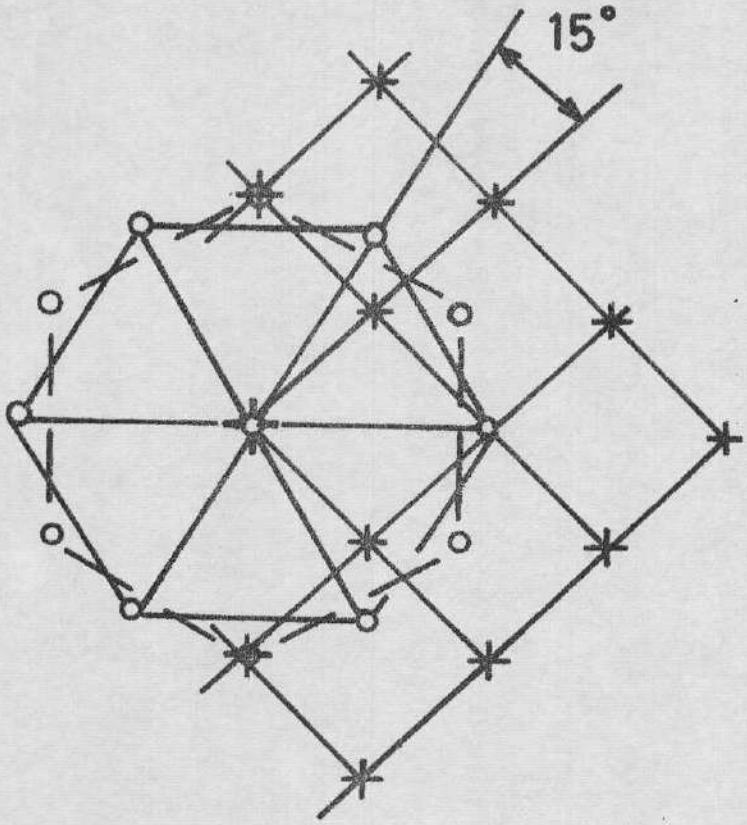
15°

Fig.6.

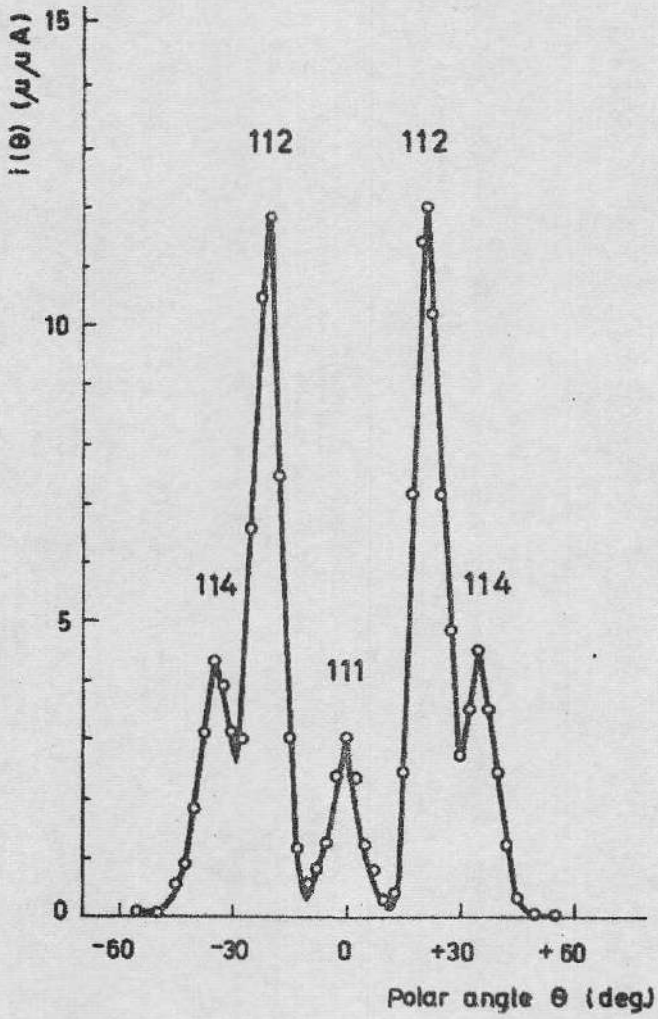
I(θ) (μμA)
15
10
5
0
112
112
114
114
111
-60
-30
0
+30
+60
Polar angle θ (deg)

Fig.7.

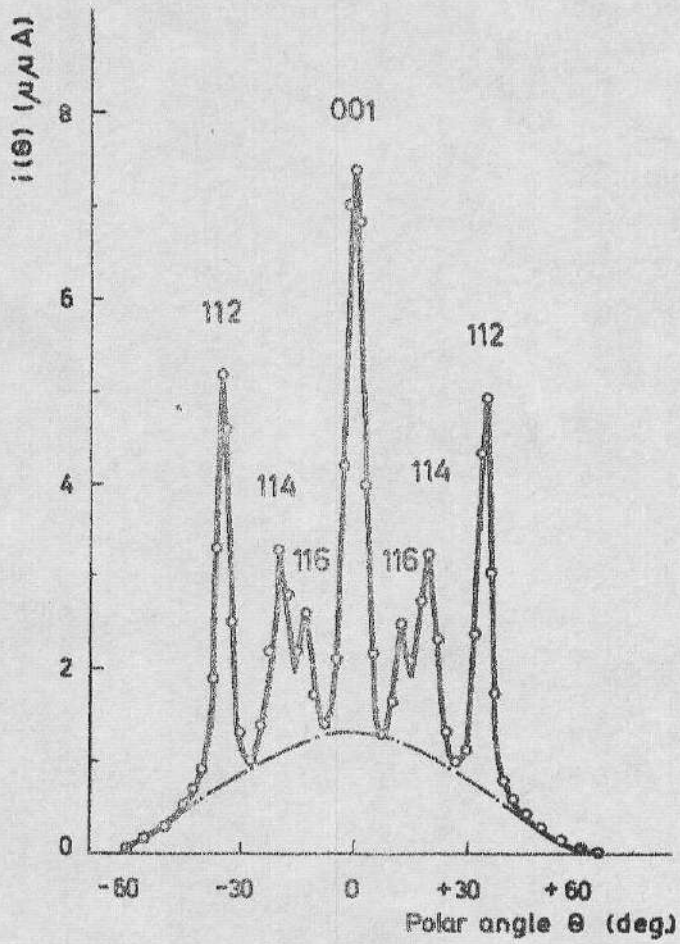
i (θ) (μμ A)
8
6
4
2
0
001
112
112
114
114
116
116
-60
-30
0
+30
+60
Polar angle θ (deg.)

Fig.9.

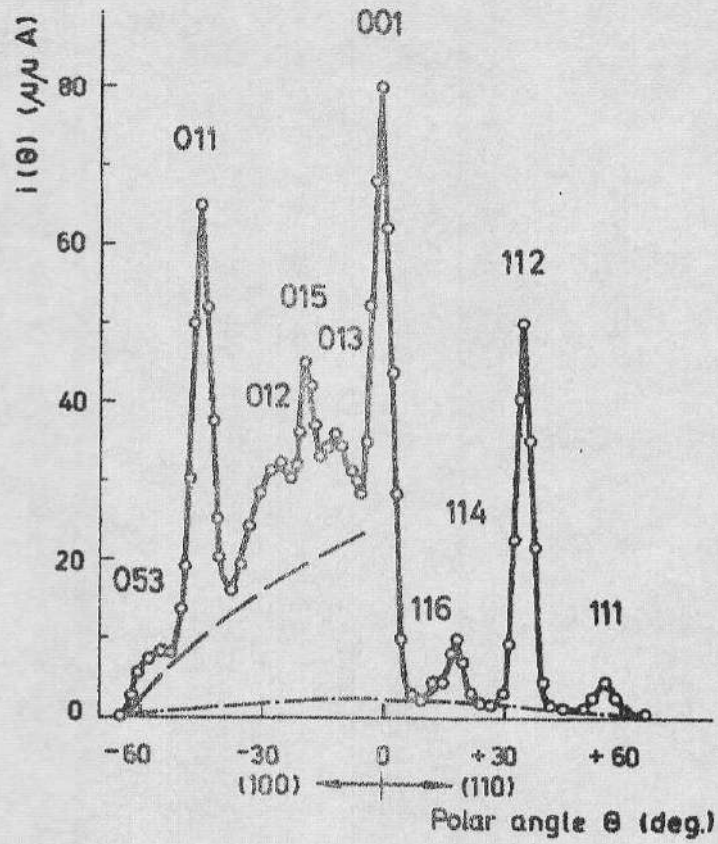
i (θ) (μμ A)
80
60
40
20
0
001
011
112
015
013
012
114
053
116
111
-60
-30
0
+30
+60
(100)
(110)
Polar angle θ (deg.)

Fig.9a.

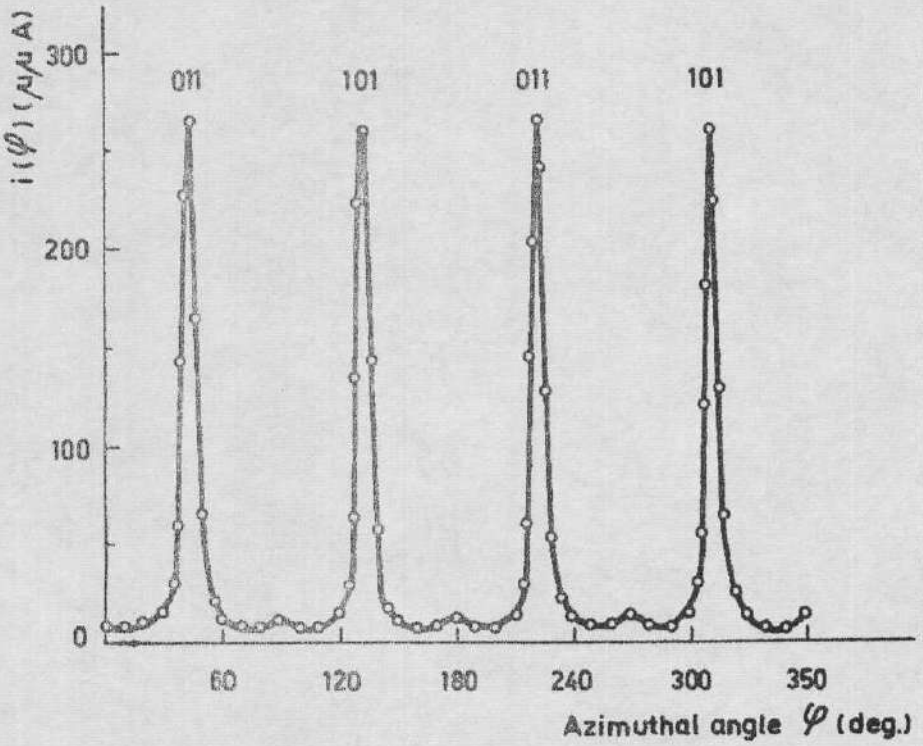
i(φ) (μμ A)
300
200
100
0
011
101
011
101
60
120
180
240
300
350
Azimuthal angle φ (deg.)

Fig. 9b.

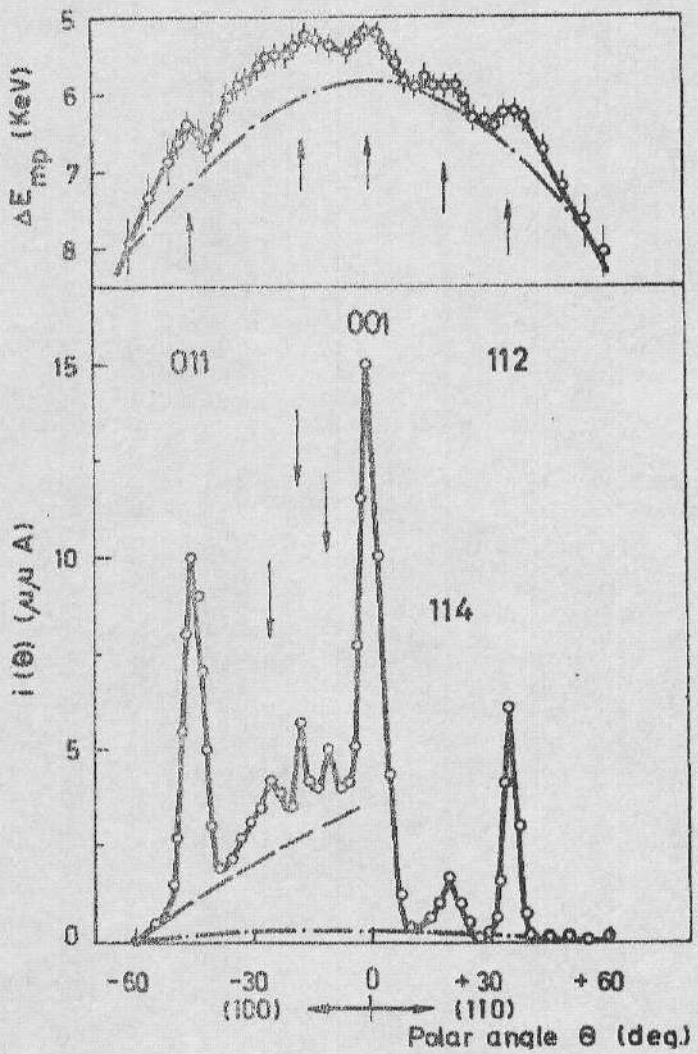
ΔE_mp (KeV)
5
6
7
8
001
011
112
114
i (θ) (μμ A)
15
10
5
0
-60
-30
0
+30
+60
(100)
(110)
Polar angle θ (deg.)

Fig.10.

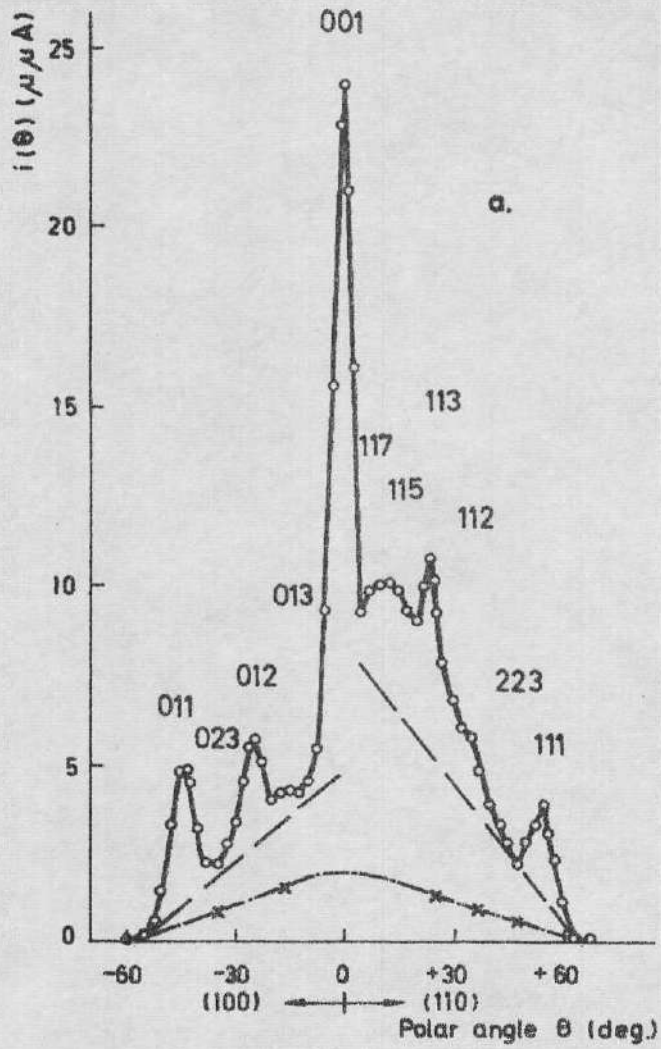
i (θ) (μμA)
a.
001
113
117
115
112
013
012
223
011
023
111
-60
-30
0
+30
+60
(100)
(110)
Polar angle θ (deg.)

Fig. 11

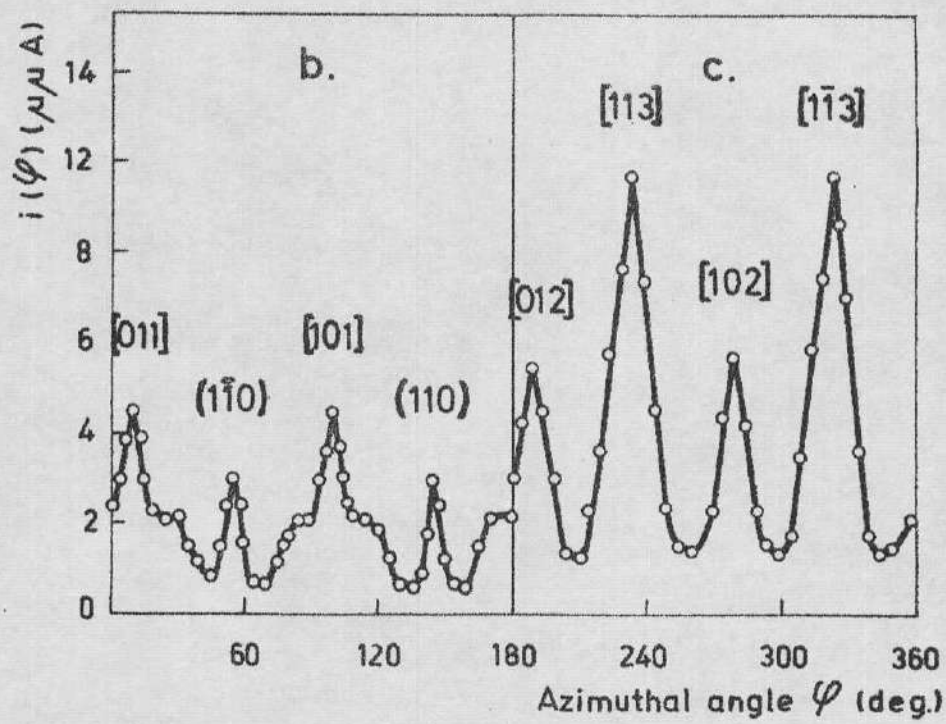
i (φ) (μμA)
b.
c.
[011]
(1̄10)
[101]
(110)
[012]
[113]
[102]
[1̄13]
Azimuthal angle φ (deg.)

DOKTORSAVHANDLINGAR
VID
CHALMERS TEKNISKA HÖGSKOLA
Ny serie Nr 64

A Simple Transparency Model For The Channeling of Low Energy Light Ions In Crystals.

by

Carl-Joel Andreen
Chalmers University of Technology
Gothenburg, Sweden.

Abstract

The degree of correlation between relative channeled intensities and channel areas is studied for D^+ ions of energies around 15 keV, transmitted through thin single crystal gold films in the forward direction. It is found that for film thicknesses around 200-400 Å a linear relationship exists between the two entities. For the {111} planes the degree of correlation is close to 100%. Planar channeling along {111} and {100} planes play an important role in obtaining the linear relationship.

INTRODUCTION

In recent years considerable attention has been paid to measurements dealing with ion penetration through crystalline material[1-11]. The fact that enhanced ion transmission is observed along low index crystallographic directions and planes has changed quite substantially the picture of the scattering of ions in crystals. The symmetry in the lattice makes the ions experience correlated small angle scattering, a fenomenon which is called the channeling effect, or the string effect.

Most of the data has been collected for incident ion energies above 0.5 MeV. Some experiments deal with heavy ions of as much as $\sim$ 100 MeV[9]. A few investigations deal with the low energy region[2,12-14]. Andreen et al. have reported about channeling through thin gold and iron films in the energy region 1 - 25 keV[12-15].

A theoretical treatment of the subject was published by Lindhard 1965[16]. For example, critical angles for channeling Ψ for crystallographic directions were given as functions of the energy E, the "string"-constant d and the Z-values of the incident and target particles. The theory focuses on the high energy region where a classical picture of the scattering process can be used with good accuracy.

The channeling effect is also observed in Rutherford scattering experiments[17]. The ion which become trapped in a directional (or a planar) channel have a smaller probability to become backscattered. The energy lost by these ions is different from the energy loss experienced by the randomly scattered particles. As a consequence one finds dips in the reflected intensity as a function of the crystal orientation. Measurements similar to the ones described above have been performed by Domeij[18]. α-radioactive Rn ions were implanted in a tungsten single crystal. The emitted α-activity was then measured as a function of the crystal orientation. It was found that dips in the emitted intensity corresponded

to low index directions and planes in the crystal. It was concluded that almost all the Rn and Po atoms ended up in lattice positions. The minimum intensity in the dips is discussed theoretically by Lindhard.

The intensity of ions transmitted through a crystal has been subject to little attention. It was shown earlier by Andreen et al. that relative transmitted intensities correlated with the area per atom $A^{<hkl>}$ along a directional channel <hkl> both for f.c.c.[12] and b.c.c.[13] structures. A transparency model used in the theory of sputtering[19] assumes that a certain number of the incident ions are absorbed by the channel during the passage through the first one or two atomic layers. These ions would therefore be ineffective to the sputtering yield S. Instead they contribute to the channeled intensity. The relative success of this model demonstrates the connection between channeling and sputtering. Onderdelinden[20] has shown that the widths of the minima in the sputtering yield agree very nicely with Lindhards theory for the string effect.

It is the purpose of this paper to study in some detail the degree of correlation between transmitted relative intensities and crystallographic parameters such as channel areas $A^{<hkl>}$ and interplanar spacings $D^{\{hkl\}}$.

APPARATUS

The ion bombardment equipment, the goniometer and the detecting system are described earlier[14,21]. The crystals used are thin films prepared by evaporation. The preparation techniques for gold and iron films can be found elsewhere[22,23]. The films are checked in an electron microscope and carefully selected according to defect concentrations and wrinkles. An optical microscope is used as a preselecting instrument to avoid visible wrinkles. The influence of different sources of error on the peak widths

and on the critical angles for channeling is reported earlier[14]. The absolute transmission coefficient is not considered here. The influence of the geometry in the apparatus is therefore greatly eleminated. Only transmitted intensity ratios normalized to specific low index channels will be discussed.

RESULTS

f.c.c.

Fig. 1 shows the transmitted intensity $i(\Theta)$ or 17 keV D^+ ions in the forward direction for a 265 Å thick gold single crystal with an <001> direction parallell to the foil normal. The ion beam is parallell to a {100} plane. The dashed line combines approximately the deepest minima in the transmitted intensity. The reason for drawing this line will be discussed later. The dot-dashed line represents the intensity along high index directions and is experimentally found to reflect the behaviour of a polycrystal with a random orientation. The intensity above the dashed line is resolved into individual peaks. The peaks are expected at Θ-values corresponding to low index channels in the crystal. One notices that very often the channel indices have a sum h+k+l which is even.

Fig. 2 shows the transmitted intensity $i(\Theta,\varphi)$ of 16 keV D^+ ions passing through a 450 Å thick gold crystal along a {111} plane. The intensity above the dashed line is resolved into individual peaks which shows that h+k+l is without exception even.

Fig. 3 shows the transmitted intensity $i(\Theta)$ of 21 keV D^+ ions passing through a 300 Å gold crystal along a {110} plane. It is interesting to notice that the random intensity fits quite precisely the minima between the individual peaks. Again h+k+l is most often even.

Fig. 4 shows the intensity already shown in Fig. 1 - 3 for the {111}, {100} and {110} planes. One single ion energy of about 8 keV is used.

The gold crystal is about 900 Å thick. The relative intensity for higher indexed directions is reduced at this lower energy and for a thicker film. The <114> direction is almost completely gone. The information concerning the position and relative importance of the peaks in Fig. 1 - 3 is concentrated in Fig. 5. This figure shows an eighth of a stereogram in the <001> orientation. The {111}, {100}, and {110} planes can be found in the stereogram. For the purpose of a later discussion a few other low index planes are also represented. These are {120}, {113} and {115} planes. Dashed lines along certain planes indicate an increased transmission. The sizes of the filled circles represent the relative importance of the directions. The positions of the experimental peaks deviate from the calculated angles by less than 0.5° on the avarage. This error is ascribed to a small misorientation of the crystal plane relative to the sample holder which may be introduced when the crystal is mounted.

Fig. 6 shows the transmitted intensity $i(\Theta,\varphi)$ through a gold crystal about 265 Å thick along a {111} plane for an extremely low incident D^+ ion energy of 3.2 keV. The other two planes, {100} and {110}, are shown in Fig. 7 for an energy of about 3.0 keV.

Tables I and II list the experimentally observed peaks for energies around 17 keV and 3 keV respectively.

b.c.c.

Fig. 8 taken from ref. 13 shows the intensity $i(\Theta)$ of 15 keV D^+ ions transmitted through a single crystal α-iron film in an <001> orientation. The crystal is about 600 Å thick. The two most important planes {110} and {100} are shown. The dot-dashed line represents the random scattering of ions. The intensity above the dashed line is resolved into individual peaks. Quite a few peaks appear in the two planes. One notice

that h+k+l is preferably odd. The positions and the relative importance of the peaks are represented in the stereogram in Fig. 9. The planes {110} and {100} are shown together with a few additional planes for the purpose of a later discussion. These planes are {112}, {130} and {111} type planes. An attempt to detect an increased intensity along the plane {112} gave a negative result. In fact no indications of other planes could be observed than the ones shown in Fig. 8. Table III lists the directions found in the two planes {110} and {100}.

Fig. 10 shows the transmitted intensity in the forward direction through two gold crystals. Both crystals are about 200 A thick and are grown in a <001> orientation. The incident ion energy is about 15 keV. The intensity is measured as a function of φ for $|\theta| = 36.5^{\circ}$ at which angle the highest peak, besides the <001> peak, could be observed in the entire detectable region of the stereogram. Fig. 11 shows the intensity detected as a function of θ for $\varphi \approx 185^{\circ}$ for the same two crystals and the same ion energy as in Fig. 10. In that figure one finds a double pattern compared to what is found for one crystal. The relative angle of rotation $\Delta\varphi$ between the two crystals is $25^{\circ} \pm 2^{\circ}$ as measured from Fig. 10. Fig. 12 shows the intensity detected as a function of Θ for a φ-value corresponding to a {100} plane in one of the crystals. Because of the rotation of the crystals relative to each other the <011> directions are not parallell as they would be if $\Delta\varphi = 0$. The intensity along one <011> channel is therefore found to be effectively decreased by the second crystal. The <001> channels are always almost exactly parallell regardless of $\Delta\varphi$. The intensity along this direction is found to be less affected.

Discussion of experiments.

From Fig. 1 - 12 it is rather obvious that certain directions in

a crystal are more transparent than others. The transmitted intensity also seems to depend on which crystallographic plane is parallell to the ion beam. If one compares the two planes {100} and {110} in Fig. 4 one finds that except for the <112> channel nothing all is seen in the {110} plane. There are, however, directions in this plane along which the crystal seems as open to the ions as along an other direction in the {100} plane. If the effective foil thickness is the same for the two directions to be compared one would expect, at least tentatively, that the transmitted intensity should be the same for equal transparencies. The transparency could be expressed as the open area $A^{<hkl>}$ between the strings seen by the incoming ions.

If one compares the intensities along the planes {100} and {111} in Fig. 4, one observes that the intensity is generally larger along the {111} plane than in the {100} plane. This is so despite the fact that the {111} plane is found in the interval $35^{\circ} \leq \Theta \leq 45^{\circ}$ and should be compared with the intensities at these Θ-angles along the {100} plane. At higher energies the intensity detected along the {110} plane may show peaks as in Fig. 3. One finds, however, that the intensity along the {100} plane always exceeds the intensity along the {110} plane for equal effective foil thicknesses. The intensity along the <013> channel may be even 25% higher than along the <112> channel. The same general observations are also valid for the intensities along the {110} and {100} planes in a b.c.c. crystal as shown in Fig. 8. No indications of any other type of plane is observed in this crystal at these energies.

One important condition which has to be fullfilled in order to make a meaningful analysis of the intensities is that the resolution of the detector system is high enough to reveal the characteristics of the crystal. In the present investigation the influence of the detector, the beam divergency and the condition of the foils on the peak widths, is estimated to be less than 5%.[14]

A big problem for the analysis of the intensities is the different effective foil thickness for different tilt angles Θ . For higher Θ-values the beam path in the foil is longer and the transmitted intensity in the forward direction is lower.

One possible way of correcting for the thickness to some degree would be to resolve the total intensity above the dot-dashed lines and devide the peak intensity with the random intensity at the same Θ-value. In this way one would obtain the order amongst the directions, which one expects from calculated channel areas $A^{<hkl>}$. One is not able, however, to account for the completely different situation along the {110} plane in Fig. 4.

At this point it seems logical to explain the meaning of the dashed lines. These lines combine the deepest minima between the peaks in a way that quite closely resembles the random intensity. The directions with Θ -values corresponding to these minima are of very high orders. It is therefore not probable that these high order channels contribute to the channeled intensity. The crystal seems, however, quite a bit more transparent to the ions along the {100} plane regardless of the value of Θ then it does along a higher order plane like the {110} plane.

Apart from a small overlap between neighbouring peakes, the intensity at the deep minima are ascribed to planar channeling. The dashed lines are thus separation lines between planar channeling and directional channeling, which is believed to account for the peakes above the dashed line. By introducing planar channeling one obtains a more reasonable relationsship between directions in the {100} and the {110} planes. The dashed lines in the {111} plane in Fig. 2 and Fig. 4 are obtained in a somewhat different way than in Fig. 1 and 3. It is observed that the planar intensity along a {100} plane (and also the random intensity) at $\Theta = 35^{\circ}$ and $\Theta = 45^{\circ}$ are related to each other through a factor of about 1.4 - 1.5. The same factor is used for the planar intensity in the {111} plane. As far as the random intensity

is concerned this factor is experimentally verified.

In ref. (14) it was found that the energy loss as a function of Θ along different planes also indicated the presence of planar channeling. Both directional and planar channeling exhibited a lower than normal energy loss. Because of this fact it seems more attractive to compensate in a rough way for the variation in foil thickness by taking the ratio $R^{<hkl>}$ between the directional intensity and the planar intensity at each peak than to use the random intensity in the denominator. The final result is of course unchanged. Tables I, II and III list the ratios $R'_{exp} = R^{<hkl>}/R^{<h_1k_1l_1>}$ for all peaks found experimentally. $R^{<h_1k_1l_1>}$ is the ratio for the most open direction in each plane. The direction $<h_1k_1l_1>$ may be either the $<001>$, $<011>$ or the $<111>$ direction. In the plane $\{110\}$ in a f.c.c. crystal the planar channeling is not observed. In Tables I and II the random intensity is then used as a rough thickness correction along this plane.

The planar intensity, whenever it appears, divided by the random intensity at the same angle Θ is approximately a constant ratio $R^{\{hkl\}}$. If this ratio is normalized to the ratio obtained for the most open plane one arrives at a relative number R''_{exp} which is expected to reveal the order of importance amongst the crystallographic planes. Table IV lists a few low index planes both in f.c.c. and b.c.c. structures. The ratios R''_{exp} are listed for all planes experimentally detected. We can thus write

$$R'_{exp} = R^{<hkl>}/R^{<h_1k_1l_1>}$$

and

$$R''_{exp} = R^{\{hkl\}}/R^{\{h_1k_1l_1\}}$$

The interpretation of Fig. 10 and Fig. 11 is based on two overlapping stereograms shown in Fig. 13 for a f.c.c. lattice. From Fig. 11 it is known that the relative rotation between the stereograms is about 25°.

The two overlapping stereograms in Fig. 13 are therefore rotated relative to each other 25° around the <001> channel. If one draws a circle centered around the <001> channels and with a radius corresponding to about $\Theta = 36.5$ which is the value of Θ in Fig. 10, one finds several points where this circle crosses either a {100} or a {111} type plane. One can immediately identify the smaller peaks in Fig. 10 to be caused by the intersection of a {100} and a {111} plane. These points are labelled with A. The difference $\Delta\varphi$ between these peaks is about 25° on the avarage. Between each pair of peaks A one observes a broad double peak. The difference $\Delta\varphi$ between the peaks B in each doublet is about 18° on the avarage. In Fig. 13 the <112> channels in each crystal is 25° apart from each other. These channels are expected at $\Theta = 35.2$, which is very close to the circle $\Theta = 36.5$. If the <112> channels contributed appreciably to the transmitted intensity in Fig. 10 there is no doubt that a shoulder should be observed on the outer edge of each peak B due to the flank of the <112> channels. This is observed for one foil but is not the case here. One therefore concludes that directional channeling is effectively decreased in the double crystal. This is also verified for the open channels <011> at $\Theta = 45°$ in Fig. 12. The intensity is decreased about 10 times because of the presence of a second film. The peaks B are significantly closer together than 25° and can not be explained by the influence of the close lying <112> channels. In Fig. 13 it is found, by following the circle, that it crosses a {111} plane twice in between the {110} planes and that the $\Delta\varphi$ value between these crossings is about 18°. One concludes that each peak in Fig. 10 involves a contribution from the plane {111}. Some of the peaks also involve a contribution from the {100} plane. The observation that the doublets are about twice as intense as the other peaks A is explained by the fact that in the φ interval between two <112> channels the beam runs almost parallell to two {111} planes. Two {133} planes pass quite close to this interval too.

A somewhat surprising observation in Fig. 11 is the presence of a broad peak at $|\Theta| \approx 22^{\circ}$. The peak even seems to consist of two peaks, one at $\Theta = 22^{\circ}$ and the other at $\Theta \approx 16^{\circ} - 17^{\circ}$. The peak at 22° may be explained by the presence of three consecutive intersections between pairs of {113} and {115} planes. The three intersections are found at $\Theta \approx 18^{\circ}$, 22° and 26°. The peaks overlap and the most probable angle for the combined peak is $\Theta \approx 22^{\circ}$. The peak at $\Theta \approx 16^{\circ} - 17^{\circ}$ is caused by the intersection of four {115} planes. No low index channel can be found in the immediate vicinity. Two <114> channels are about 13° off in φ. Any directional channeling along these channels should be effectively decreased below the detecting level because of the second foil. The conclusion drawn from these observations is that planar channeling exists also along {113} and {115} planes.

The peak due to the four {115} planes is less intense, as expected from interplanar distance values $D^{\{hkl\}}$.

One fact, concerning the indices of the planes {hkl} which are observed, is that h, k and l are all odd in a f.c.c. lattice. The only exception is the {100} plane. No indication of the presence of planar channeling along other types of planes other than the ones indicated by dashed lines in Fig. 5, is found.

COMPARISON WITH SIMPLE THEORY

At this point it seems suitable to introduce some very simple geometrical parameters by help of which a straightforward comparison with experiment is made possible. Let us consider the lattice atoms as mathematical points. The density of atoms $\varrho^{<hkl>}$ along the direction <hkl> is the inverse of the "string" constant d in Lindhards theory. The area per atom $A^{<hkl>}$ perpendicular to the direction <hkl> is intimately related

to $\varrho^{<hkl>}$ through the relation

$$A^{<hkl>} / \varrho^{<hkl>} = V$$

where V is the volume of the unit cell. For f.c.c. and b.c.c. lattices V is $\frac{a^3}{4}$ and $\frac{a^3}{2}$, respectively. The interplanar spacing $D^{\{hkl\}}$ is mentioned above. Less important for the present analysis is the density $\varrho^{\{hkl\}}$ of atoms in a plane $\{hkl\}$. A few comments will be made which involves this parameter. In the following discussion $A^{<hkl>}$ and $D^{\{hkl\}}$ will be used mostly. All the parameters are easily expressed in terms of the indices h, k and l for a direction $<hkl>$ or a plane $\{hkl\}$. The positions of the different channels in the stereograms are calculated from the expressions.

$$tg\ (\Theta - \Theta_o) = l^{-1} \cdot (h^2 + k^2)^{1/2}$$

and

$$tg\ (\varphi - \varphi_{\{100\}}) = h/k$$

where Θ_o is zero for a <001> oriented crystal and $\varphi_{\{100\}}$ is the azimuthal angle corresponding to the $\{100\}$ plane.

Further we find that

$$\text{for f.c.c. } A^{<hkl>} = \begin{cases} \frac{a^2 \cdot Q^{<hkl>}}{2} & h+k+l \text{ even} \\ \frac{a^2 \cdot Q^{<hkl>}}{4} & h+k+l \text{ odd} \end{cases}$$

$$\text{and for b.c.c. } A^{<hkl>} = \begin{cases} a^2 \cdot Q^{<hkl>} & h, k \text{ and } l \text{ odd} \\ \frac{a^2 \cdot Q^{<hkl>}}{2} & \text{one of } h, k, l \text{ odd or even,} \end{cases}$$

$$\text{for f.c.c. } D^{\{hkl\}} = \begin{cases} a \cdot Q^{\{hkl\}} & h, k \text{ and } l \text{ odd} \\ \dfrac{a \cdot Q^{\{hkl\}}}{2} & \text{one of } h, k, l \text{ odd or even} \end{cases}$$

$$\text{and for b.c.c. } D^{\{hkl\}} = \begin{cases} a \cdot Q^{\{hkl\}} & h+k+l \text{ even} \\ \dfrac{a \cdot Q^{\{hkl\}}}{2} & h+k+l \text{ odd,} \end{cases}$$

$$\text{for f.c.c. } Q^{<hkl>} = \begin{cases} \dfrac{2Q^{<hkl>}}{a} & h+k+l \text{ even} \\ \dfrac{Q^{<hkl>}}{a} & h+k+l \text{ odd} \end{cases}$$

$$Q^{<hkl>} = \text{and for b.c.c.} \begin{cases} \dfrac{2Q^{<hkl>}}{a} & h, k \text{ and } l \text{ odd} \\ \dfrac{Q^{<hkl>}}{a} & \text{one of } h, k, l \text{ odd or even} \end{cases}$$

and

$$\text{for f.c.c. } Q^{\{hkl\}} = \begin{cases} \dfrac{4Q^{\{hkl\}}}{a^2} & h, k \text{ and } l \text{ odd} \\ \dfrac{2Q^{\{hkl\}}}{a^2} & \text{one of } h, k, l \text{ odd or even} \end{cases}$$

$$\text{and for b.c.c. } Q^{\{hkl\}} = \begin{cases} \dfrac{2Q^{\{hkl\}}}{a^2} & h+k+l \text{ even} \\ \dfrac{Q^{\{hkl\}}}{a} & h+k+l \text{ odd} \end{cases}$$

where $Q^{<hkl>} = Q^{\{hkl\}} = (h^2 + k^2 + l^2)^{-1/2}$ and a is the lattice constant. One observes that for equal conditions on h, k and l

$$\left(\frac{A}{Q}\right)^{<hkl>} = \begin{cases} \frac{a^3}{4} & \text{f.c.c.} \\ \frac{a^3}{2} & \text{b.c.c.} \end{cases}$$

and

$$\left(\frac{D}{Q}\right)^{\{hkl\}} = \begin{cases} \frac{a^3}{4} & \text{f.c.c.} \\ \frac{a^3}{2} & \text{b.c.c.} \end{cases}$$

For a directional channel with a large channel area the density of atoms along the channel direction is high. Similarly for a set of planes with a large interplanar distance the density of atoms in the planes is also high. It is as clear from the systematics of the parameters as it is clear from the experiments that certain directions and planes are favoured relative to others both in f.c.c. and b.c.c. structures. The larger values of any of these four parameters represents the favoured directions or planes.

A close look at the parameters reveal a few interesting facts. In both f.c.c. and b.c.c. structures the probability for a plane to be favoured is 1/3. It can be shown quite easily for f.c.c. lattices that in order for two directions $<h_1\ k_1\ l_1>$ and $<h_2\ k_2\ l_2>$ to be found in a favoured plane for which h, k and l are all odd, they have to fullfill the condition that

$$\left.\begin{matrix} h_1 + k_1 + l_1 \\ h_2 + k_2 + l_2 \end{matrix}\right\} = \text{even}$$

At the same time there is one condition to be fullfilled concerning the sequence of the indices within the symbol $< hkl >$. This condition is that the odd index can not be placed in the same position in the symbols for the two directions. As a consequence, the direction $< h_1 + h_2 ; k_1 + k_2 ; l_1 + l_2 >$, which is found in the same plane, has always an even sum of the indices which can not be reduced by a common factor as is possible in other planes. As a result favoured planes only contain favoured directions. This is not the case for b.c.c. structures. Here the favoured planes contain both favoured and unfavoured directions. However, unfavoured planes contain only unfavoured directions. There is thus a clear difference between the two types of lattices in this respect. It is believed that this behaviour is reflected in the experiments, where it was found that more than twice as many planes could be observed in f.c.c. than in b.c.c. crystals for energies and foil thicknesses of about the same values.

Tables I, II and III list the $A^{<hkl>}$ -values for the most important planes relative to the $A^{<h_1k_1l_1>}$ -value for the most open channel in each particular plane. The tables compare the ratio $R'_{theor.} = (A^{<hkl>}/A^{<h_1k_1l_1>})_{theor.}$ with the experimental numbers. Table IV lists the $D^{\{hkl\}}$ -values for a few low index planes relative to the $D^{\{h_1k_1l_1\}}$ -value for the most important plane in that particular type of lattice. This ratio is denoted $R''_{theor.}$. As far as the order amongst the directions in a plane or amongst the planes is concerned the correlation between theoretical and experimental numbers is almost perfect. If one compares the numbers a little closer one finds that the difference between theory and experiment increases as the values of h, k, and l increases. This is true for both directions and planes. Fig. 14 shows the experimental numbers R'_{exp} obtained from the ratio of directional to planar channeling, $R^{<hkl>}$, as functions of the theoretical numbers $R'_{theor.}$ in Tables I and II. It is observed that for the higher energies in Table I the functions are relatively straight lines until

very close to the endpoint. The endpoints are found to correspond to one single value of $A^{<hkl>}$ of 0.045 a^2. The experimental numbers for the {110} plane are namely related to the <001> channel while the {111} and {100} planes are related to the common <011> channel.

The other possible method of cerrecting for variations in foil thickness makes use of the ratio between the total intensity above the random intensity divided by the random intensity. The result of this method gives a quantitative correlation which is much worse than the one shown in Fig. 14. For the most open plane {111} the correlation shown in Fig. 14 is good. A correction, of the theoretical ratios $R'_{theor.}$ for the hard sphere radius tends to lower the theoretical line. To compensate for this in the experiments an ever higher contribution from low index planes is demanded.

The second method is not able to account for what is called planar channeling in this investigation. Neither is it capable of explaining the peaks marked with filled triangles in Fig. 15. These peaks sometimes appear at intersections between low index planes where no low order direction is found in any of the crystals. The numbers R'_{exp} and R''_{exp} are functions of the energy E. For energies large compared to the energy corresponding to the mean range $\bar{R}$ these numbers tend to become more and more constant.

The discussion so far has shown that directional channels play a dominant role at low energies and in thin crystal films. Additional support to this interpretation is given by the results obtained from an investigation of critical angles for channeling[15]. The critical angles were measured without taking notice of the effect of intersecting planes. The agreement with Lindhards theory for low ion energies was good. One could find, however, that the experimental critical angles for the <112> channel as a function of energy were slightly too large. A correction due to an effect from intersecting low index planes is also largest for this channel.

FURTHER DISCUSSION

The hard sphere radius mentioned above is a simple minded but convenient concept to demonstrate the fact that directional channels are predominant at low energies and for thin crystals. Corrected values $A^{<hkl>}_{corr.}$ and $D^{\{hkl\}}_{corr.}$ may be quite a bit smaller than the uncorrected ones. The planar channels are, however, more strongly affected by a correction than the directional channels. Overlapping spheres may block a plane $\{hkl\}$ completely while the direction $<hkl>$ still is open. The increasing difference between experimental and theoretical numbers in the Tables may partly be explained by increasing hard sphere radius as the energy is decreased. There are additional factors involved which help to explain the predominance of directions at low energies. In real crystals the lattice atoms undergo thermal vibrations. Besides these vibrations a channeled particle is also sensitive to defects of various kinds along the channel path. An ion which starts out nicely trapped in one type of directional channel may thus be scattered out of the directional channel into a planar channel or into the random beam by the thermal vibrations or by defects along the channel. The probability for such an event increases as the penetrated depth increases and as the temperature increases.

In order to explain the experimental results by Domeij et al[24], Erginsoy[25] assumed a new mechanism through which the ion beam within a channel looses ions proportional to the remaining intensity. This mechanism was then able to account for the shape of the extra long range tails, supertails, in the measured range distributions. Davies et al[26] recently showed, however, that the tails in that experiment were due to an interstitial diffusion of the injected ions, having nothing to do with ordinary channeling. The diffusion process was predicted by McCaldin[27] (1965) before the supertails were ever observed. The idea introduced by

Erginsoy is still attractive for moderate ranges. Different kinds of defects and the thermal vibrations are very likely to cause an intensity loss of the beam along its path. It is thus possible that beyond a certain depth almost only planar channeling will be observed. It was shown earlier by Erginsoy et al[4] that for high energy protons (several MeV) the transmitted intensity through a thick crystal along a low index direction could be accounted for by adding the planar contributions from all planes intersecting at that particular direction. The present investigation shows that this cannot be done for low energy ions in thin crystals. For proton energies of about a few hundred keV, Eisen [30,28] shows that the interpretation of the transmitted spectrum needs the introduction of directional effects besides the planes. The very fact that it is possible to resolve the total channeled intensity into many low index directions, with relative numbers which correlate nicely with simple geometrical parameters, shows that at very low energies the directional channels are predominant. Crystallographic planes are believed to be seen at these low energies too.

According to Lindhard the ions experience a potential caused by a crystallographic plane only along very high index directions in that plane. Along the low index directions the planar potential vanishes. The theory is, however, based on strings and planes isolated in space, a situation which is drastically different from a situation where strings and planes are put together to form a lattice. For very open directions and for widely separated planes like for example the $<011>$, $<001>$ and $<112>$ channels and the $\{111\}$ and $\{100\}$ planes in a f.c.c. lattice the approximation on which the theory is based may be appropriate. It can be doubted, however, that in a real crystal the planar potential is negligable along a low index channel in that plane.

When entering the crystal some ions may be forced into a channeling state parallell to a plane although most of the ions probably end up in a directional channel. As indicated above the situation may change as the beam travels through the material. One cannot exclude the possibility that, due to defects along a directional channel and vibrations of the strings forming the channel, ions leave the directional channels and via the planar channels end up in the random beam. Planar channels are expected to be less sensitive to defects but more sensitive to vibrations because of the smaller critical angles. One may therefore find a completely different situation as the penetrated depth increases. The influence of the nearest neighbour strings on the peak width even for high index channels may be doubled for good reasons. It was shown already by Nilson and Thompson that the effective transverse potential for protons travelling down a $<110>$ channel in gold was less than 100 eV already 0,25 Å from the $<110>$ string. 0,5 Å from the string the potential is about 10 times lower.

The influence of positional assymmetry of the scattering centres along the channel is, however, believed to affect the string constant. The four strings which form a channel $<hkl>$ have the same string constant $d_{<hkl>}$. If two of the border strings are shifted a distance less than $d_{<hkl>}$ along its own direction a situation may arise where the effective string constant $d_{<hkl>}$ is decreased.

The successful way of resolving the intensity into individual peaks with a width that does not decrease noticably with increasing values of h, k and l suggests that the string constant along the direction $<hkl>$ does not increase as fast as expected from simple geometrical calculations.

SUMMARY

It has been shown that the normalized ratios of directional to planar channeling correlate nicely with simple geometrical parameters[29]. The correlation is in fact so close that one concludes that for low energy light ions in thin crystal films the directional channels are the predominant ones. For higher order channels the peak width does not decrease according to Lindhards predictions probably due to channel wall assymmetries. The ion beam looses intensity along its path presumably due to defects and lattice vibrations. Planes are also seen but cannot account for the directional peaks.

ACKNOWLEDGEMENT

The author would like to thank Prof. R.L. Hines for the excellent working conditions provided in his laboratory at Northwestern University, Evanstone, Ill., U.S.A. and for his hospitality during my stay there. The cooperation with Fred Morris, Donald Weber and William Krakow is also deeply acknowledged.

The work is supported by Atomic Energy Commission of the United States of America.

REFERENCES

1. M.T. Robinson and O.S. Oen
Appl. Phys. Letters 2, 30 (1963)

2. R.S. Nelson and M.W. Thompson
Phil. Mag. 8, 1677 (1963)

3. G. Dearnaley
IEEE Trans. Nucl. Sci. 11, 249 (1964).

4. C..Erginsoy, H.E. Wegner and W.M. Gibson
Phys. Rev. Letters 13, 530 (1964)

5. M.W. Thompson
Phys. Rev. Letters 13, 756 (1964)

6. A.R. Sattler and G. Dearnaley
Phys. Rev. Letters 15, 59 (1965).

7. E. Bøgh, J.A. Davies and K.O. Nielsen
Phys. Letters 12, 129 (1964).

8. W.M. Gibson, C. Erginsoy, H.E. Wegner and B.R. Appleton
Phys. Rev. Letters 15, 357 (1965).

9. S. Datz, T.S. Noggle and C.D. Moak
Phys. Rev. Letters 15, 254 (1965).

10. C. Erginsoy
Phys. Rev. Letters 15, 360 (1965)

11. B.R. Appleton, C. Erginsoy, H.E. Wegner and W.M. Gibson
Phys. Letters 19, 185 (1965).

12. C.J. Andreen, R.L. Hines, W. Morris and D.E.Webel
Phys. Letters 19, 116 (1965).

13. C.J. Andreen, E.F. Wassermann and R.L. Hines
Phys. Rev. Letters 16, 782 (1966).

14. C.J. Andreen and R.L. Hines
Phys. Rev. 151, 341 (1966).

15. C.J. Andreen and R.L. Hines
Physics Letters 24A, 118 (1967)

16. J. Lindhard
Mat. Fys. Medd. Dan. Vid. Selsk. 34, 14 (1965).

17. E. Bøgh and E. Uggerhöj
Phys. Letters 17, 116 (1965),
Nucl. Instr. and Methods 38, 216 (1965).

18. B. Domeij
Arkiv för Fysik 32, 179 (1966).

19. A.L. Southern, W.R. Willis and M.T. Robinson
J. Appl. Phys. 34, 153 (1963).

20. D. Onderdelinden
Appl. Phys. Letters 8, 189 (1966).

21. R.L. Hines and R. Arndt
Phys. Rev. 119, 623 (1960)

22. D.W. Pashley
Phil. Mag. 4, 324 (1959).

23. J.W. Mathews
Appl. Phys. Letters 7, 225 (1965).

24. B. Domeij, F. Brown, J.A. Davies, G.R. Piercy and E.V. Kornelsen
Phys. Rev. Letters 12, 363 (1964).

25. C. Erginsoy
Phys. Rev. Letters 12, 366 (1964).

26. J.A. Davies and P. Jespergård
Can. J. Phys. 44, 1631 (1966).

27. J.O. McCaldin,
Progress in Solid State Chemistry (Pergamon Press, London), Vol. 2, p. 9 1965.
Nucl. Instr. and Methods 38, 153 (1965).

28. F.H. Eisen
Physics Letters 23, 401 (1966).

29. While writing the manuscript a similar view on the subject was presented to me by Drs. B. Fagot and C. Fert, Toulouse, France for which I am deeply grateful. See
B. Fagot and C. Fert,
J. de Microscopie 5, 389 (1966)
J. de Microscopie 4, 21 (1965).

CAPTIONS

Fig. 1. The transmitted intensity $i(\Theta_{\perp})$ of 17 keV D^+ ions is shown as a function of Θ along a {100} plane. The crystal is about 265 Å thick. The dashed line separates the directional channeling from planar channeling. The dot-dashed line represents the intensity in high index directions outside the {100} plane. Individual directions are resolved and indexed.

Fig. 2. The transmitted intensity $i(\Theta,\varphi)$ of 16 keV D^+ ions is shown as a function of Θ and φ along a {111} plane. The crystal is 450 Å thick. The dashed line separates planar channeling from directional channeling. The dot-dashed line represents the transmitted intensity in high index directions just outside the (111) plane. Individual directions are resolved and indexed.

Fig. 3. The transmitted intensity $i(\Theta)$ of 21 keV D^+ ions is shown as a function of Θ along a {110} plane. The crystal is about 300 Å thick. The dot-dashed line represents the intensity in high index directions outside the {110} plane. No planar channeling from the {110} plane can be detected. Individual directions are resolved and indexed.

Fig. 4. The transmitted intensity $i(\Theta,\varphi)$ of 8 keV D^+ ions for a gold film about 900 Å thick is shown as functions of Θ and φ along the three planes {111}, {100} and {110}. The dashed lines separate directional from planar channeling. Dot dashed lines represents the intensity in high index directions outside the planes. Individual directions are resolved and indexed. Fewer directions are observed at this low energy.

Fig. 5. An eighth of a stereogram is shown for a <001> oriented f.c.c. crystal. Filled circles represent low index directions. The radii of the circles indicate the relative importance of the channel. Besides the $(\overline{1}11)$, (100) and $(1\bar{1}0)$ planes one finds a few additional low index planes. These are the {120}, {113} and {115} type planes.

Fig. 6. The transmitted intensity $i(\Theta,\varphi)$ of 3.2 keV D^+ ions is shown as a function of Θ and φ along a {111} plane. The crystal is about 265 Å thick. The dashed line separates directional channeling from planar channeling. The dot-dashed line represents the intensity in high index directions. Very few directions are observed at this low energy.

Fig. 7. The transmitted intensity $i(\Theta)$ of 3.0 keV D^+ ions is shown along the {100} and the {110} planes. The crystal is about 265 Å thick. The dot-dashed line represents the intensity in high index directions outside the planes. Only very few channels can be resolved. No planar channeling is believed to be present.

Fig. 8. The transmitted intensity $i(\Theta)$ of 15 keV D^+ ions is shown as function of Θ along the planes {110} and {100}. The crystal is a 600 Å thick α-iron film. The dashed lines separate directional channeling from planar channeling. The dot-dashed curve shows the intensity in high index directions outside the planes. Individual directions are resolved and indexed.

Fig. 9. An eighth of a stereogram is shown for a <001> oriented b.c.c. crystal. Filled circles represents low index directions. The radii of the circles indicate the relative importance of

the channels. Besides the $(1\bar{1}0)$ and (100) planes a few other low index planes are seen. These are the {111}, {112} and {130} type planes.

Fig. 10. The transmitted intensity through two single crystals, each 200 Å thick, of 15 keV D^+ ions is shown as a function of φ. Θ is about 36.5° which corresponds to the intense peaks in Fig. 11. The smaller peaks are intersections between {111} and {100} planes.

Fig. 11. The transmitted intensity through the same two crystals as in Fig. 10 is shown as a function of Θ for $\varphi = 185^\circ$. The weak peaks are caused mainly by intersections between {113} planes. The dot-dashed line indicate the random intensity.

Fig. 12. The transmitted intensity along a {100} plane in the double crystal in Fig. 10 ($\varphi = 85^\circ$) is shown as a function of Θ. Several peaks are visible on both sides of the <001> peak which do not correspond to low index directions.

Fig. 13. Two overlapping stereograms rotated relative to each other about 25° are shown for a f.c.c. lattice with a {100} plane parallell to the crystal surface. The radii of the open circles indicate the relative importance of the directions. The dashed line is part of the circle $\Theta = 36.5^\circ$ as in Fig. 10. The lines L_1 and L_2 show the path of the beams in Fig. 11 and Fig. 12 respectively. Triangles show the positions of all the peaks found in these figures.

Fig. 14. The experimental relative numbers in Tables I - III are shown as functions of the theoretical numbers in the same tables. One observes a good correlation between experiment and theory for both directions and planes.

Table I The relative number $R'_{theor.} = A^{<hkl>}/A^{<h_1k_1l_1>}$ is listed for several low index directions in the three planes {111}, {100} and {110} shown in Figs. 1 - 3. The directions are listed in decreasing order of importance in each plane. One observes that a good correlation exists between experimental and theoretical numbers.

Table II The relative number $R'_{theor.} = A^{<hkl>}/A^{<h_1k_1l_1>}$ is listed for several low index directions in the three planes {111}, {100} and {110} shown in Figs. 6 and 7. The directions <hkl> are listed in decreasing order of importance. As far as the order amongst the channels is concerned the correlation is still very good. The difference between experimental and theoretical numbers is larger at lower energies.

Table III The relative number $R'_{theor.} = A^{<hkl>}/A^{<h_1k_1l_1>}$ is listed for several low index directions in the planes {110} and {100} shown in Fig. 8. The directions are listed in decreasing order of importance. The correlation between experimental and theoretical numbers is good.

Table IV The relative number $R''_{theor.} = D^{\{hkl\}}/D^{\{h_1k_1l_1\}}$ is listed for several low index planes in both f.c.c. and b.c.c. lattices. The planes are listed in decreasing order of importance for both types of structures. The correlation between experimental and theoretical numbers is good. Fewer planes are visible in the b.c.c. lattice than in the f.c.c. lattice.

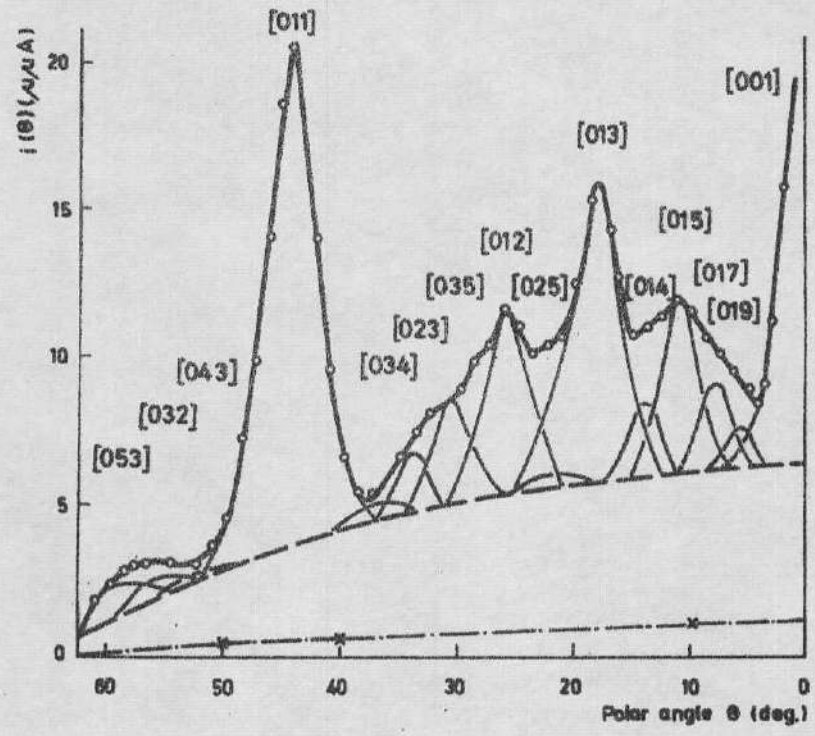
i (θ) (μA)
20
15
10
5
0
[011]
[001]
[013]
[015]
[012]
[035]
[025]
[014]
[017]
[019]
[023]
[034]
[043]
[032]
[053]
60
50
40
30
20
10
0
Polar angle θ (deg.)

Fig.1.

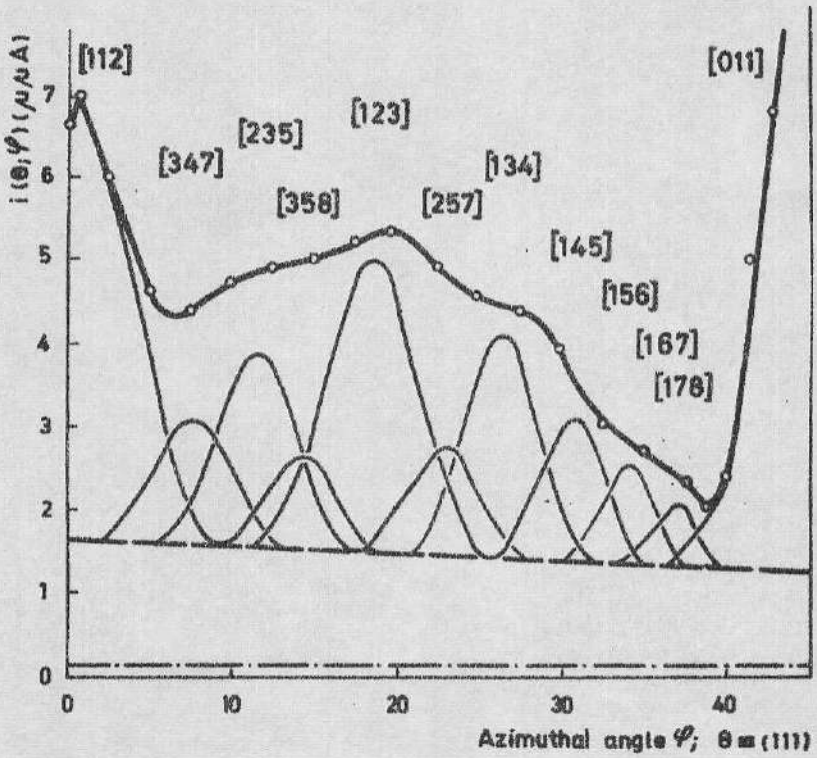
i (θ;φ) (μA)
7
6
5
4
3
2
1
0
[112]
[011]
[123]
[235]
[347]
[134]
[358]
[257]
[145]
[156]
[167]
[178]
0
10
20
30
40
Azimuthal angle φ; θ = (111)

Fig.2.

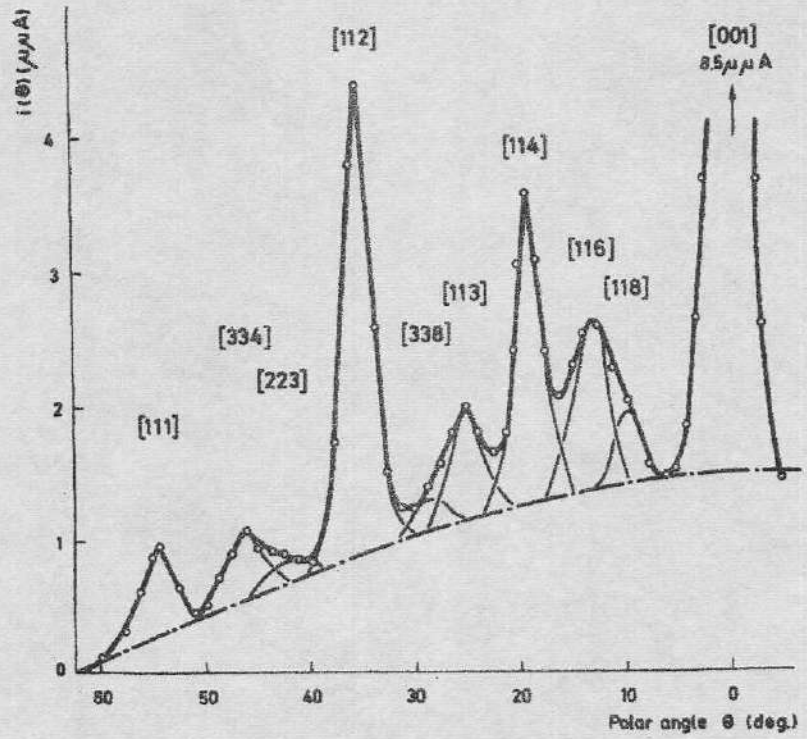
i(Θ) (μμA)
[112]
[001]
8.5μμA
[114]
[116]
[113]
[118]
[334]
[338]
[223]
[111]
Polar angle Θ (deg.)

Fig.3.

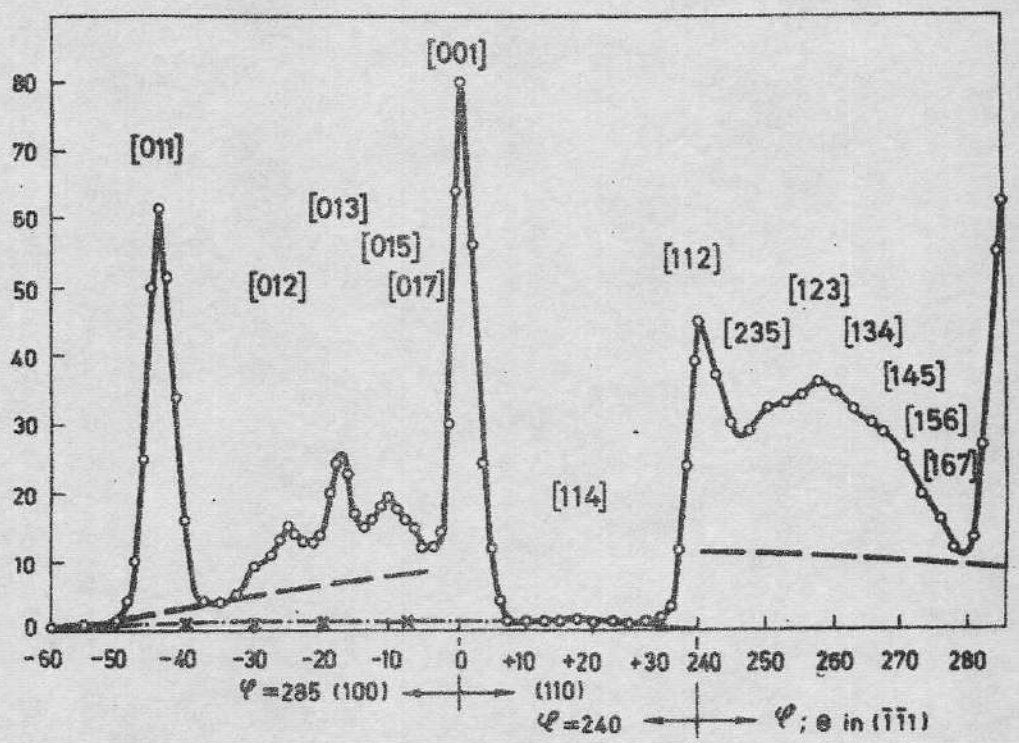
[001]
[011]
[013]
[015]
[012]
[017]
[112]
[123]
[235]
[134]
[145]
[156]
[167]
[114]
φ=285 (100)
(110)
φ=240
φ; Θ in (1̄1̄1)

Fig.4.

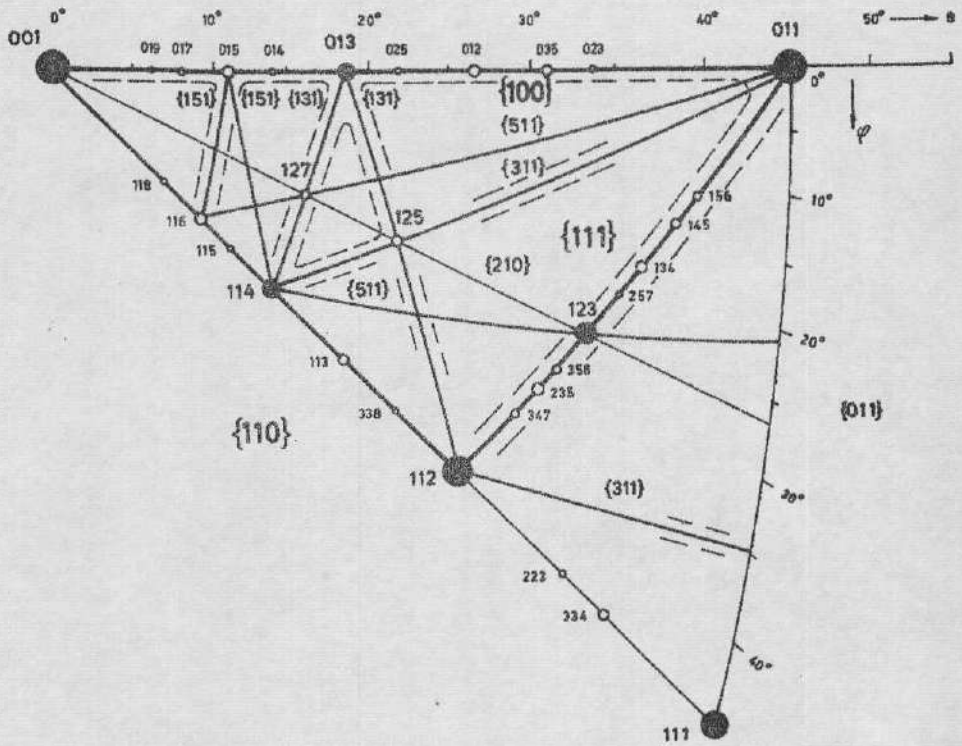
001
011
013
{100}
{151}
{131}
{511}
{311}
{111}
{210}
{110}
{011}
{311}
127
125
123
114
112
111
φ

Fig.5.

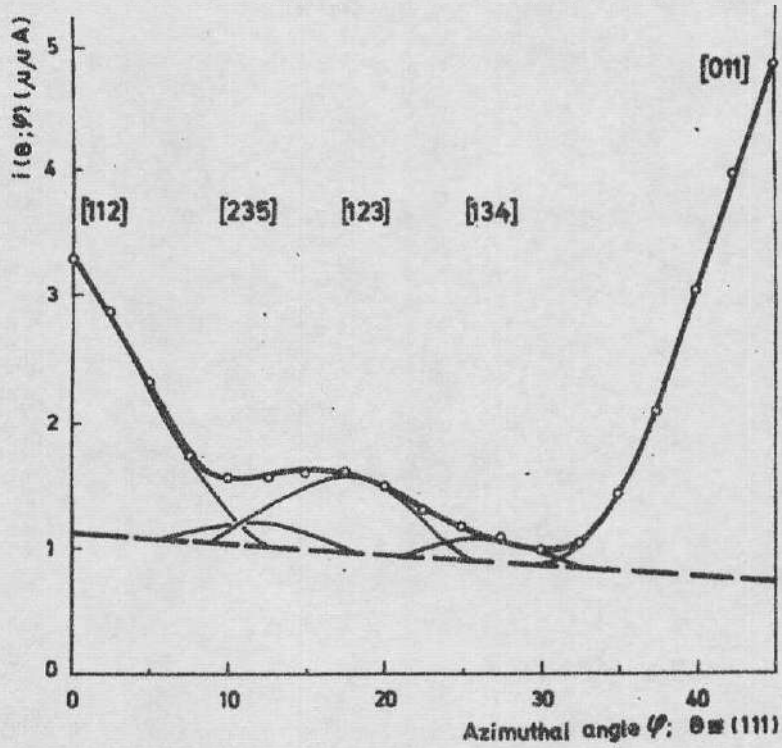
[011]
[112]
[235]
[123]
[134]
Azimuthal angle φ; θ ≡ (111)

Fig.6.

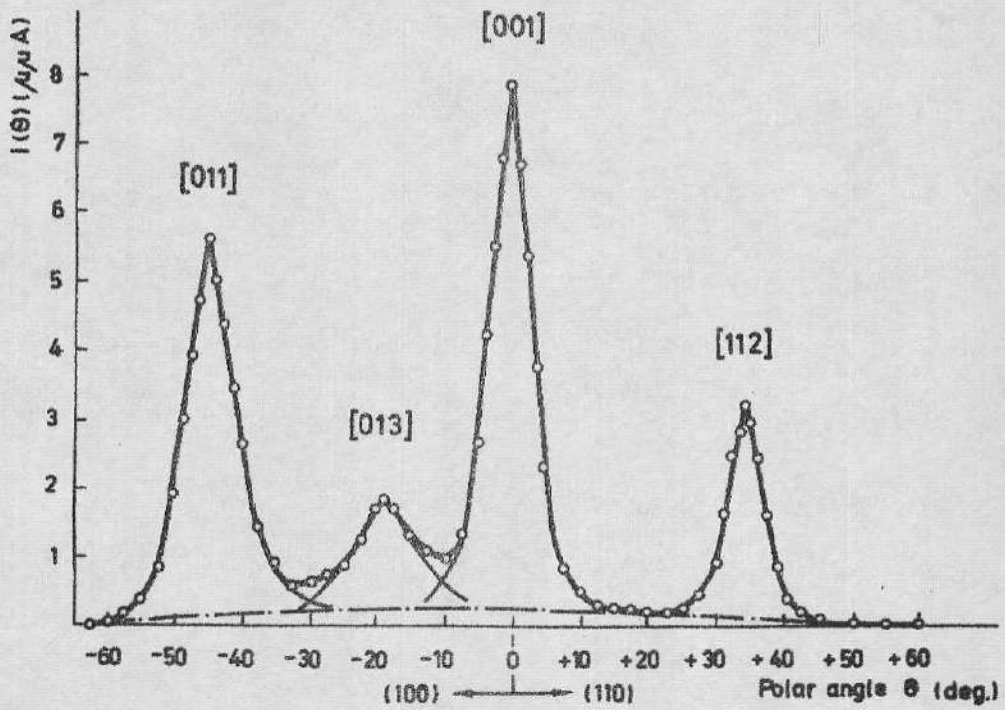
i(θ) (μμA)
[001]
[011]
[013]
[112]
(100)
(110)
Polar angle θ (deg.)

Fig.7.

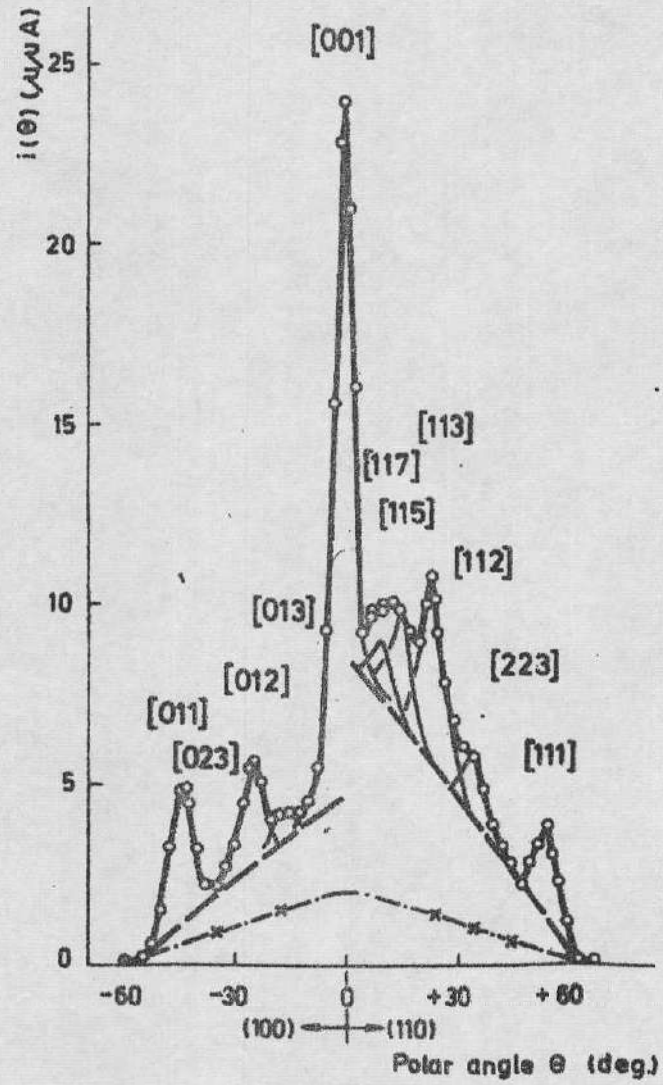
i(θ) (μμA)
[001]
[113]
[117]
[115]
[112]
[013]
[012]
[223]
[011]
[023]
[111]
(100)
(110)
Polar angle θ (deg.)

Fig.8.

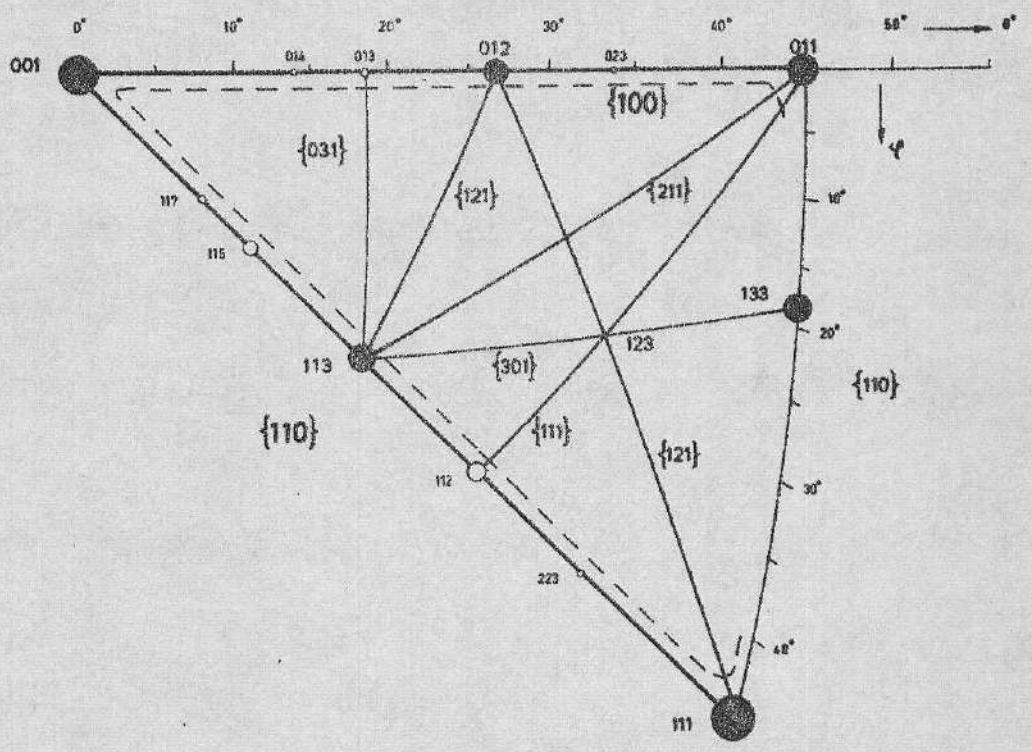
001
012
011
{100}
{031}
{121}
{211}
133
123
113
{301}
{110}
{111}
{121}
{110}
111

Fig.9.

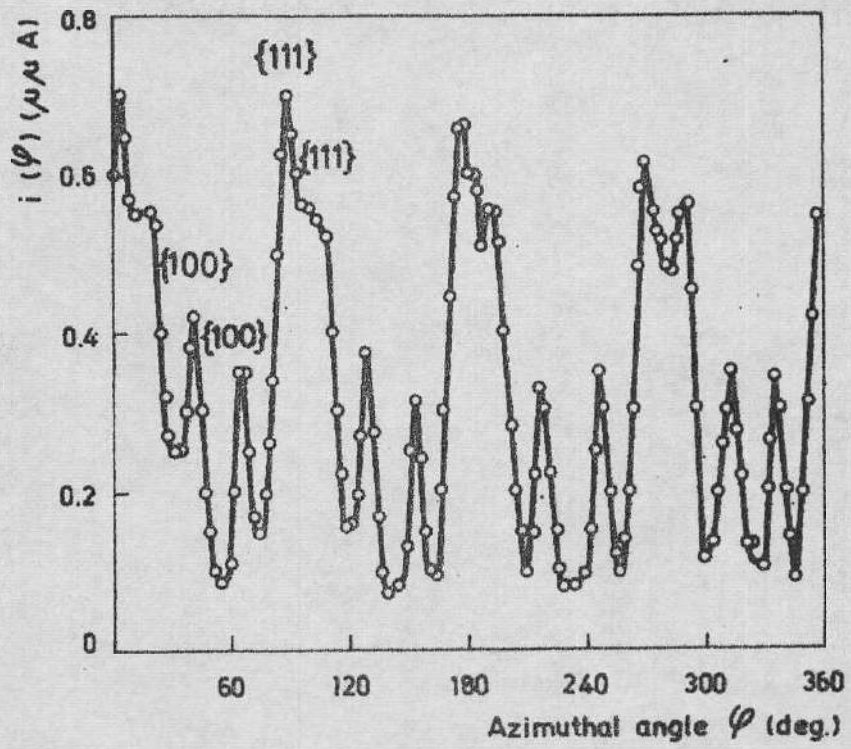
i (φ) (μA)
0.8
0.6
0.4
0.2
0
{111}
{111}
{100}
{100}
60
120
180
240
300
360
Azimuthal angle φ (deg.)

Fig.10.

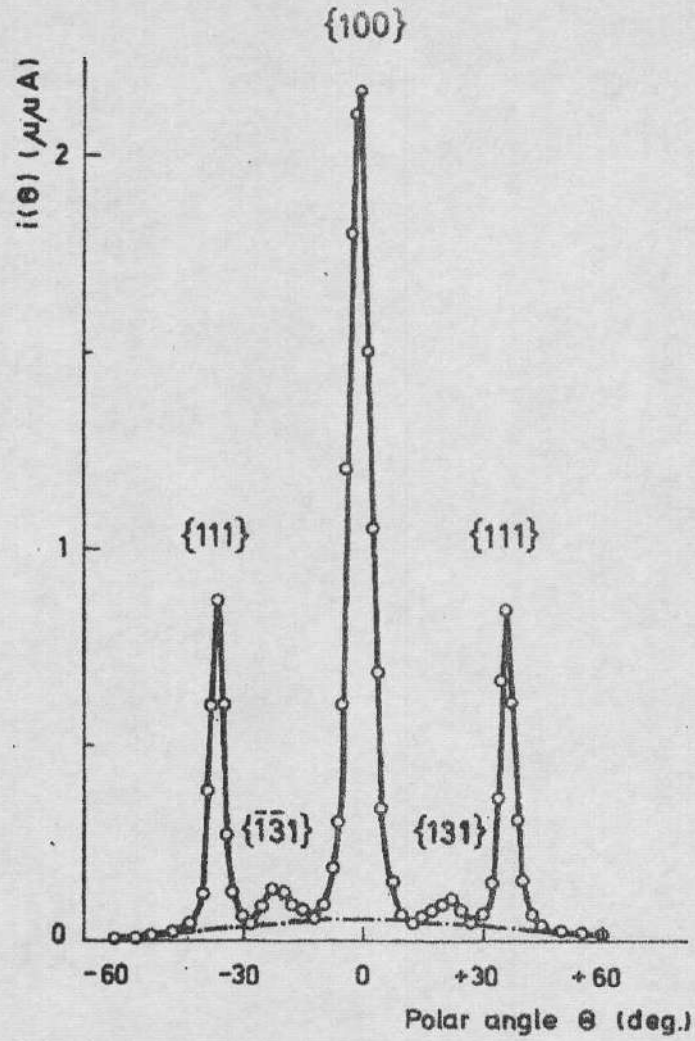
{100}
i(θ) (μμA)
2
1
0
{111}
{111}
{1̄31}
{131}
-60
-30
0
+30
+60
Polar angle θ (deg.)

Fig.11.

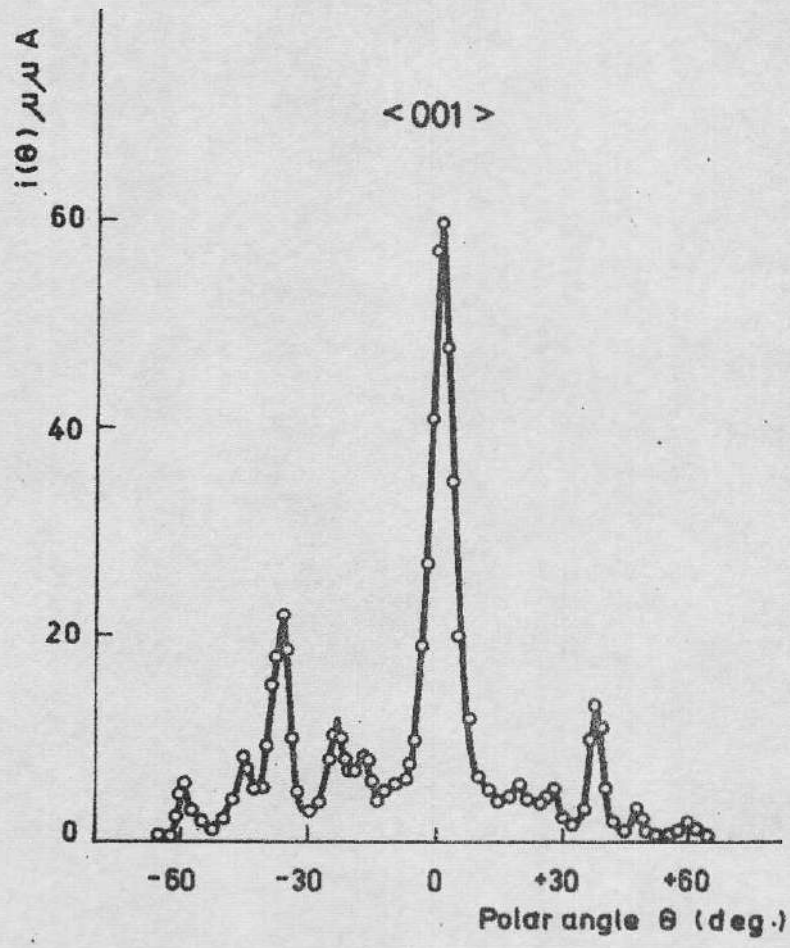
i(θ) μμA
<001>
60
40
20
0
-60
-30
0
+30
+60
Polar angle θ (deg.)

Fig.12.

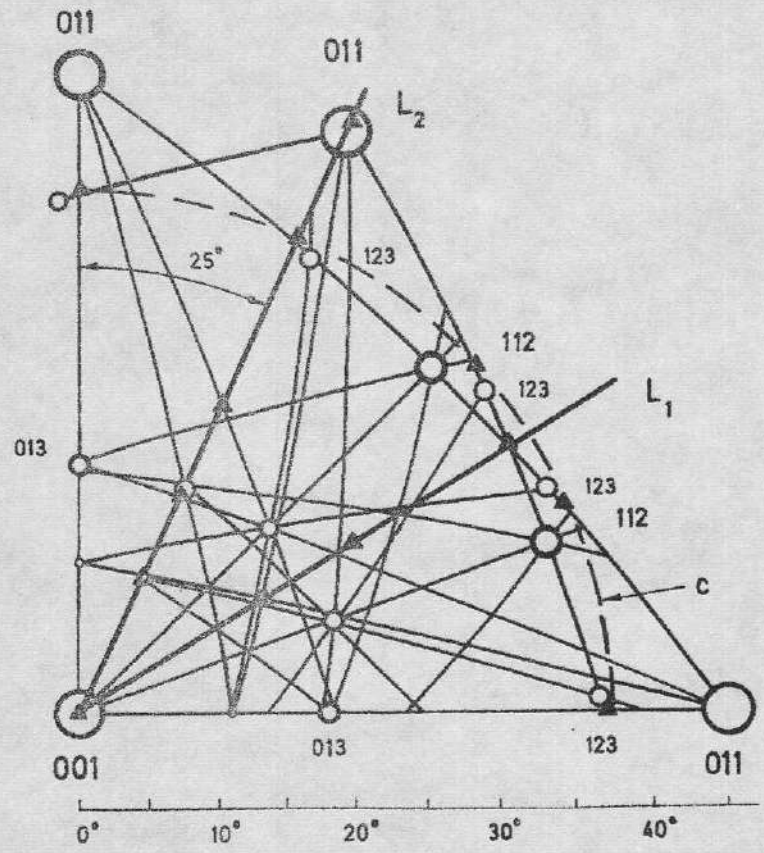
011
011
L2
25°
123
112
123
L1
013
123
112
C
001
013
123
011
0°
10°
20°
30°
40°

Fig.13.

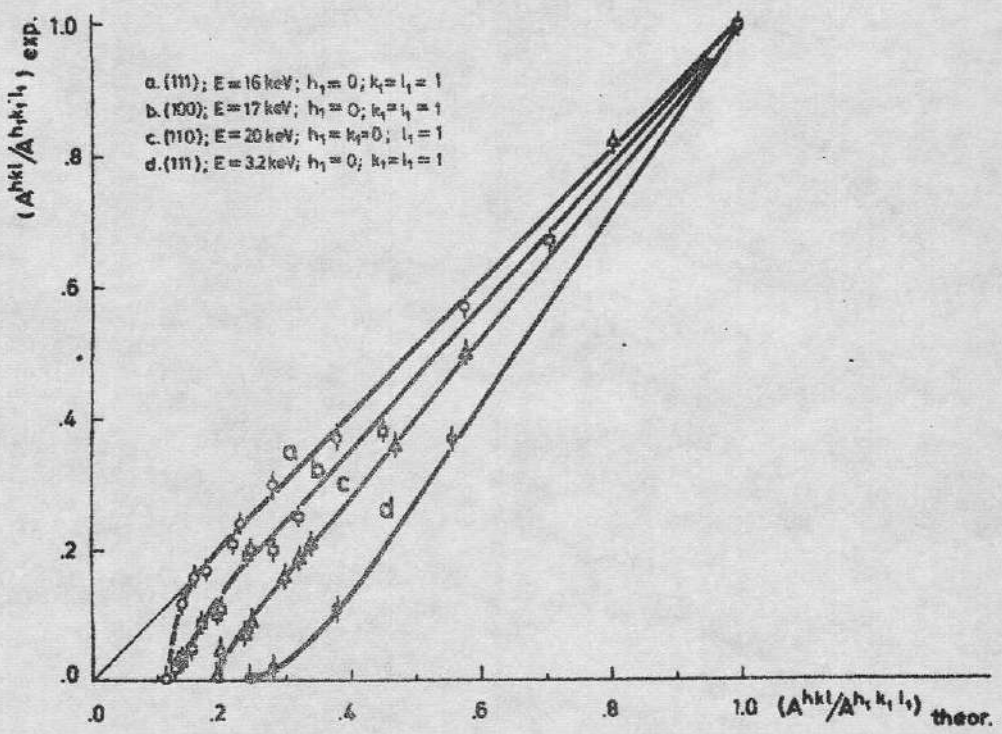
a. (111); E = 16 keV; h1 = 0; k1 = l1 = 1
b. (100); E = 17 keV; h1 = 0; k1 = l1 = 1
c. (110); E = 20 keV; h1 = k1 = 0; l1 = 1
d. (111); E = 32 keV; h1 = 0; k1 = l1 = 1
(Ahkl/Ah1k1l1) exp.
(Ahkl/Ah1k1l1) theor.
1.0
.8
.6
.4
.2
.0
.2
.4
.6
.8
1.0
a
b
c
d

Fig.14

Plane {111}			Plane {100}			Plane {110}		
hkl	$A^{<hkl>}/A^{<011>}$ theor	R'_{exp}	hkl	$A^{<hkl>}/A^{<011>}$ theor	R'_{exp}	hkl	$A^{<hkl>}/A^{<001>}$ theor	R'_{exp}
011	1.00	1.00	011	1.00	1.00	001	1.00	1.00
112	0.58	0.57	001	0.71	0.67	112	0.81	0.88
123	0.38	0.37	013	0.45	0.38	111	0.58	0.49
134	0.28	0.30	012	0.32	0.25	114	0.47	0.35
235	0.23	0.24	015	0.28	0.20	334	0.34	0.20
145	0.22	0.21	035	0.24	0.19	116	0.32	0.18
156	0.18	0.17	053	0.24	0.20	113	0.30	0.16
347	0.16	0.16	017	0.20	0.11	118	0 25	0.09
257	0.16	0.16	023	0.195	0.10	223	0 24	0.07
167	0.15	0.11	032	0.195	0.10	338	0 22	0.04
178	0.13		014	0.17	0.09	1,110	0 20	0.03
358	0.14	0.12	019	0.156	0.05	115	0 19	~0.02
189	0.115	~0	034	0.14	0.03			
			043	0.14	0.04			
			025	0.13	~0.02			

Table I

Plane {111}			Plane {100}			Plane {110}		
hkl	$A^{<hkl>}/A^{<011>}$ theor	R'_{exp}	hkl	$A^{<hkl>}/A^{<011>}$ theor	R'_{exp}	hkl	$A^{<hkl>}/A^{<001>}$ theor	R'_{exp}
011	1.00	1.00	011	1.00	1.00	001	1.00	1.00
112	0.56	0.37	001	0.71	0.41	112	0.81	0.39
123	0.38	0.11	013	0.45	0.11	111	——	0.0
134	0.28	0.02	012	0.32	<0.05	114	——	0.0
235	0.23	<0.02	——	——	——			

Table II

Plane {110}			Plane {100}		
hkl	$A^{<hkl>}/A^{<111>}$ theor	R'_{exp}	hkl	$A^{<hkl>}/A^{<001>}$ theor	R'_{exp}
111	1.00	1.00	001	1.00	1.00
001	0.87	0.83	011	0.71	0.68
113	0.52	0.40	012	0.45	0.20
112	0.35	0.20	013	0.32	0.04
115	0.33	0.17	023	0.28	0.02
117	0.24	0.08	014	0.24	<0.01
223	0.21	<0.02			

Table III

f.c.c.			b.c.c.		
hkl	$D^{\{hkl\}}/D^{\{111\}}$ theor	R''_{exp}	hkl	$D^{\{hkl\}}/D^{\{110\}}$ theor	R''_{exp}
111	1.00	1.00	110	1.00	1.00
100	0.87	0.27	100	0.71	0.40
110	0.61	—	112	0.58	—
113	0.52	~0.05	013	0.45	—
120	0.39	—	111	0.41	—
112	0.35	—			
115	0.33	<0.02			
122	0.29	—			

Table IV

DOKTORSAVHANDLINGAR
VID
CHALMERS TEKNISKA HÖGSKOLA
Avhandling Nr 64

Blocking of D^+ ions in single crystal gold films.

by
C-J Andreen
Chalmers University of Technology
Gothenburg, Sweden.

ABSTRACT

Blocking effects are believed to be observed along the directions <011>, <001>, <112> and <123> in gold. Planar blocking along {111} and {100} type planes is also suggested. The experimental result, involving a complicated combination between planar and directional effects due to both channeling and blocking, cannot by subject to mathematical analysis at the present time.

INTRODUCTION

Gibson[1] et al have shown that in transmission through a thin crystal some particles loose more energy than normal. It is believed that energy is lost to atoms in a row or in a plane by correlated collisions in high electron density regions. A highly anisotropic atomic density provided by a crystal structure thus makes it possible for a certain part of the transmitted particles to experience this larger than normal energy loss. Erginsoy[2] call these particles, blocked particles. Some particles exhibit a lower than normal energy loss. These particles are called channeled particles.

Gemmell and Holland[3] investigated the blocking effect on (d;p) and similar reactions in a silicon crystal. 4 -, 7 -, and 11 MeV protons, 4 MeV deuterons and 10 MeV α-particles were used. 4 MeV protons incident on a germanium crystal were also used. Domeij and Björkqvist[4] studied the emission of about 5 MeV α-particles from implanted Rn and Po atoms. Blocking of α- particles was observed along low index directions and planes. In these investigations the radiation originated from lattice sites.

The purpose of this paper is to present some measurements on the blocking of low energy D^+ ions transmitted through thin gold single crystal films. Evidence for axial as well as planar blocking will be presented. The width of the blocking dips are discussed to some extent.

APPARATUS

The probability for an ion to become blocked along a low index crystallographic direction or plane is smaller than the probability for the same ion to become channeled. It is therefore a necessity to move the detector away from the beam direction a certain angle α. In order to observe the blocking effect the angle α is larger for low energies. The experimental arrangement has been described earlier[5,6]. α may be varied from -3° to $+58^\circ$ relative to the beam direction. This additional degree of freedom makes it possible to shoot ions into one directional channel and to detect the transmitted beam along another directinal

channel. The design of the goniometer limits the number of combinations of channels to the ones in low index planes which intersect at the <001> direction.

Fig. 1 a - h shows the different detector and crystal arrangements used in the figures below. The direction of the incident beam is fixed and represented by the heavy vertical arrows. The most interesting channels available with the limited flexibility of the goniometer - detector system are the <011>, <001> and <112> channels. They have either the {100} or the {110} plane in common. Two directional channels in a {111} plane cannot be combined at the present time.

Single crystal gold films may be prepared by epitaxial growth on a rocksalt - silver substrate. The detailed techniques can be found elsewhere[7]. In this experiment one <100> oriented single crystal is used in all figures. The thickness is about 600 Å. The incident beam consists of 18 keV D^+ ions, except in the last figure where the energy is somewhat higher. The ion beam is not energy analyzed neither before nor after the penetration of the crystal because of intensity limitations. The film is, however, completely free from pinholes.

RESULTS AND DISCUSSION

Fig. 2 shows the transmitted intensity $i(\varphi)$ of ions detected at $\alpha = 45^\circ$ as a function of the azimuthal angle φ of rotation around the foil normal, along which the incident beam is directed. The ions thus enter the foil along the <001> channel ($\Theta = 0$) and are detected along the <011> channel. One observes four rather deep dips at φ -values which will be shown below to correspond to {100} -planes. It has been found earlier[6] that an enhanced intensity of ions along low index directions or planes correspond to a smaller than normal energy loss. Although the energy loss is not measured in this investigation, it is expected that a decrease in intensity of transmitted ions below the "random" intensity corresponds to a larger than normal energy loss. This is verified experimentally by Gibson et al[1] at higher energies. On each side of the dips one observes the characteristic shoulders reported by Domeij[8] and others. The ions contributing to the shoulders compensate to about 50 % for the blocked ions in the dip. One finds no evidence at all for a blocking

effect along the {110} planes which would be expected exactly in between the observed dips.

Fig. 3 shows the reversed ion path compared to Fig. 2. The ions are shot into the crystal at $\theta = 45^{\circ}$ and detected along the <001> direction ($\alpha = 45^{\circ}$). The general profile is the same as far as the dips and the shoulders are concerned. The width of the dips is about the same too. However, it is obvious that the intensity level in high index planes, the random intensity, is lower by about a factor 2 in Fig. 2. An explanation for this seems to need the introduction of the channeling effect. The circumstance that ions are constantly incident along the <001> axis means that quite a few ions miss the detector because of channeling along the <001> direction. The random intensity at $\alpha = 45^{\circ}$ is therefore lower. When the ions are incident 45° off the normal they become channeled along the <011> type channels only at four very limited angular intervals as the angle φ is rotated through 360°. The <011> channel is able to absorb more ions into directional channeling than the <001> channel, {111} planes intersecting at the <011> direction may also be of influence. One would therefore expect the random intensity to be lower in Fig. 3. This is also the case. When the beam is incident at $\theta = 45^{\circ}$ the reflection of ions backwards may change and influence the detected random intensity too. One thus finds that it is difficult to separate quantitatively directional and planar effects in Fig. 2 and Fig. 3. In both these figures the <001> and <011> directions are connected through the {100} plane. Two effects may be present due to this plane. The relatively high atom density along the plane {100} may block the incoming ions causing an energy loss which is larger than normal. The probability of being scattered out of the detector direction is thus higher. The{100} plane may also give planar absorption which becomes visible only at ϕ-values corresponding to {100} planes. Both effects may explain the dips in Fig. 2 and Fig. 3. The {110} planes are not seen at all.

Fig. 4 shows the ions which are incident at $\theta = 35^{\circ}$ and detected at $\alpha = 35^{\circ}$, the <001> channel. In Fig. 5 the path direction is reversed and the ions are constantly entering the <001> channel and are detected at $\alpha = 35^{\circ}$. A comparison between the two last figures indicates again that the <001> channel absorbs ions so that the intensity in a random direction for $\alpha = 35^{\circ}$ is smaller when the ions are incident along the foil normal. The general behaviour of the two curves is the same. The

amplitude of the intensity variations is larger in Fig. 4. One very striking feature is the appearance of dips at azimuthal angles corresponding to {110} planes. These dips were not observed in Fig. 2 or Fig. 3 where the polar angle Θ had values more favourable for the {110} plane to show up than in Fig. 4 and 5. These broad dips are due to the <112> direction and the {111} plane. The side dips on each side of the <112> dips are traces of the {111} plane which intersect at the < 112> direction and which becomes visible close to this direction. The dip due to the {111} plane is expected to be very broad because of the fact that the beam moves almost parallell to the plane for some time. However, the extremely broad base of the dips centered about the <112> channels indicates that the directional channels <123> are also seen. These channels are expected about 18° degrees off on each side of the <112> channel. It is most improbable that the {111} plane can be seen as far out from the <112> channel as 30° which is the critical angle for the extremely broad dip. A probable way of resolving the components under the broad dip is indicated in Fig. 4, one observes again dips due to {100} planes. The depth is lower compared to Fig. 2 or Fig. 3. It is important to point out here that the <001> and <112> channels or the <001> channel and the {111} plane are not connected to each other through a low index plane which has been shown to exhibit deviations from a random plane. For example there has been no indication of the {110} plane contributing to channeled intensities. In Fig. 2 and Fig. 3 the {110} plane does not show up either as pointed out above. The dips centered around the <112> directions thus do not involve any influence from planar channeling. The conclusion is that the directional channels <112> as well as the channels <123> are causing blocking effects.

Fig. 6 shows a situation where the ions are shot into the crystal at 40° from the foil normal. The detector is parallell to the <001> channel. The shape of the four relatively broad dips is explained by the presence of two {111} planes and one {100} plane. The angular interval $\Delta\varphi$ between a {111} and a {100} plane at $\Theta = 40^{\circ}$ is about 11° which is consistent with Fig. 6. The random intensities in Fig. 5 and Fig. 6 are about the same. This is not in contradiction with what is said above about the influence of channels on the random intensity level. One notices that already 5 degrees of the <112> channel along the {110} plane, the broad dips due to <112> and <123>

directions and {111} planes in Fig. 5 are completely gone. This shows again that no anomalies occur due to {110} planes.

From the discussion here it seems clear that a combination of both axial and planar effects are responsible for many dips. Definite exceptions are the dips due to the <112> and <123> channels in Fig. 5. These dips indicate the new effect, called blocking[2]. It is believed that Fig. 2 to Fig. 4 and Fig. 6 involve both axial and planar blocking. The separation of axial from planar effects is, however, impossible.

The channeled intensity $i(\varphi)$, detected in the forward direction, is shown in Fig. 7 for $\theta = 45^\circ$. The four sharp channeling peaks at $\varphi = 45^\circ$, 135°, 225° and 315° correspond to <011> channels. Fig. 8, shows the transmitted intensity $i(\varphi)$ in the forward direction for $\theta \approx 35^\circ$. The different directional and planar indices are given. Fig. 7 and 8 serve as calibration curves for the orientation of the crystal. Fig. 9 shows the typical intensity profiles $i(\theta)$ along the {100} and {110} planes as a function of θ. One concludes from Fig. 7 - 9 that the single crystal gold film used in the experiment is as good as any of our crystals grown by evaporation.

Finally Fig. 10 shows the intensity of ions which are shot into the crystal at $\theta \approx -35^\circ$ relative to the foil normal and detected at $\alpha = +35^\circ$ (Fig. 1h). The total angle relative to the <001> channel is therefore $\sim 70^\circ$. The goniometer is not designed for this large angle. This can be observed at $\varphi = 45^\circ$, 135° and 318° where the detected current is negative. The ion beam hits the goniometer axis and creates secondary electrons enough to be detected. The interesting feature in Fig. 10 is, however, the narrow peaks at $\varphi = 0^\circ$, 90°, 180° and 270°. These φ-values correspond to the positions of {110} planes. A comparison with Fig. 4 shows that one can evidently obtain either peaks or dips along the {110} plane after a total angle of scattering of $\sim 35^\circ$, depending upon wether the detector is set at the <001> direction, on one side of the incident beam, or is set at 35° on the opposite side of the beam.

A very probable explanation for the existence of the four narrow peaks in Fig. 10 cannot be given. The width of the peaks is smaller than the width of the four deep dips in the {100} planes in Fig. 2 or 3. The peaks in Fig. 10 may originate from channeling and more specifically from planar channeling along {110} planes. If this is a correct interpretation we have here the very first indication of planar channeling of D^+ ions below 25 keV energy along the {110} planes. Compared to the {111} and {100} planes the effect is negligable.

CRITICAL ANGLES

A comparison between Fig. 2 and Fig. 7 shows that the critical angles are significantly larger in Fig. 2. The width of the dips in Fig. 3 is also broader than in Fig. 7, but slightly narrower than in Fig. 2. It was shown earlier[6] that the total width σ of a peak in the transmitted distribution i s a combination of the entrance and exit widths, σ_1 and σ_2, respectively, of the form

$$\sigma^{-2} = \sigma_1^{-2} + \sigma_2^{-2}$$

If one assumes that the effective foil thickness traversed by the ions in Fig. 2 and Fig. 3 is the same and that the total width σ is independent of a reversal of the ion trajectory, one would expect that

$$\vec{\sigma} = \overleftarrow{\sigma}$$

where the arrows indicate opposite path directions. The fact that this is not the case indicates that the ions do not feel the different directions and planes parallell to the beam and detector directions to the same degree during the passage of the crystal. One concludes from Fig. 2 and Fig. 3 that the ions which are scattered through 45° reflect to a higher degree the directions and the planes parallell to the detector direction (σ_2) and to a lower degree the directions and planes parallell to the incident beam (σ_1). This seems to be consistent with the observation that channeling along the directions and planes parallell to the incident beam is responsible for the different background levels in Fig. 2 and Fig. 3. This is also supported by the difference observed between Fig. 4 and Fig. 9. In Fig. 4 the detector is constantly parallell to the <001> channel. One observes a well defined dip along the {110} plane. In Fig. 10 the detector is not parallell to any low index direction. A narrow peak is observed this time along a {110} plane. The dips in Fig. 4 therefore seem to be due to blocking along the <001> channel while the less pronounced dips in Fig. 5 seem to be due to blocking along the <112> channel. If channeling was responsible for the dips one would expect the dips to be deeper in Fig. 5 than in Fig. 4. The critical angles for channeling of the peaks in Fig. 7 are found to be about 6°. This value is consistent with a average energy of the ions in the foil of about 15 keV[9]. This is a normal situation for a foil thickness of 500 - 600 Å. The widths of the dips in Fig. 2, Fig. 3 and Fig. 7 are shown in Table I.

The width of the dips are found to be broader than one would expect from a calculation of the critical angles for channeling from Lindhards low energy formula[9]. Taking into account the large energy loss in the foil due to the extra path travelled by the ions, a comparison between calculated and measured widths indicate that the ions in the dips still have lost more energy than normal.

SUMMARY

The investigation has shown that part of the ions transmitted through a single crystal exhibit a lower than normal probability to emerge from the crystal along certain directions. This seems to be partly due to the so called blocking effect. In most cases, shown in the figures, the blocking is believed to be a rather complicated combination of planar and directional effects. It seems quite convincing from a systematic study of the figures that axial blocking is present. The low index directions involved are the <011> , <001> , <112> and <123> directions. The low index planes that seem to be involved are the {111} and {100} planes. It is important to stress that the experiments on blocking presented here are somewhat different from the experiments reported by Domeij and others. In the latter cases the radiation originated from lattice sites and the influence of channeling was thus excluded. In this investigation the ions detected parallell to the beam are channeled while some ions detected at large angles are blocked. The blocking effect as it is observed here is believed to be the result of a correlated Coulomb scattering experienced by the ions during part of the time of transmission through the crystal. During the rest of the time the blocked ions may be randomly scattered in the crystal. This situation is too complicated to be subject to detailed analysis at the present time. If one by channeling only means a correlated Coulomb scattering, the blocking effect can be labelled a channeling effect with a larger than normal energy loss. The word canalisation is suggested for both phenomena. Canalisation in regions where the distance r from a string is larger than a ($r > a$)[2] is called channeling. For $r < a$ one may use the word blocking for the canalisation effect.

ACKNOWLEDGEMENT

The author would like to take this opportunity to thank Dr. R.L. Hines for the excellent working conditions provided at the Physics Dept., Norhtwestern University. The work is supported by the Atomic Energy Commission of the United States of America.

REFERENCES

1. W.M. Gibson, C. Erginsoy, H.E. Wegner and B.R. Appleton
Phys. Rev. Letters 15, 357 (1965).

2. C. Erginsoy
Phys. Rev. Letters 15, 360 (1965).

3. D.S. Gemmell and R.E. Holland
Phys. Rev. Letters 14, 945 (1965).

4. B. Domeij and K. Björkqvist
Physics Letters 14, 127 (1965).

5. R.L. Hines and R. Arndt
Phys. Rev. 119, 623 (1960).

6. C.J. Andreen and R.L. Hines
Phys. Rev. 151, 341 (1966).

7. D.W. Pashley
Phil. Mag. 4, 324 (1965).

8. B. Domeij
Arkiv f. Fysik 32, 179 (1966).

9. J. Lindhard
Mat. Fys. Medd. Dan. Vid. Selsk. 34, No 14 (1965).

CAPTIONS

Fig. 1. The figure shows the different crystal and detector arrangements a - h corresponding to the 8 figures 2 - 9 below. The incident beam direction is indicated by the heavy vertical arrows. In all cases the detector is parallell to the plane which the two indicated low index directional channels are found.

Fig. 2. The transmitted intensity at $\alpha = 45^{\circ}$ is shown as a function of φ. The incident beam is constantly parallell to the <001> channel (Fig. 1a). The four dips correspond to the positions of {100} planes. The {110} planes are not seen.

Fig. 3. The transmitted intensity at $\alpha = 45^{\circ}$ is shown as a function of φ. The beam is incident at $\theta = 45^{\circ}$ (Fig. 1b). The four dips appear at the same φ-values as in Fig. 2. The {110} planes are not seen.

Fig. 4. The transmitted intensity at $\alpha = 35^{\circ}$ is shown as a function of φ. The beam is incident at $\theta = 35^{\circ}$ (Fig. 1c). Dips appear at φ-values corresponding to {100}, {110} and {130} planes. The very broad dips are interpreted as beeing due to the {111} planar channels and the <112> and <123> directional channels.

Fig. 5. The transmitted intensity at $\alpha = 35^{\circ}$ is shown as a function of φ. The beam is constantly incident parallell to the <001> channel (Fig. 1d). The interpretation of the curve is about the same as the one given for Fig. 4. The intensity variations are smaller.

Fig.6. The transmitted intensity at $\alpha = 40^{\circ}$ is shown as a function of φ. The beam is incident at $\theta = 40^{\circ}$ (Fig. 1e). The broad dips are interpreted as being due to the blocking from one {111} plane on each side of the {100} plane.

Fig. 7. The transmitted intensity in the forward direction ($\alpha = 0$) is shown as a function of φ. The beam is incident at $\theta = 45^{\circ}$ (Fig. 1f). The four sharp peaks indicate the φ-values of the {100} planes.

Fig. 8. The transmitted intensity in the forward direction ($\alpha = 0$) is shown as a function of φ (Fig. 1g). Some indices of crystallographic planes and directions are given. Fig. 7 and 8 together serve as calibration curves for the orientation of the crystal.

Fig. 9. The transmitted intensity in the forward direction ($\alpha = 0$) is shown as a function of θ in the two planes {100} and {110}. The curve is taken from ref. 6 showing numerous directional channels as indicated plus the presence of the {100} plane indicated by the dashed line. The dot-dashed line is the random intensity as a function of θ.

Fig. 10. The transmitted intensity at $\alpha = + 35^{\circ}$ is shown as a function of θ. The beam is incident at $\theta = - 35^{\circ}$ (Fig. 1h). The rather sharp dips at φ-values corresponding to {110} planes may be an indication of a planar channeling along these planes. The negative current at $\varphi = 45^{\circ}$, 135° and 318° is caused by secondary electrons.

Table I

The Table shows the σ-values for three different combinations of θ and φ. The third cimbination represents a channeling condition. σ is the characteristic half width of the dips.

θ deg.	α deg.	σ deg.
0	45	10,5 ± 0,3
45	45	9,1 ± 0,3
45	0	6,3 ± 0,2

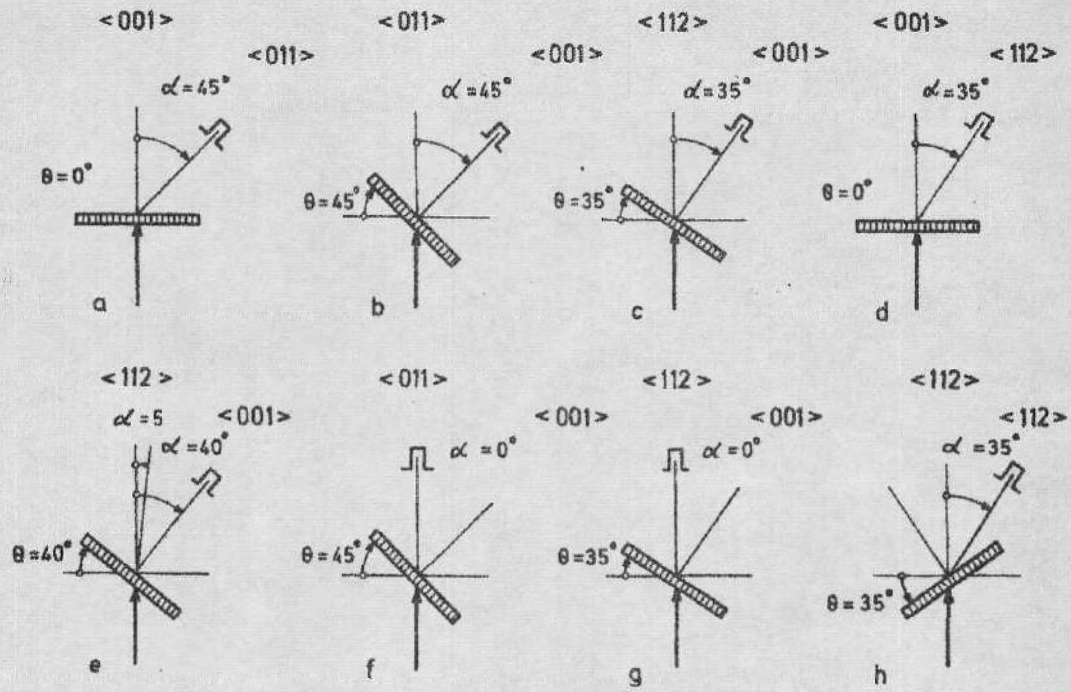
<001>
<011>
α=45°
θ=0°
a
<011>
<001>
α=45°
θ=45°
b
<112>
<001>
α=35°
θ=35°
c
<001>
<112>
α=35°
θ=0°
d
<112>
<001>
α=5
α=40°
θ=40°
e
<011>
<001>
α=0°
θ=45°
f
<112>
<001>
α=0°
θ=35°
g
<112>
<112>
α=35°
θ=35°
h

Fig.1.

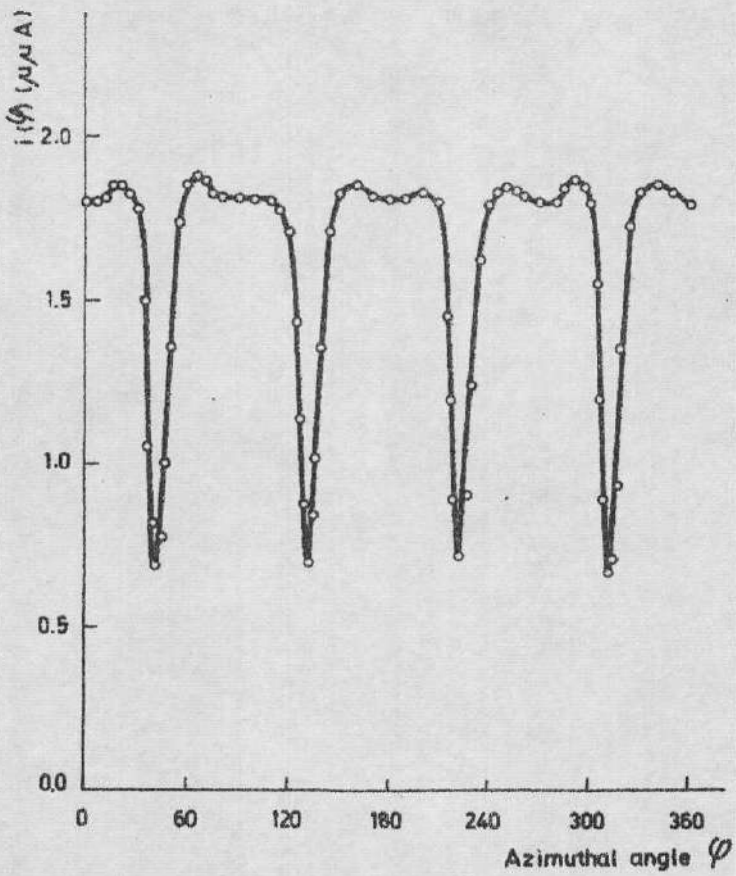
i(φ) (μA)
2.0
1.5
1.0
0.5
0.0
0
60
120
180
240
300
360
Azimuthal angle φ

Fig.2.

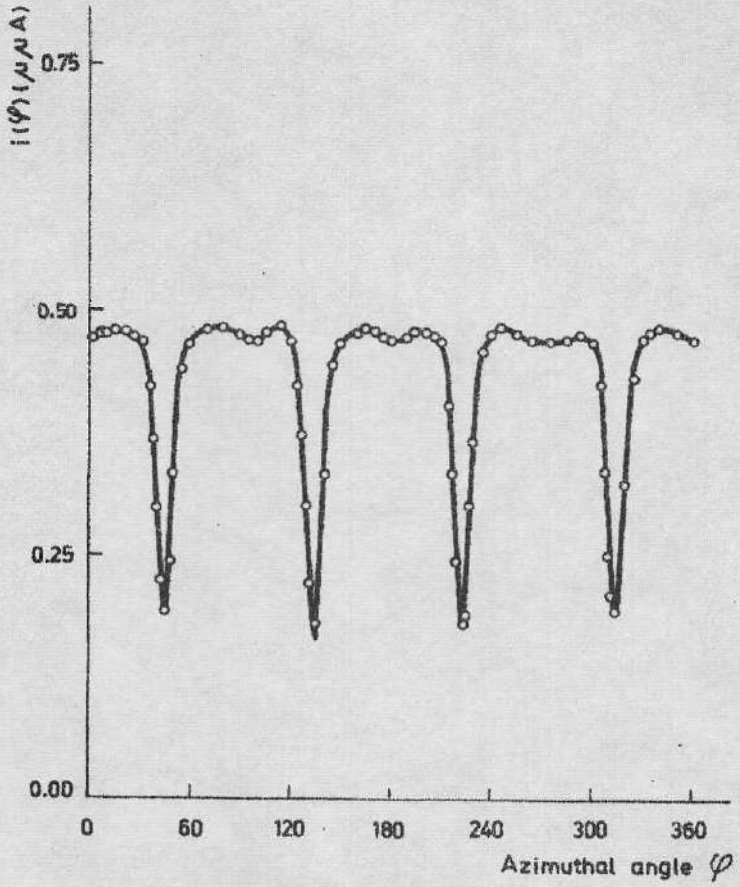
i(φ) (μA)
0.75
0.50
0.25
0.00
0
60
120
180
240
300
360
Azimuthal angle φ

Fig.3.

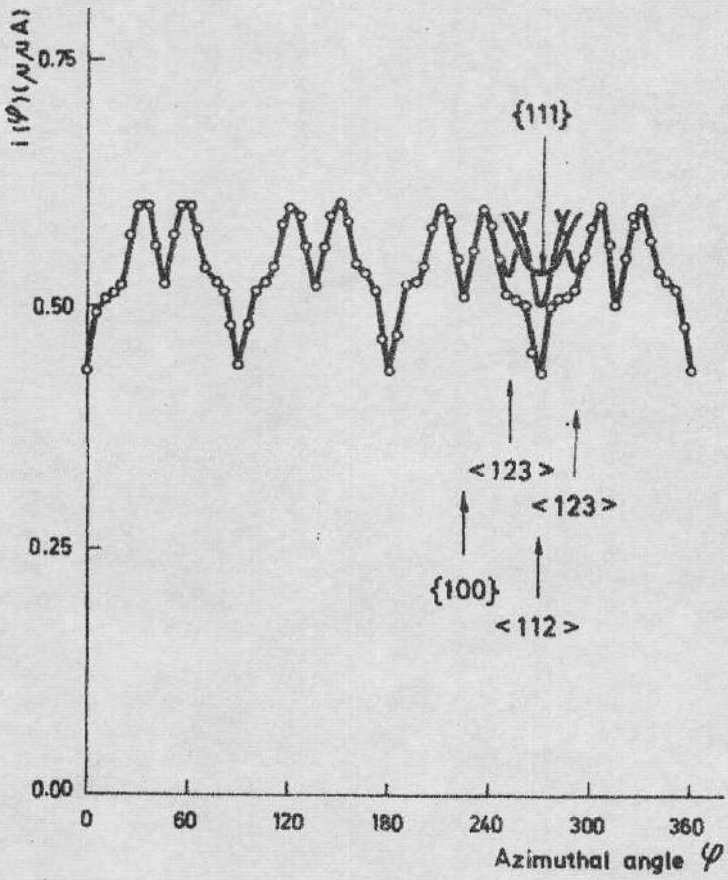
i(φ) (μA)
0.75
0.50
0.25
0.00
{111}
<123>
<123>
{100}
<112>
0
60
120
180
240
300
360
Azimuthal angle φ

Fig.4.

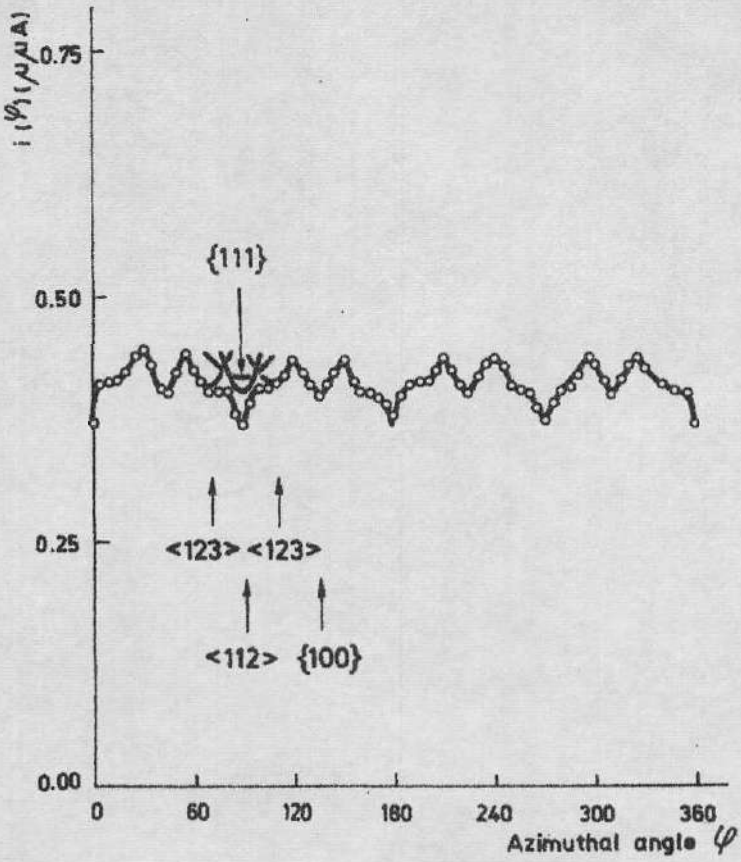
i (φ) (μA)
0.75
0.50
0.25
0.00
{111}
<123> <123>
<112> {100}
0 60 120 180 240 300 360
Azimuthal angle φ

Fig.5.

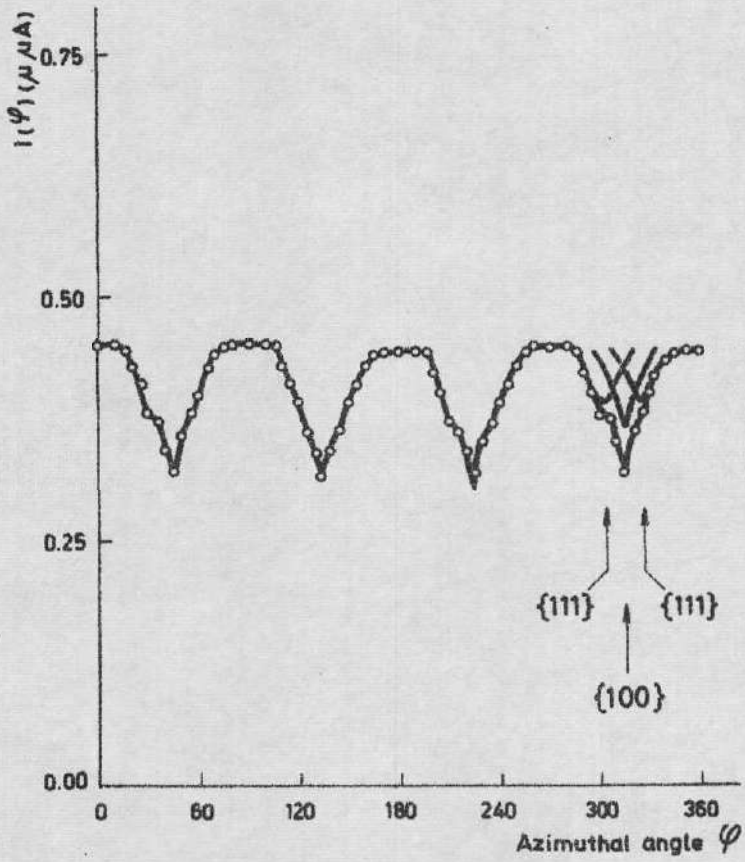
i (φ) (μA)
0.75
0.50
0.25
0.00
{111} {111}
{100}
0 60 120 180 240 300 360
Azimuthal angle φ

Fig.6.

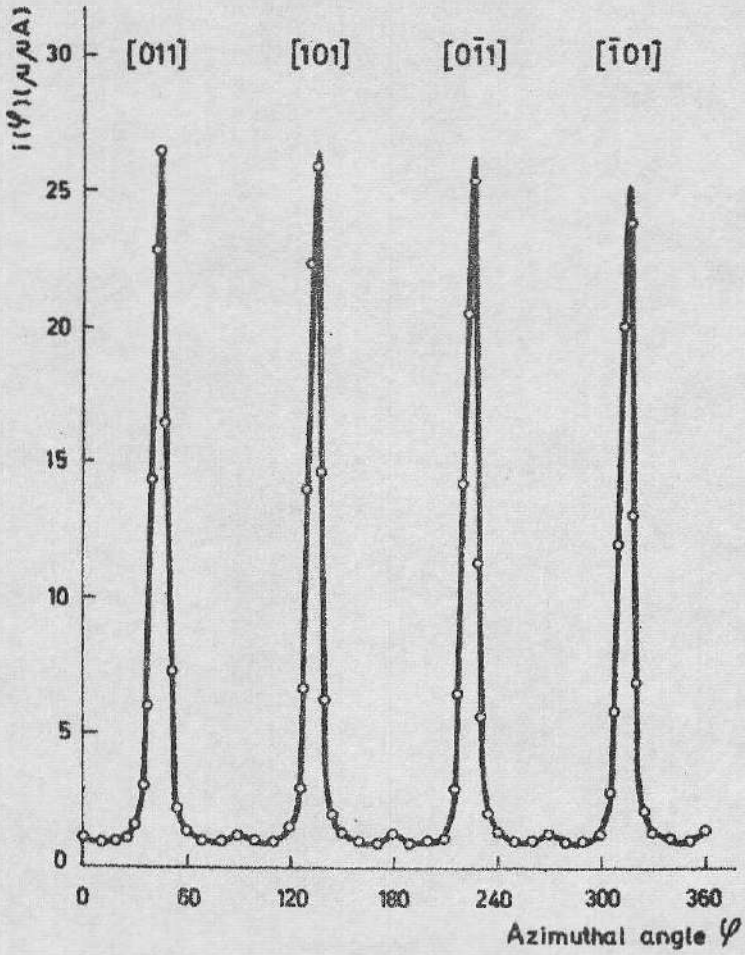
[011]
[101]
[0$\bar{1}$1]
[$\bar{1}$01]
i(φ)(μA)
30
25
20
15
10
5
0
0
60
120
180
240
300
360
Azimuthal angle φ

Fig.7.

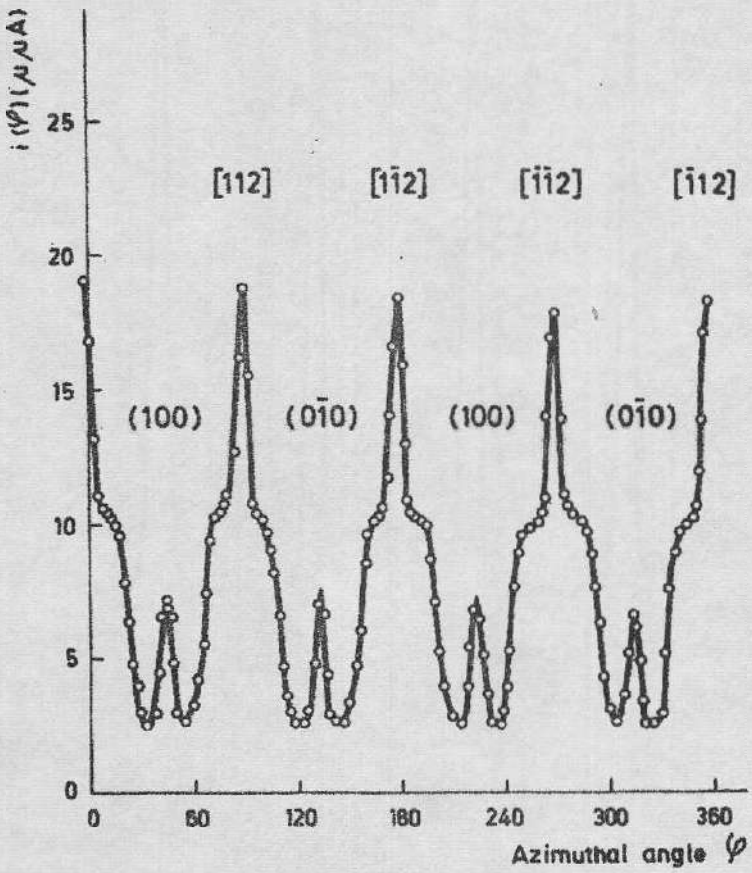
[112]
[1$\bar{1}$2]
[$\bar{1}\bar{1}$2]
[$\bar{1}$12]
(100)
(0$\bar{1}$0)
(100)
(0$\bar{1}$0)
i(φ)(μA)
25
20
15
10
5
0
0
60
120
180
240
300
360
Azimuthal angle φ

Fig.8.

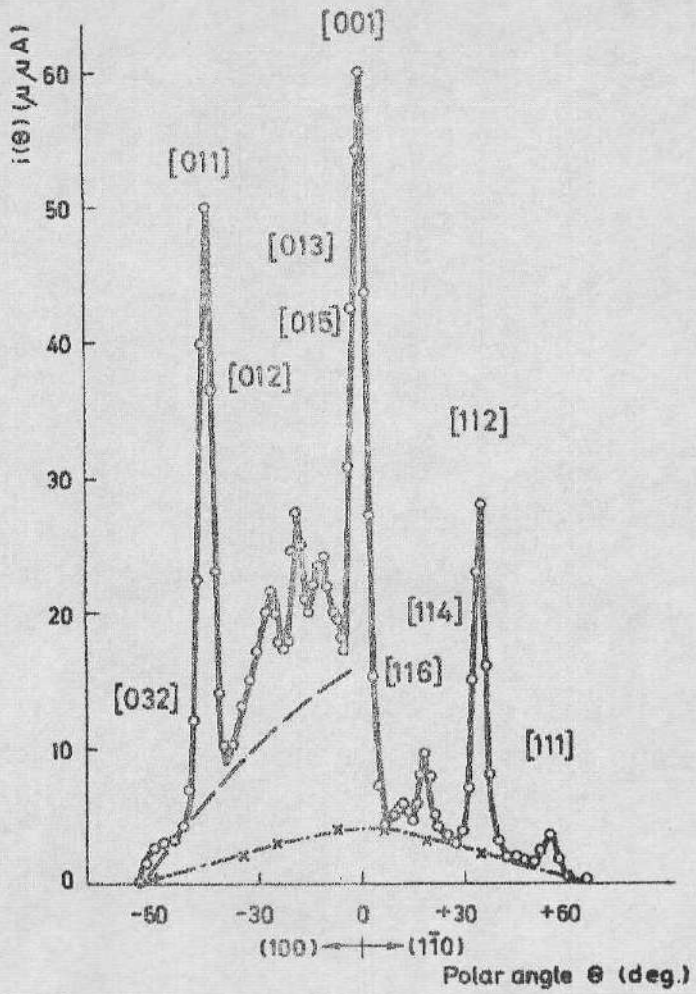
[001]
[011]
[013]
[015]
[012]
[112]
[114]
[116]
[032]
[111]
i(θ) (μμA)
60
50
40
30
20
10
0
-50
-30
0
+30
+60
(100)
(1$\bar{1}$0)
Polar angle θ (deg.)

Fig.9.

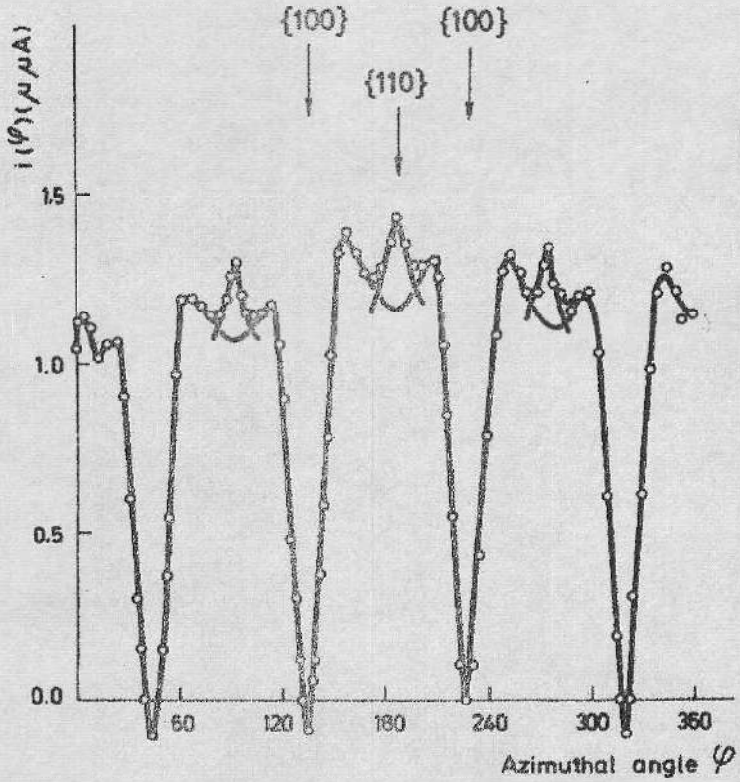
{100}
{100}
{110}
i(φ) (μμA)
1.5
1.0
0.5
0.0
60
120
180
240
300
360
Azimuthal angle φ

Fig.10.